LASER INTERFEROMETER GRAVITATIONAL WAVE OBSERVATORY
- LIGO -
==========
LIGO SCIENTIFIC COLLABORATION

Technical Note	**LIGO-T1300433–v3**	2013/06/04

Instrument Science White Paper

LIGO Scientific Collaboration

Distribution of this document:

LIGO Scientific Collaboration

California Institute of Technology
LIGO Project, MS 100-36
Pasadena, CA 91125
Phone (626) 395-2129
Fax (626) 304-9834
E-mail: info@ligo.caltech.edu

Massachusetts Institute of Technology
LIGO Project, Room NW22-295
Cambridge, MA 02139
Phone (617) 253-4824
Fax (617) 253-7014
E-mail: info@ligo.mit.edu

LIGO Hanford Observatory
Route 10, Mile Marker 2
Richland, WA 99352
Phone (509) 372-8106
Fax (509) 372-8137
E-mail: info@ligo.caltech.edu

LIGO Livingston Observatory
19100 LIGO Lane
Livingston, LA 70754
Phone (225) 686-3100
Fax (225) 686-7189
E-mail: info@ligo.caltech.edu

http://www.ligo.org/

Contents

1 Introduction

The LIGO Scientific Collaboration (LSC) conducts research and development directed toward the improvement of the current generation of LIGO and GEO interferometers as well as toward the development of concepts, prototypes, components, and modeling for future interferometer configurations.

The research is roughly separated into the following categories and working groups:

- The Advanced Interferometer Configurations Working Group (AIC)
- The Quantum Noise Working Group (QNWG)
- The Lasers and Auxiliary Optics Working Group (LAWG)
- The Optics Working Group (OWG)
- The Suspensions and Isolation Working Group (SWG)

The intent of this white paper is to provide a synopsis of the current and future R&D directions of these working groups.

Interferometer developement is a broad topic. An obvious part of the effort is in the design, building, and characterization of test systems and prototypes for the current detectors. Another element, of growing importance as we push the envelope of system performance, is the physics of materials and condensed matter systems. As this often requires scientists and skills beyond the existing groups, the Collaboration must expand these efforts in order to succeed in the larger goal of gravitational wave astrophysics. Finally, much of the ongoing and planned research commands interest in and of itself; adaptive optics, precision measurement, and quantum interactions with matter are both integral elements of gravitational wave detectors and exciting areas of physics.

Current instrument science research efforts focus on three related projects with three distinct time scales:

- **Incremental improvements to Advanced LIGO.** These are specific, small scale targets of opportunity that promise sensitivity improvements for astrophysical sources. As our experience with Initial and Enhanced LIGO demonstrate, These activities will almost certainly play a role in mitigating unforeseen problems in Advanced LIGO. The results of this ongoing research and development will be incorporated into the current observatories as-needed from now through the era of commissioning and first detections.

- **Upgrades of Advanced LIGO.** These efforts focus on incorporating Third Generation (3G) technologies into the existing observatories. The most likely upgrade path consists of incremental installation and upgrade phases followed by a science run. In this way there will be a continuous transition from the baseline Advanced LIGO configuration to the 3G LIGO detectors. Included in this scope are things such as (but not limited to) squeezed light injection, squeezing filter cavities, novel mirror coatings, new mirror substrate materials, cryogenic suspensions and optics, and heavy, composite test masses. These upgrades need to be ready for installation after the Advanced LIGO has made the first detections and completed several science runs (2018 - 2020).

- **Development of a Fourth Generation detector.** There is also a strong scientific motivation to build a substantially improved instrument in the same spirit as the European Einstein Telescope [1] (ET). We refer to this future instrument as a Fourth Generation (4G) detector. The design for such a detector may include new sites/facilites, underground infrastructure, longer beamtubes, and substantially heavier test masses. The epoch for the implementation of such a detector could possibly be ∼2025-2030.

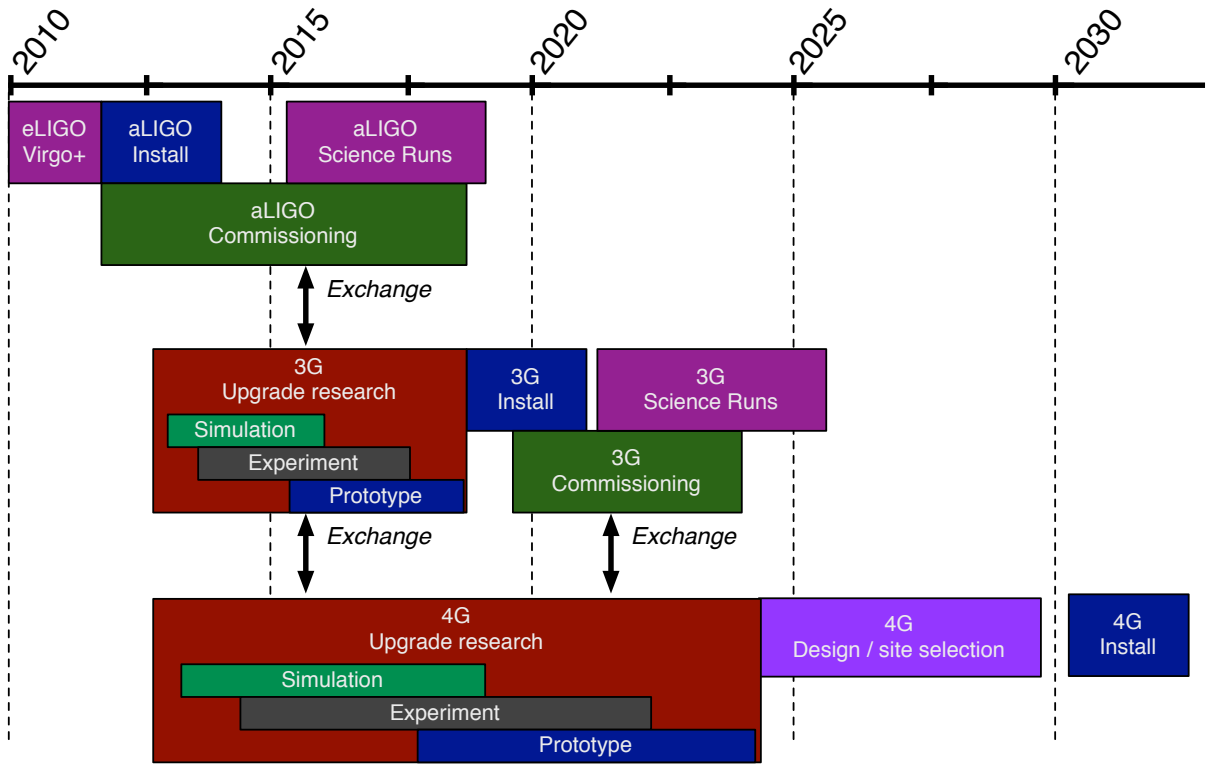

Figure 1: Timeline for 2G, 3G, and 4G gravitational wave detectors.

Figure 1 presents an estimated timeline for these efforts. Although the activities have different time scales, there is a vital and necessary exchange of knowledge, technology and personnel during every stage. As with Initial and Enhanced LIGO, the success of the aLIGO and 3G programs depends on the input from a robust next-generation research program, and vice-versa. This white paper represents the current thinking of the LSC technical working groups. From experience, we know that it will be updated routinely based on our ongoing R&D and both the experimental and observational results of Advanced LIGO.

2 Constraints

In this section, we outline a program that identifies the constraints applicable to the 3G and 4G detectors. Appendix A summarizes the status of Advanced LIGO circa mid-2012. Figure 2 presents our current best understanding of the noise sources that will limit Advanced LIGO in the high power, broadband tuning configuration. The sensitivity is determined by shot noise at high frequencies, by mirror thermal noise in the middle frequencies, and by a combination of thermal, seismic and quantum radiation pressure noises at low frequencies.

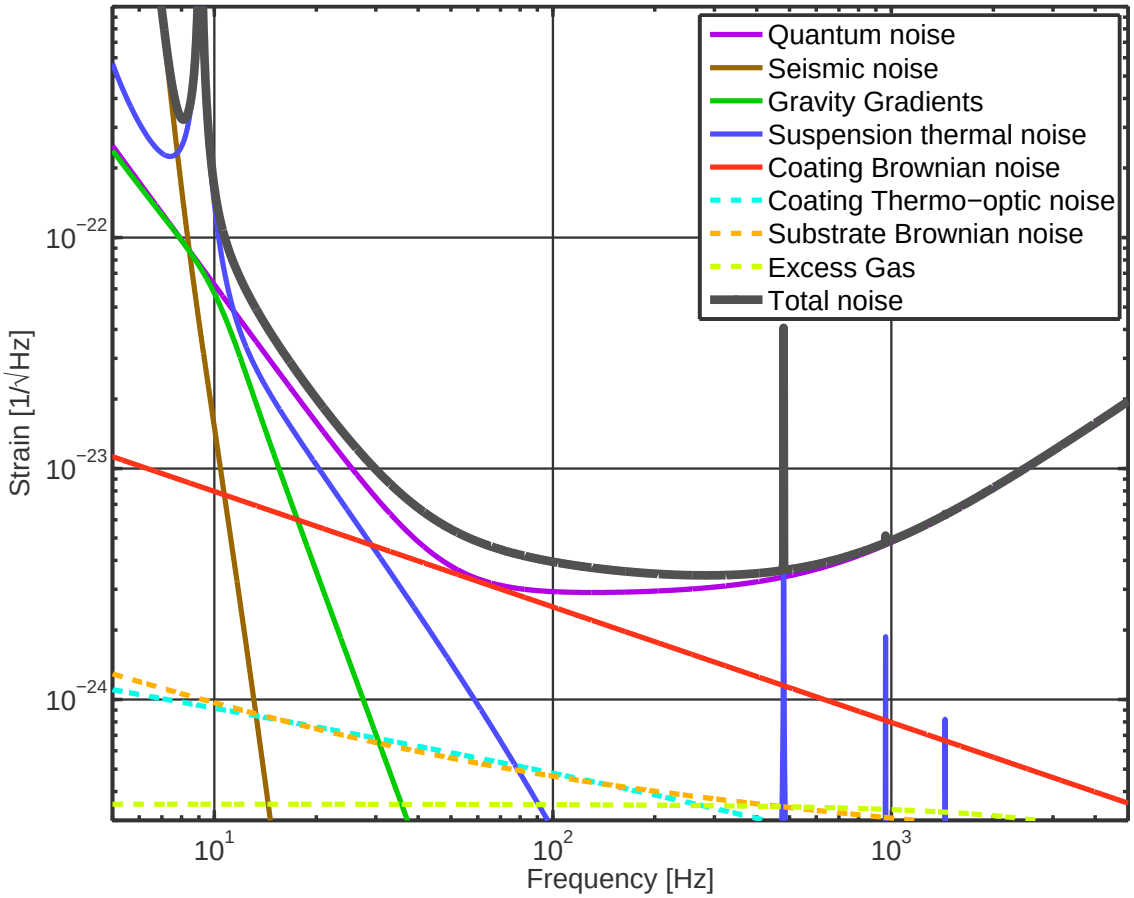

Figure 2: Baseline aLIGO Noise Budget (GWINC v2.0). 125 W input power; broadband RSE tuning.

The 3G and 4G detectors will study novel astrophysics and gravitational phenomena employing technology beyond the current state of the art. These sources are well described in the ET Design Study [1] as well as a technical note being prepared within the LSC [2]. The predicted gravitational wave sources emit in a variety frequency bands with a variety of durations, which places a corresponding requirement on the detector sensitivity. Ideally, the design of the 3G and 4G detectors will match the gravitational wave sources and the noise performance will be optimized accordingly. The required sensitivity then dictates the detector technology and design. This design methodology is illustrated schematically in Figure 3. This methodology fails in the current situation without gravitational wave detection – the input astrophysics remains speculative. In the following discussion, the process is reversed.

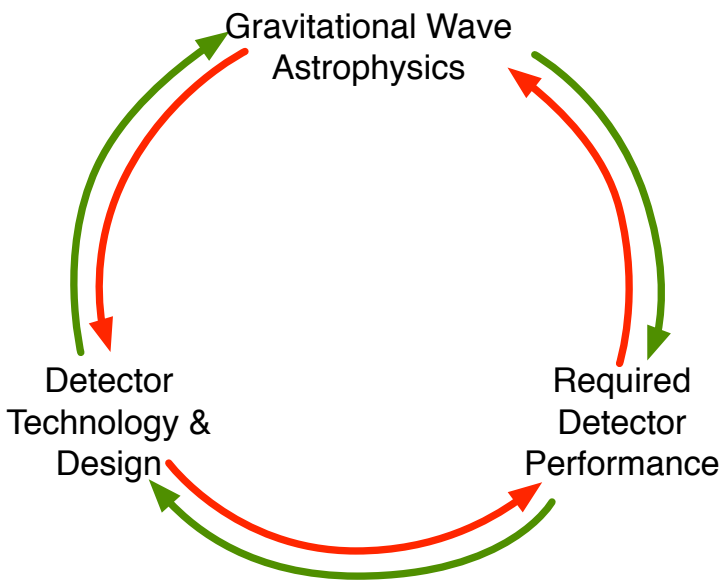

Figure 3: The interplay between astrophysics, sensitivity, and technology in detector design.

A straw man detector design based on reasonable extensions of current technology is used to calculate the dominant detector noise terms. The resulting instrument sensitivity is then used to evaluate the accessible astrophysics, which in turn influences the instrument design.

In Section 3, we describe a recent excercise to develop Strawman designs for the next generation LIGO detectors. In this context, Strawman implies that the design precedes a conceptual design and is chiefly used to explore possible designs and possibly rule them out.

3 Advanced Interferometer Configurations

The AIC group has two chief purposes:

- Coordinate the integration of interferometers systems and make trade-offs between components to optimize the sensitivity.
- Design the sensing and feedback control for the interferometer length, alignment, and wavefront (thermal compensation) systems.

3.1 Configurations

From January 9–12, 2012 the LIGO Scientific Collaboration (LSC) Instrument Science Working Groups held a workshop to begin studying designs for third generation interferometers to be installed at the existing LIGO sites.

The purpose of this workshop was to compare the sensitivity of a few different designs. These Strawman Designs came from three teams (Red, Green and Blue) in an attempt to explore all reasonable design space and to create a basis for comparing different design ideas. The Red Team was lead by Stefan Hild, the Green Team by Stefan Ballmer and the Blue Team by Rana Adhikari. They are briefly described in the following sections. The details of the Strawman Designs are found in [3] and also in [4] for the Red Design.

This workshop was an excercise to start working towards a conceptual design of LIGO-III. As described here and in the above-mentioned report, a great deal of analysis and experimentation is required before we know enough to choose between the various possible designs.

3.1.1 Common remarks on the designs

Here general common remarks on the designs are listed:

- The interferometers will be located at the existing LIGO sites. No extension of the arm lengths is possible at these sites.
- The existing LIGO vacuum envelope is used. An additional short vacuum tube may be used for a speedmeter or squeezing filter cavity.
- All designs reuse existing ISIs with possible enhancement for the heavier masses and improvement of the sensors and actuators. Modification of the external seismic support structure is allowed.
- Mirror suspensions should be updated as all designs assume heavy masses of more than 100 kg for reduction of radiation pressure noise and suspension thermal noise.
- All designs consider coating thermal noise to be the main issue in achieving noise improvement around 100 Hz. The designs attempt to mitigate the issue by using larger beam spots on the mirrors and/or by other coating technologies, or perhaps non-Gaussian beam shapes.

- All designs require Newtonian noise cancellation with seismometer arrays.
- All designs keep the standard aLIGO configuration, namely dual-recycled Fabry-Perot Michelson, while all of them employ frequency dependent squeezing with an input filter cavity of 100-m class length for reduction of quantum noises.

The key parameters used for the calculation of the sensitivities are shown in Table 1.

3.1.2 Red Design

The Red Design tries to mitigate limiting noises of aLIGO by extending concepts of the current aLIGO design. In the following list a brief overview of the assumed changes are given. A more detailed description for each fundamental noise source can be found in [4].

- **Suspension Thermal Noise:** The team assumed fused silica suspensions at room temperature, with the length of the last stage being increased from 0.6 to 1.2 m. In addition, the weight of the test mass was increased to 160 kg and the fiber geometry was accordingly adapted. These changes provide a suspension thermal noise reduction of about a factor 3 to 4 above 10 Hz.
- **Seismic Noise:** The increased length of the last suspension stage also reduces the seismic noise by a factor 2. No subtraction techniques have been included.
- **Newtonian Noise:** Newtonian noise is subtracted by a factor of 5 with seismometer arrays.
- **Coating Thermal Noise:** An overall reduction of coating noise by a factor 3.2 is assumed. Increasing the beam size by a factor 1.6 reduces the coating noise by a factor 1.6. In addition, a further reduction of a factor 2 is given by either improved coatings, the application of Kahlili cavities, or the use of waveguide mirrors, or the application of alternative beam shapes.
- **Quantum noise:** The same interferometer configuration and optical power as for aLIGO is assumed. The quantum noise improvements originate from an increased test mass weight and the injection of frequency dependent squeezed light. An initial squeezing level of 20 dB (inside the squeezing source) and losses of 9% plus the roundtrip loss in the filter cavity are considered. These result in an observed quantum noise reduction of about 9 dB. The employed filter cavity has a length of 300 m and a roundtrip loss of 30 ppm.

The Strawman Red noise budget and the corresponding sensitivity described in this section are shown in Figure 4. The resulting sensitivity improvement with respect to the Advanced LIGO baseline is shown in the lower subplot of the figure. For all frequencies above 50 Hz the Strawman Red sensitivity can provide an improvement of a factor 3. In the range from 8 to 30 Hz the improvement is about a factor 4. The sensitivity curve presented here corresponds to a binary neutron star inspiral range of 614 Mpc.

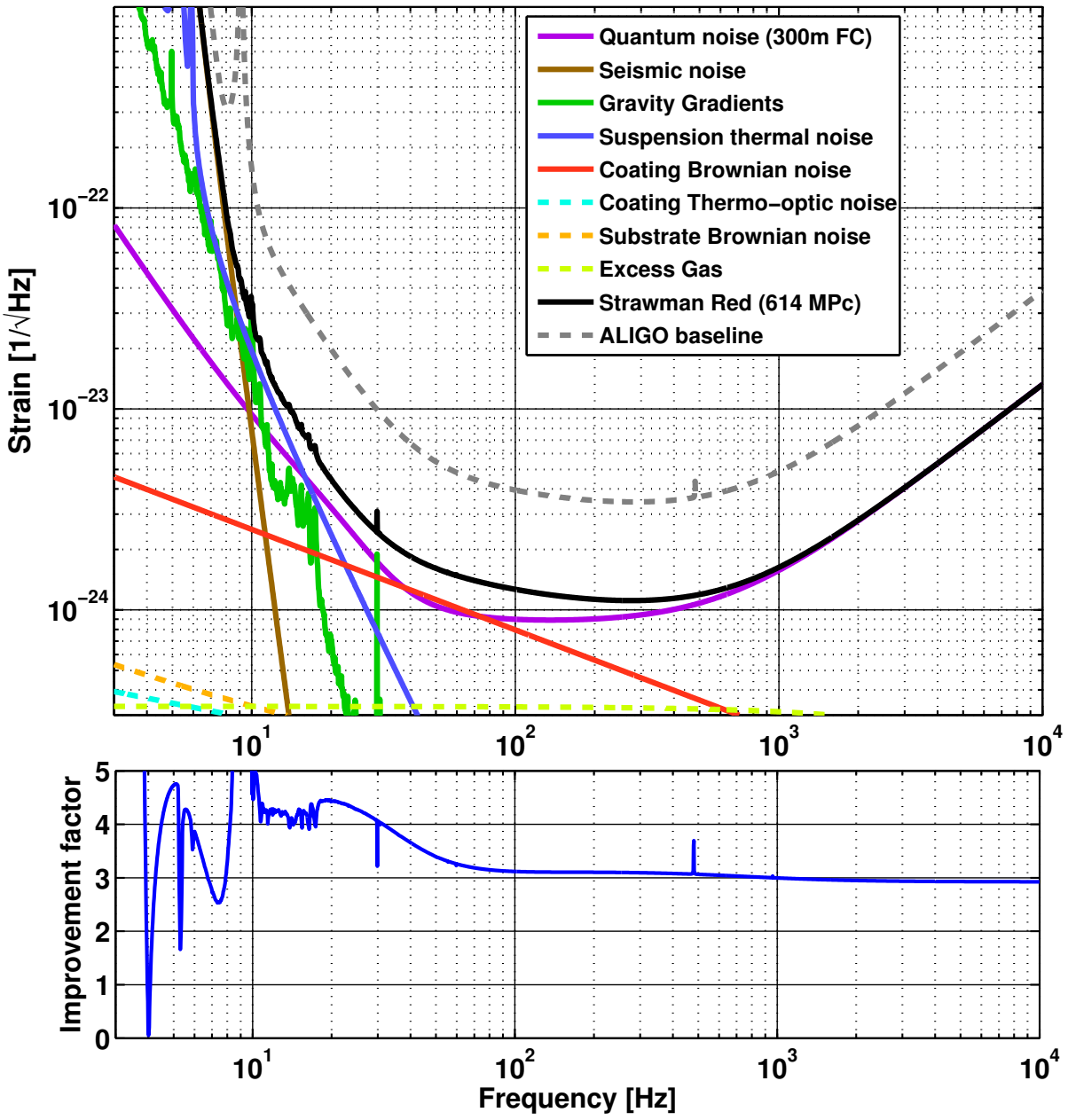

Figure 4: Noise budget for the LIGO-3 Strawman Red design (upper subplot) and the linear improvement factor compared to Advanced LIGO (lower subplot).

3.1.3 Blue Design

The Blue Design tries to mitigate limiting noises of aLIGO by replacing the material of the mirrors and suspensions as well as operating a detector at cryogenic temperature of 120 K.

- **Large cryogenic Silicon mirror:** In order to obtain broadband improvement of the sensitivity, 150 kg Silicon mirrors at the operating temperature of 120 K are considered.
- **Silicon cryogenic suspension:** Silicon ribbons (and perhaps blade springs) in the final stage suspension at 120 K are employed.
- **Newtonian noise:** Newtonian noise is subtracted by a factor of 30 with seismometer arrays.
- **High power 1560 nm laser:** 1560 nm wavelength lasers operating at 300–700 W are employed. Arm cavity powers will reach 2–5 MW.
- **Coating Thermal Noise:** The beam spot size is kept at the aLIGO size to avoid optical degeneracy issues and epitaxial coatings on the test masses are employed for a mirror thermal noise improvement of 3 to 10.
- **Quantum noise:** Squeezed light injection (10 dB) and a 300 m filter cavity for frequency dependent squeeze angle is assumed.

The Strawman Blue noise budget and the corresponding sensitivity described in this section are shown in Figure 5. The sensitivity curve presented here corresponds to an binary neutron star inspiral range of 700 Mpc.

3.1.4 Green Designs

The green team investigated two distinct design ideas:

- Combining the ideas of Fabry-Perot cavities and Herriott delay lines, forming resonant delay lines.
- The use of a suspension point interferometer on the penultimate mass (or separately suspended from the penultimate mass) as high frequency interferometer of a xylophone. The low frequency interferometer remains on the (ultimate) test mass.

Other design elements are copied or compatible with ideas from the other groups.

- baseline design with 1064 nm laser and silica optics at room temerature, but compatible with cryogenic operation at 1560 nm wavelength,
- $\sim$160 kg test mass
- improved suspension for a reduction in suspension thermal noise
- Newtonian noise substraction via seismometer arrays

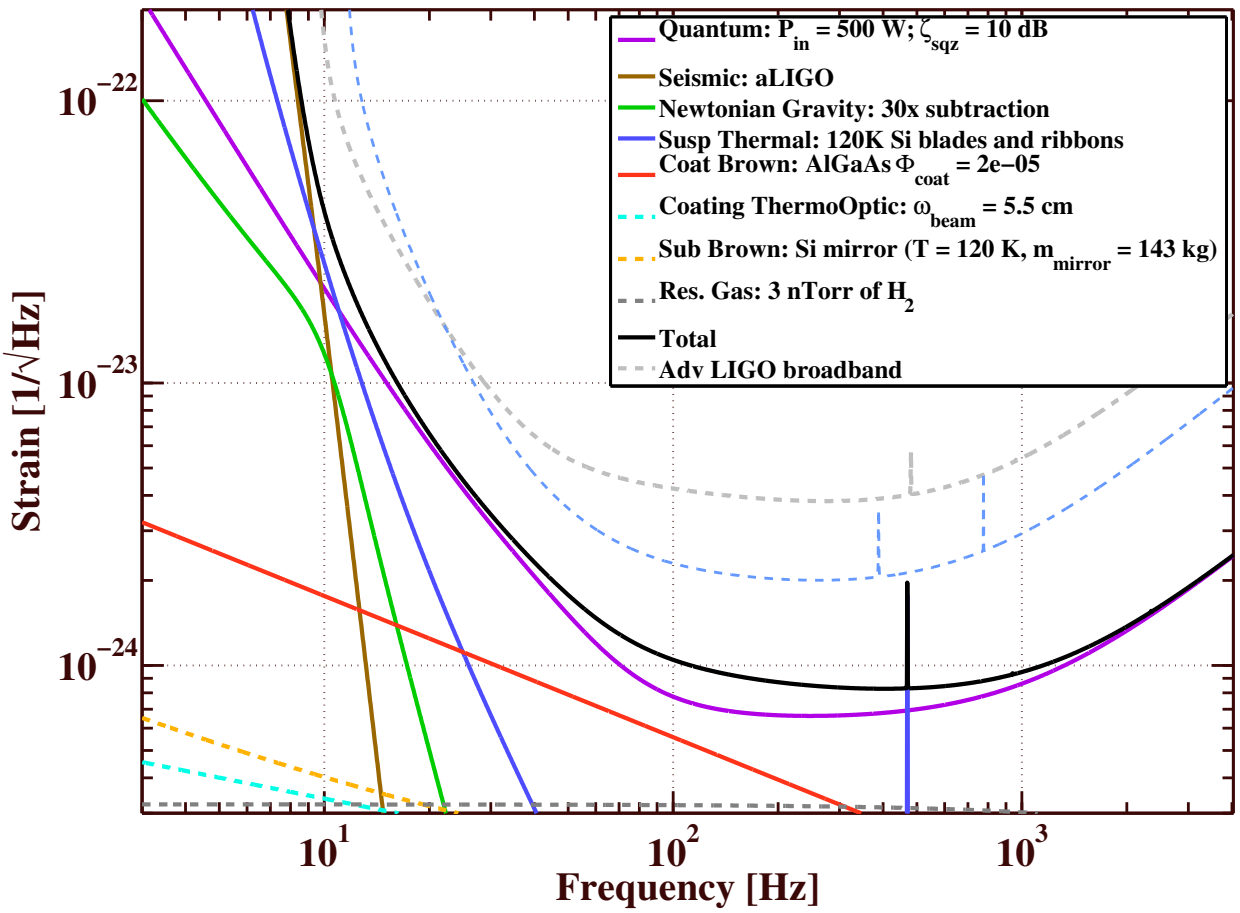

Figure 5: Noise budget for the LIGO-3 Strawman Blue design.

- Squeezed light injection (10 dB) and a 100 m filter cavity for frequency dependent squeezing.

Resonant Delay Line (RDL) interferometer:

In the Green RDL design, a Herriott delay line combined with a Fabry-Perot cavity is considered in order to increase the sampled surface area of the optic to reduce the coating Brownian noise without using marginaly stable arm cavity. Such multiply folded arm cavities can be built in either travelling wave or standing wave configuration [3].

Example Green RDL Design sensitivity is shown in Figure 6. For the calculation, standing wave resonant delay line with 4 spots per mirror, beam spot increase of $w \times 1.5$ over aLIGO, mass=160 kg, and 10dB squeezing are employed. For other parameters see table 1. The sensitivity curve presented here corresponds to an binary neutron star inspiral range of 514 Mpc.

SPI/Xylophone interferometer:

Another detector configuration proposed by the Green Team is actually a hybrid of two separate design methodologies: SPI and Xylophone. In addition to the traditional SPI [5, 6],

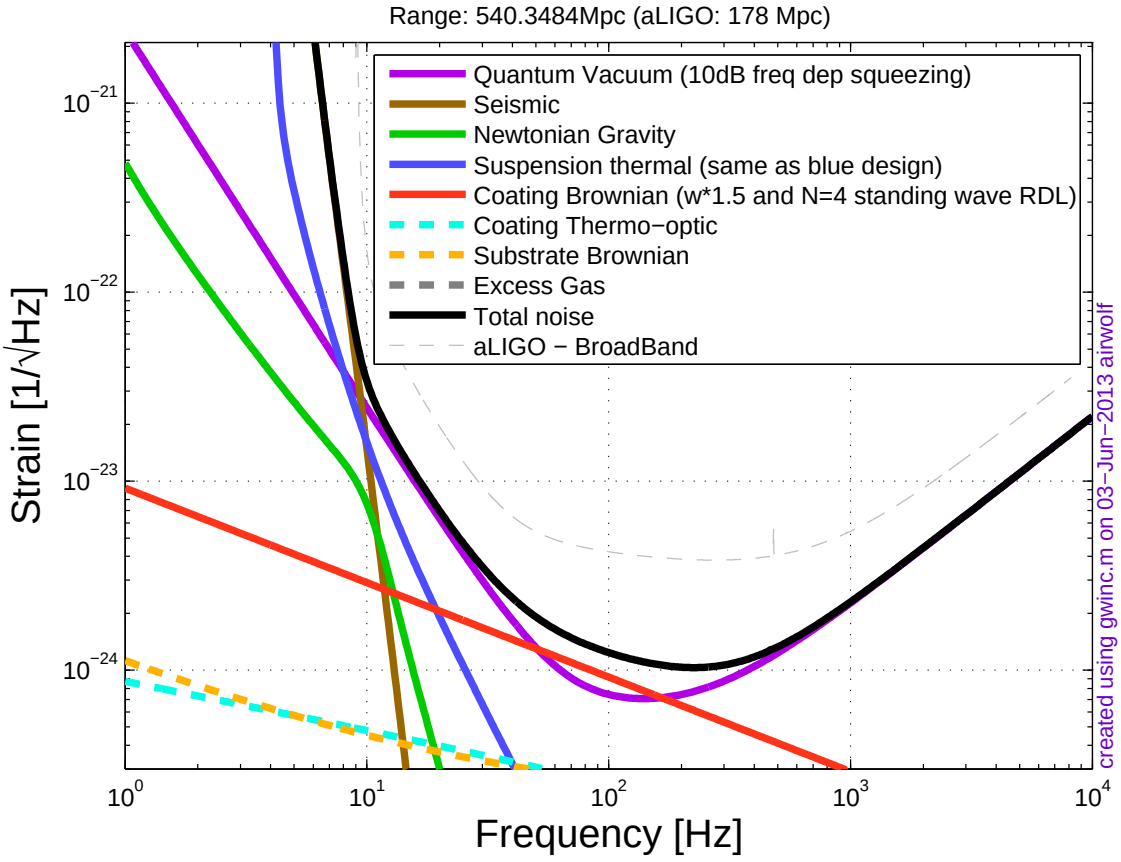

Figure 6: Noise budget of the Green Resonant Delay Line approach.

the auxiliary interferometer formed by the penultimate stage of the suspension (PUM) is used to sense gravitational waves, as well as the ultimate stage (UM). By changing the parameters of the individual IFOs (e.g. mass, dimensions, laser power, etc.), the two detectors can be made to have optimal sensitivity in different bands i.e."xylophone detector".

The PUM is made to have a lower mass than the UM, and the laser power of the upper IFO is higher than that of the lower stage. The result is that the upper IFO has better quantum-limited performance at high frequencies, where its lower shot noise dominates, while the lower stage prevails at low frequencies, where it is dominated by its lower radiation pressure noise. Finally, since the upper IFO is not used for GW detection at low frequencies, it can be used in this band as a sensitive displacement noise suppressor. The displacement noise fed through to the UM — including the radiation pressure noise of the PUM stage — is then just the fully suppressed, closed-loop residual noise of the upper IFO, filtered further by the passive final pendulum stage.

Figure 7 is an example sensitivity of the SPI/Xylophone detector. The combined sensitivity curve presented here corresponds to an binary neutron star inspiral range of 618 Mpc.

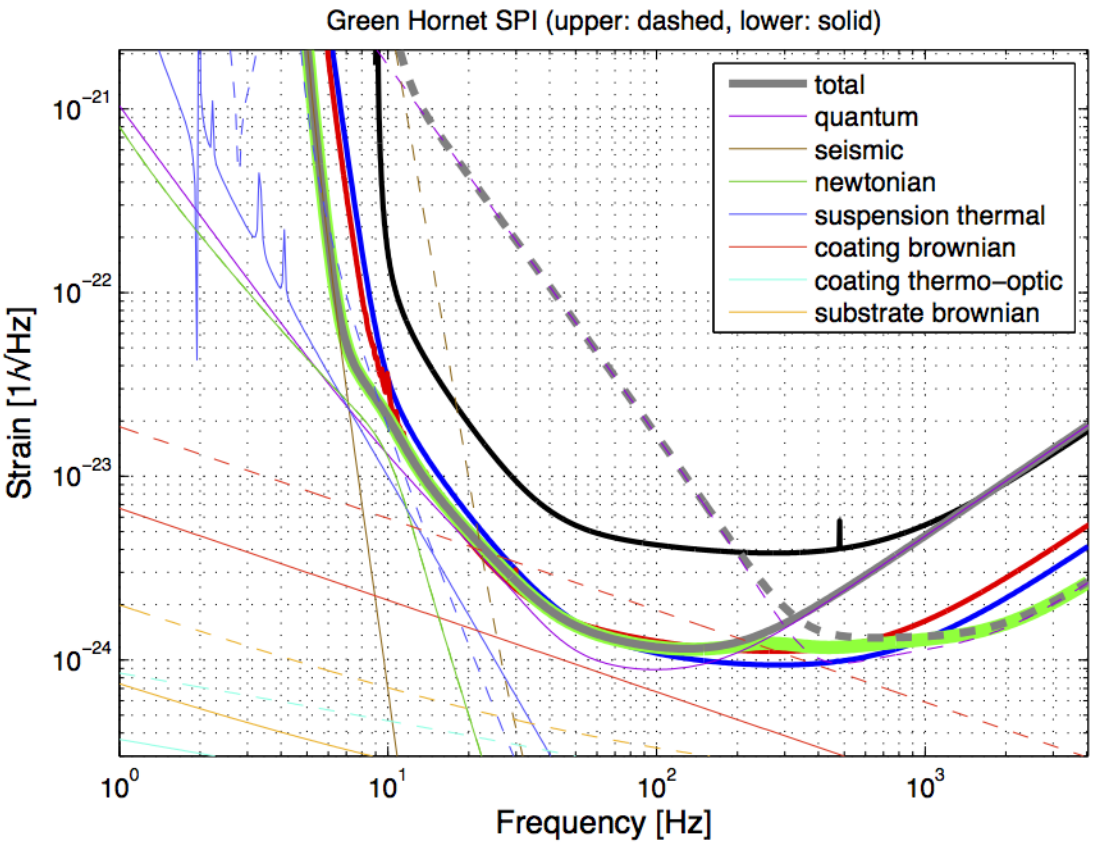

Figure 7: Noise budget for the Green Hornet SPI, given the parameters in [3]. Traces for the upper IFO are dashed and those for the lower IFO are solid, and the total combined GH noise is in thick solid green. The thick blue and red curves are the Blue and Red team noise curves, respectively, and the thick black curve is the aLIGO broadband noise curve.

3.1.5 Comparison

Table 1 shows the comparison of the key parameters of the detector designs. Figure 8 shows the comparison of the sensitivity curve between the designs including the nominal aLIGO.

3.1.6 Required research and development

While the Strawman Designs will require some common research for the development of their subsystems for the most part they will require different levels of research effort for the development of their various subsystems. Here some of the main research topics are highlighted.

- **Suspensions:** The Red, Green and Blue designs will all require new quadruple suspension systems (SUS) designed to support the much heavier test masses. New design including the suspension thermal noise optimization is required. The Blue design involves a silicon cryogenic suspension. This require a thorough study of the new suspension materials. The Green SPI design needs the integration of the PUM interferometer into the suspension design.

IFO Cases	Blue	Red	Green RDL	Green SPI (PUM/UM)	aLIGO
Mirror Mass [kg]	143	160	160	14/157	40
Mirror Material	Silicon	Silica	Silica	Silica	Silica
Mirror Temp [K]	120	295	295	295	295
Sus Temp [K]	120	295	295	120	295
Sus Fiber	0.6m Si	1.2m SiO2	TBD	0.6m Si	0.6m SiO2
Fiber Type	Ribbon	Fiber	TBD	Ribbon	Fiber
Input Power [W]	450	125	125	250/50	125
Arm Power [kW]	3200	800	210	1503/295	800
Wavelength [nm]	1560	1064	1064	1064	1064
NN Sub	30	5	10	30	1
Coating Type	AlAs:GaAs	SiO:TaO	SiO:TaO	SiO:TaO	SiO:TaO
Beam Size [cm]	5.3 / 6.2	8.5 / 10	8.3 / 9.3	(4/4) / (11/11)	5.3 / 6.2
SQZ Factor [dB]	10	20	20	20	0
F. C. Length [m]	300	300	100	100/100	N. A.

Table 1: Baseline parameters for aLIGO and the Strawman IFO configurations

- **Seismic Isolation Systems:** All three suspension designs are based on an Internal Seismic Isolation (ISI) system which can operate with a total payload equal to that of aLIGO. Although the current ISI is supposed to be able to handle the heavier mass/suspensions, confirmation from the engineering point of view is necessary. The Red design, which uses longer pendulums, will require modification of the BSC chambers as well as the ISI supports and the HEPI controls.

- **Newtonian Noise Subtraction:** All three designs will require Newtonian Noise Subtraction using seismometer arrays. This is also a part of the risk reduction effort for aLIGO and is already underway at the sites and other laboratories.

- **Lasers:** The Blue Design requires a 500-600 W laser operating at 1560 nm. While such a laser is not currently available, there is considerable commercial and academic activity today focused on fiber lasers.

- **Core Optics:** For ∼150 kg silicon and silica core optics the technology for making the boules is already in hand. Grinding and polishing should also not be a big problem for either material. There is an engineering challenge to perform the metrology for such large substrates. Acquiring 150 kg pieces of silicon of 'float-zone' quality is not currently possible and may not be in the future without some industrial motivation.

- **Optical Coatings:** We probably need to carry out parallel study on the three sources of optical loss related to the coatings including coating thickness nonuniformity which leads to figure error, prompt scattering from microroughness and scattering from "inclusions" or "defects" in the coatings. The amount of the effort will depends on the material of the substrate. The Blue design will require the development of new generation of crystalline optical coatings. For the crystalline coatings one important area of research will be the attachment of the coatings to the mirror substrate and measurements of the mechanical loss of coatings applied to appropriate optical substrates and

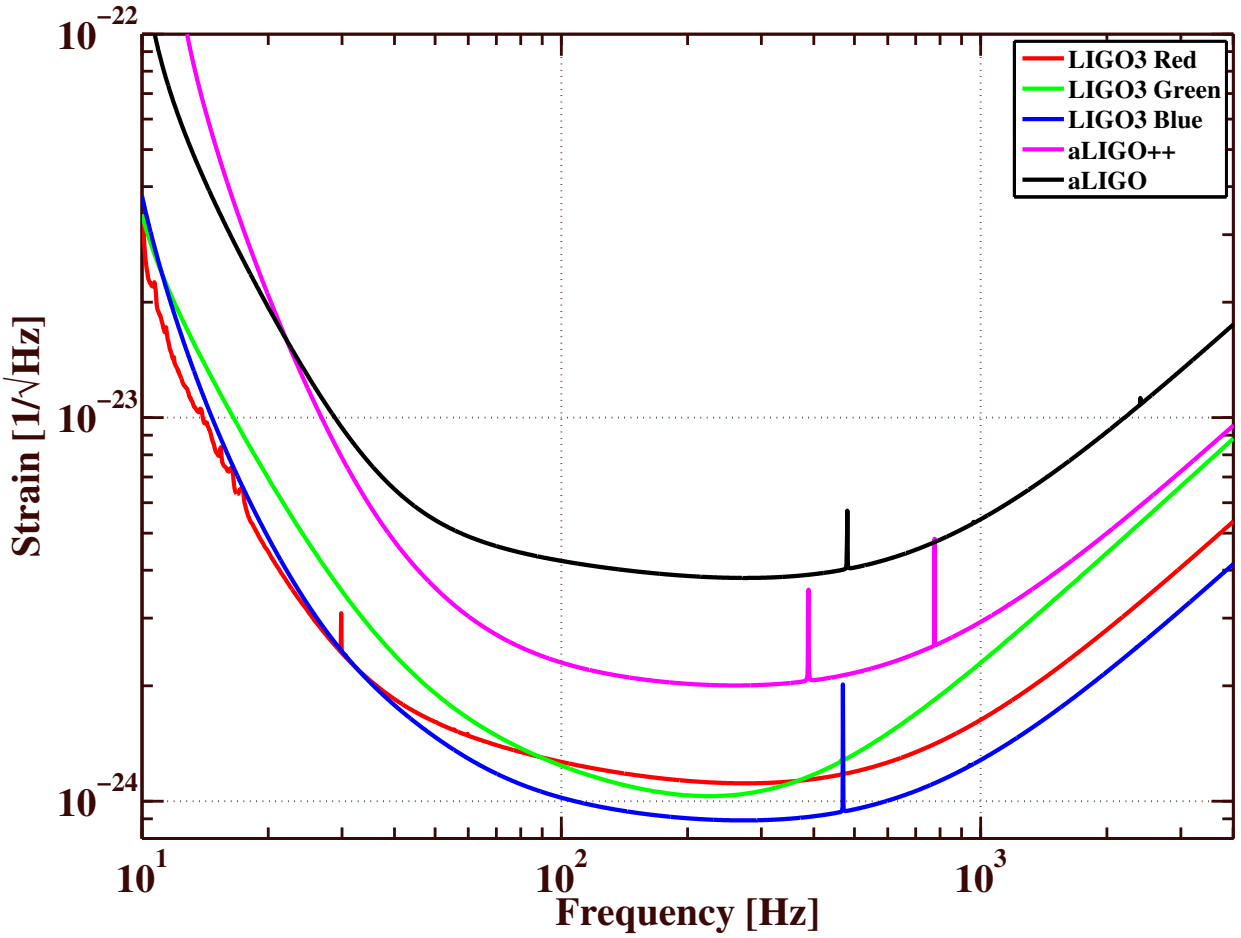

Figure 8: Comparison of the 3 LIGO-3 design concepts as well as the Advanced LIGO baseline. Also shown is an estimate of an intermediate upgrade (aLIGO++) including: 6 dB of squeezing injection with a short filter cavity as well as improved coatings (e.g. AlGaAs applied via epitaxial liftoff giving an improvement factor of 2 in strain)

characetrizations of its optical qualities. After laboratory scale favorable results on the coating, a longer term collaborative effort with coating vendors must be undertaken.

- **Coatings Thermal Noise Reduction:** The coating thermal noise reduction in progress on the aLIGO coatings and this should be continued. The Red design alone could require work on a resonant waveguide (RWG) mirror approach. These coatings would require research in almost all areas of coating development. The Red design also considers the use of the Khalili cavity. This requires experimental demonstrations of the technique in terms of the control and noise aspects.

- **Input Optics:** All designs may require larger input beams thus requiring larger input optics. The Green SPI Design requires significant upgrade of the input optics in order to accommodate two interferometers in a single vacuum manifold. The Blue design should replace every optic the beam passes through. Also the higher input power may lead to the need for a thermal compensation system for some of the critical input optics.

- **Thermal Compensation:** A Khalili cavity will require a dedicated TCS to ensure the coupling of the beam to the Khalili cavities as designed. RWG may need more research on the TCS. For the Blue design, the cryogenic fused silica compensation plate at higher power would require additional research.
- **Auxiliary Optics:** Stray light control will need to be reevaluated for all designs becuse of the increased seisitivity. TMS will also need additional investigation because of the larger beams employed. For the Blue design, High efficiency photodiodes at 1560nm will need to be explored. Arm Length Stabilization (ALS) system for deterministic lock is necessary to be replaced by other technique including phase lock using a frequency comb technique or a heterodyne interferometry with pseudo-random modulation.
- **Frequency Dependent Squeezing:** This is discussed in Section 23.

3.2 Interferometer Sensing and Control

The Interferometer Sensing and Control (ISC) consists of three areas (LSC, ASC, and TCS). In addition to these, general remarks about the control systems and the interferometer simulations are made in the AIC context.

The dominant issue of ISC is to maintain IFO stability while not introducing control noise. The following is an overview of the three subsystems:

Length Sensing and Control (LSC): The LSC manages the interference conditions of the fundamental mode in the interferometer in order to maintain a high sensitivity to GWs. The longitudinal distances between the mirrors are adjusted so that they fulfill particular interference conditions.

Alignment Sensing and Control (ASC): The ASC primarily controls the 1st-order optical modes in the interferometer by adjusting the angular orientation of the mirrors. In addition to the LSC, this system is also necessary to maintain interferometer sensitivity. Although the angular motion of the mirrors are locally stabilized by the vibration isolation and the suspension systems, the global control is necessary in order to realize stable interferometer operation.

Thermal Compensation System (TCS): The TCS controls the higher-order modes in the interferometer. The importance of the TCS, and our understanding of it, has been increasing with increasing circulating power in first generation detectors and their enhancements. The sensing of thermal aberrations, which lead to higher-order mode production and instability of interferometer control, is discussed below while the TCS actuators are described in Section **??**.

3.2.1 Length Sensing and Control

The Advanced LIGO interferometers consist of five coupled cavities that must resonate simultaneously to reach the operating point. The LSC receives the length sensing signals from the photodiodes and sends them to the actuators on the suspensions so that those five degrees of freedom stay at the operating point. Between the sensing and the actuation, the signals are processed by servo filters so that stable feedback control of each loop is established.

The aLIGO LSC employs a combination of RF heterodyne detection and DC readout [7]. This RF sensing scheme comprises the Pound-Drever-Hall technique, Schnupp modulation, and third harmonic demodulation technique [8] as a baseline design. The DC readout scheme provides sensing of the GW signal with shot noise performance superior to that of RF detection, along with more immunity to laser noises when combined with an Output Mode Cleaner (OMC). DC readout also clears the way for the use of squeezed light injection to reduce quantum noise (see section 4).

These sensing techniques have been independently demonstrated by the Enhanced LIGO [9, 10] and GEO600 [11, 12] interferometers, and other prototype interferometers [13, 14, 15]. The task for the aLIGO interferometer commissioning team is to integrate these well known techniques and find any hidden issues. As a scale model of the full aLIGO interferometers, the Caltech 40m prototype plays an important role in this effort by giving us a first look at potential problems.

Detuning of the signal recycling cavity is also a part of the design. This detuning improves the sensitivity of the device for neutron star mergers by lowering the noise level at around 200 Hz where the quantum noise is the dominant noise source of the tuned-recycling case. However, the previous experiences at GEO600 and Caltech 40 m show the presence of obstacles to be overcome in lock acquisition and noise couplings [16, 17]. Although the first phase of aLIGO will use the broadband signal extraction, the issues of the detuning should be revisited with simulations and the prototype experiments.

The LSC system for 3G/4G detectors will likely also rest on the above technologies. Details of the system, however, will greatly depend on the optical configuration to be deployed as the future detectors may face further complication with more mirrors and cavities (e.g., filter cavities for squeezed light, or a sloshing cavity for QND interferometer readout – c.f. section 4). Once the optical configuration is set, the detailed analysis of the LSC plan should follow. In addition to the techniques already used in aLIGO, new complications may require new techniques such as multiple carriers and/or multiple lasers with single or multiple wavelengths.

An example of an upcoming ISC challenge is the filter cavity which will be required for filtering squeezed light before it enters the interferometer. This cavity will require length control via a carrier frequency which is not the same as the carrier light circulating in the interferometer (to avoid polluting the squeezed state with scattered photons). The filter cavity will also present an alignment control problem similar to the input mode-cleaner. Similarly, the phase of squeezed light source itself must be controlled with respect to the interferometer.

For the 3G/4G detectors, the idea of the Suspension Point Interferometer [5] may also be investigated as it could be a practical solution to mitigate the vibrational noise caused by the heat link of the cryogenic cooling system.

Lock acquisition A new feature of the aLIGO LSC is the use of independent laser sources in the Arm Length Stabilization (ALS) system [18, 19, 20]. This system enable us to lock the long arm cavities in a deterministic way with the guidance of auxiliary beams injected from the end mirrors.

Advanced LIGO will achieve lock using two single arm interferometers to control the arm cavity mirrors independently of the Michelson and signal recycling cavities. The arm cavity locking requires stable frequency-doubled lasers at each end station, with each laser frequency referenced to the master laser in the vertex, 4 km distant. For Advanced LIGO, these lasers are stabilized after first locking the arm cavities. For higher finesse cavities in LIGO 3G and 4G, there may be a need for an improved laser stability. Research into stabilized lasers using length controlled fibers, isolated reference cavities, and atomic frequency references may all address this need.

In addition to stable lasers, the more complex LIGO 3G interferometers may require additional lock acquisition techniques. Low noise phase meters similar to the LISA phase meter provide an option for determining the relative position of all the interferometer optics simultaneously. This includes the possible use of the pseudo random phase modulation for digital interferometry. Although these phase meter techniques require an order-of-magnitude improvement over current sensitivities, a phase meter lock acquisition system could be deployed on Advanced LIGO and provide substantial risk mitigation.

High power photo-detection Unlike previous generations of interferometers, the Advanced LIGO, 3G, and 4G interferometers will detect substantial amounts of DC photocurrent at signal frequencies below 10 Hz. In this region, photodiodes are subject to excess 1/f noise that degrades their performance. Research to characterize, understand, and improve upon photodiodes will be necessary to detect the signals from high power interferometers.

In addition to the DC photocurrent, the RF power received by the RF detectors will also increase. Increasing the SNR in the RF detectors will directly reduce the auxiliary controls noise (a limit in nearly all GW interferometers) and so needs to be explored carefully.

Output Mode-Cleaner Future interferometers use high finesse mode cleaning cavities to prepare the input laser beam for use in the interferometer and to ensure that the output photodetectors sense only the interferometer's fundamental spatial mode.

The DC sensing noise of the OMC observed in eLIGO is just barely compatible with aLIGO displacement noise. The 1/f behavior of the DC sensing noise starts rolling up below about 40 Hz, fortunately the requirement does the same. For future detectors, this will have to be reduce by $\sim$1 order of magnitude.

The mode matching between the interferometer and the OMC is particularly critical for future interferometers in which loses will be critical, as discussed in the next section. Output

mode matching presents a particular difficulty as it varies with the interferometer thermal state. The eLIGO interferometers saw numbers as bad as 65% matching, (e.g., 35% signal and squeezed light loss). Current research explores the use of deformable mirrors for adaptive mode matching, together with "Bull's Eye" wavefront sensing for measurement [21].

Squeezing Injection of squeezed vacuum from the dark port improves the shot noise level of the interferometer. The recent development of GEO600 with the squeezer demonstrated clear improvement of shot noise level by 3.5 dB [11]. Similar performance was demonstrated at the LIGO Hanford site with the H1 interferometer before it was dismantled for aLIGO installation [9]. Every 3 dB of squeezing is equivalent to a factor of 2 in power. In this sense, the squeezing injection can be considered to be risk mitigation for high power issues.

The trade-off of using squeezing injection are: light scattered back from the squeezed light source which can threaten the interferometer sensitivity in the 50-300 Hz region, increased radiation pressure noise which may decrease sensitivity below 50 Hz (mitigated by filter cavities), the technical complication of additional control systems. Furthermore, the use of squeezed light requires a very low loss readout chain for the gravitational-wave signal path.

Optical loss in the squeezer path into the interferometer, and in readout chain which carries the GW signal and squeezed light to the detection photo-diodes, limit attainable reduction of shot noise. For example, a total loss of 25% limits the reduction of the shot noise attainable via injection of squeezed light to 6 dB (equivalent to a factor of 4 power increase). In all tests to-date (LIGO H1 and GEO600), the dominant loss has been due to imperfect mode-matching of the squeezed light source to the interferometer and output mode-cleaner.

Another significant loss results from the multitude of Faraday isolators placed between the squeezer and the main interferometer (see also Section 7.4.2). The need for multiple isolators stems from the need to prevent light from being scattered off the squeezed light source and returning to the interferometer. Thus, in addition to reducing the loss in the isolators, the needed isolation can be decreased by decreasing the scattering of the squeezed light source and by decreasing its motion at frequencies relevant to gravitational-wave detection (e.g., by putting the squeezer's optical parametric oscillator, or OPO, on an isolated platform in vacuum). Resolving these issues will open the door for extracting the usefulness from further enhanced squeezing factors.

3.2.2 Alignment Sensing and Control

DC alignment sensing The alignment sensing and control subsystems simultaneously control two degrees of freedom for each optic in the interferometer. Advanced LIGO will employ DC sensing to detect the arm cavity and recycling cavity positions. Future improvements will be aimed at lowering the 1/f noise in the photodetectors, increasing the number of pixels, and combining position and length sensing in a single photodetector.

At some readout ports, the photodetectors are constrained by a combination of low light levels, high static RF signals, and small signals. To further complicate matters, the detectors must simultaneously measure multiple RF sidebands. Future research includes Monte-Carlo based RF circuit optimization, direct RF signal subtraction, and multi-pixel sensors with

integrated readout chips.

Sidles-Sigg instability High circulating power in a kilometer-scale Fabry-Perot cavity can lead to an alignment instability in which a radiation pressure driven anti-spring overcomes the mechanical restoring force of the cavity's suspended optics (Sidles-Sigg instability) [22]. The Advanced LIGO interferometers were designed to avoid instability, but this is still a potential threat for the 3G/4G detectors. Essentially, higher power leads to greater instability which can only be suppressed with high-bandwidth active alignment control. As the bandwidth of the ASC loops approaches the gravitational-wave band of the detector, noise from the alignment control signals is introduced into the detection band and can spoil the interferometer sensitivity. The investigations to mitigate this instability should be carried out in both practical and innovative aspects: reduction of the control noise level of the ASC system and exploration of any new scheme to directly suppress the instability (e.g., optical trapping of alignment degrees of freedom).

Towards ASC of 3G/4G detectors As the optical system incorporates more components, the Alignment Control System gets increasingly complicated.

Already in current interferometers, we will be required to develop new techniques to control the alignment of the OMC [23], the squeezed light source, and the filter cavities, in addition to the already complicated ASC of the main interferometer.

The higher power operation of the interferometer in future detectors will involve coupling of the higher order modes into the field content at the dark port. This coupling will depend on the angular motion of the mirrors and will make the ASC requirements more stringent. To address the issue, deep investigation of the interferometer behavior with simulation is required in the design phase.

Actually, the control noise of the ASC system has consistently been one of the main limiting technical noises in the low frequency band for all interferometric gravitational wave detectors. As the band of gravitational-wave detection moves down, and the bandwidth of alignment control increases, both for suppressing higher-order modes and optical instability, the ASC problem becomes increasingly difficult. We will eventually reach the noise limit of the conventional DC/RF readout schemes and be forced to develop a novel angular readout system, or other means of stabilizing interferometer alignment which do not require readout.

3.2.3 Thermal aberration sensing and control

Mitigation It will be necessary to apply thermal compensation methods to stabilize the recycling cavities, due to thermal lensing in the input mirror substrates, and to maintain the radii of curvature of the test masses against thermo-elastic distortion effects resulting from circulating light absorbed in the mirror coatings. Both bulk and spatially-resolved compensation will be required [24].

One method to maintain a uniform temperature profile is by coating the barrel of the optic with a thin layer (a few microns) of a metal, or other thermal conductor, with high IR emissivity (e.g., gold). This technique is planned for the Advanced LIGO compensation

plates, and it may be possible to expand it to other important optics, possibly including the test masses. Coating the barrel of optics has implications for other aspects of the design including thermal noise, charge mitigation, and parametric instabilities [25].

Another method for maintaining thermal uniformity is a scanning (or, more generally, a directed-beam) thermal compensation system that can vary the compensation profile in real time. Such systems can, in principal, offer precise thermal compensation, but come at the cost of additional control systems and related noises [26]. This will require research on carbon dioxide lasers, to reduce noise and possibly boost power, and on low-noise sensing and actuation. A variety of techniques for beam direction (galvo mirrors, crossed AOMs, MEMs) will need to be investigated.

Local radiant heaters are used in interferometers to provide bulk curvature corrections to mirrors without injecting displacement noise (e.g., the aLIGO ring-heaters). These must have a uniform heating pattern at the mirror to minimize astigmatism. Future work on radiant heaters will improve the heaters' radiant uniformity and introduce tailored non-uniformities to account for non-axisymmetric features of the interferometer optics. Other future research would make the heaters more physically robust, and minimize their electrostatic interaction with the test masses [27].

Thermal aberrations can be corrected not only by adding heat to the mirror to flatten the heat pattern caused by absorbed interferometer light, but also by directly removing the heat from the absorbed interferometer light itself, through radiative cooling to a nearby cold surface. Such a technique has been proven in principle but not developed into a useful technique for high power interferometry.

Wavefront modeling The development of realistic models of the performance of the interferometers is also crucial to achieving the performance goals of Advanced LIGO and its upgrades. FFT-based simulation tools are currently used for setting requirements optical surfaces, coatings, apertures, etc., as well as for for investigating thermal effects [28]. Although FFT-based modeling is in principle more powerful than modal models based on sets of Hermite- or Laguerre-Gauss modes, the modal model codes are faster, and the results are easier to understand. Consequently, it is important to continue the development and support of modal models capable of including thermal loading in interferometers.

Wavefront diagnostics Each of the mirrors in Advanced LIGO will have slightly different absorption characteristics and therefore will react differently when subjected to laser powers projected for Advanced LIGO (see T1100250-v2 [29]) It is useful to develop methods that allow for remote monitoring of the condition of a test mass or beam splitters using optical wavefront sensing methods. On-axis and off-axis Hartmann wavefront sensing have been developed for measuring the absorption-induced wavefront distortion in the test masses and beam splitter. The measured noise limited sensitivity of the Hartmann sensor itself is $\lambda/15{,}000$, and experiments have measured wavefront changes smaller than $\lambda/3000$ [30]. When applied to off-axis tomographic measurements, the current measured accuracy is $\lambda/120$, limited by factors other than the Hartmann sensor itself [31]. Further research is aimed at improving this performance. Avenues for improvement include simple and stable injection

schemes for Hartmann probe beams into working interferometers and incoherent probe beam sources with high power and low noise.

In addition to the Hartmann style sensors, we may use phase cameras (essentially multi-pixel RF Wavefront Sensors). These could be used to implement real-time wavefront correction. Primitive phase cameras have been used in iLIGO and iVirgo, but there were problems due to the scanning induced backscatter. Future phase cameras should allow for wavefront sensing of individual sidebands simultaneously without any moving parts.

3.2.4 General Control Issues

Fast data acquisition Currently the data acquisition rate of LIGO CDS is limited to a sampling rate of typically 16 kHz to 64 kHz. For some specific purposes high speed data acquisition will add convenience for comissioning. In the first phase this can be a ring buffer to store the data for (for example) ∼10 min to catch lock acquisition/lost events or fast transient noise of laser intensity/frequency.

Adaptive Noise Cancellation Adaptive noise cancellation techniques will be widely used in the Advanced LIGO interferometers and the future detectors. Basically, noise cancellation based on Wiener filters eliminates the noise in a target signal correlated to witness channels.

This family of techniques has a wide area of application such as seismic noise reduction, Newtonian noise subtraction, and magnetic/acoustic noise cancellation. Residual coupling of auxiliary LSC degrees of freedom to the main GW signals, which presented a sensitivity limit in the initial and Enhanced LIGO interferometers, may also be reduced by adaptive noise cancellation.

Up to now, a basic scheme with linear adaptive noise cancellation is being tested on the CDS system at the 40 m prototype [32]. This technique has also been applied to seismic noise subtraction during Enhanced LIGO [32]. In the future, in addition to the linear noise subtraction, subtraction of bilinear noise should also be investigated as it may prove useful in removing a variety of noise sources from the GW signal.

Automatic Optimization As the interferometer configuration gets more complicated, the difficulty of optimizing system parameters increases significantly. For example, we have to deal with the different range and frequency dependence of the multiple sensors and actuators at each stage of the suspension and isolation system, as opposed to the single pendulum suspensions use in iLIGO. Optimization of hierarchical control will depend on the noise level of the interferometer, which may change in time, making the traditional approach of by-hand optimization untenable.

Many of the optimization procedures in the future interferometers will need to be automated within the interferometer control system, and some may need to be dynamically adjusted. This approach should be applied in Advanced LIGO and expanded in the future detectors with continuous effort toward automatic optimization or “machine learning”. New involvement and collaboration with researchers of this particular field is encouraged.

Modern control Along with adaptive noise cancellation and automatic optimization, other applications of modern control theory to interferometer gravitational wave detectors should be considered.

Feedback control of interferometer gravitational wave detectors has mostly relied on the classical control theory up to now. The classical control theory, developed in the 1950s, is still effective as one of the approaches for control applications. However, control theory has continued over the intervening 60 years and significant improvements to the classical approach are available.

Modern control theory, which is also already 30∼40 years old, offers various possibilities to improve the interferometer control. First of all, the modern control theory includes all of the concepts of classical control. Therefore we can realize what we could do with the classical control. Secondly, modern control has high compatibility with digital control with multiple inputs and outputs as it is based on linear algebra. Thirdly, optimization of the control is theoretically supported. This can help us to reduce use of knowledge and intuition based on extensive past experiences in the design of the control system.

Furthermore, the model of the control object can be built in the controller in the modern control theory. This model, called estimator, is quite similar to the idea of the simulated plant (discussed below). It may be straightforward to realize the simulated plant and the estimator at the same time in the modern control approach. In addition to the modern control theory, extensive application of adaptive control is going to be attempted. Adaptive feedforward method will be employed to the entire interferometer control where the signal cancellation is applicable. Also, the interferometer control bandwidth can be adaptively changed accordingly with noise level of the environment. This can be realized by the modern control and automated optimization of control.

An example of this type of application is the modal-damping work done on the aLIGO suspensions at MIT [33]. The challenge faced in suspension control, and also elsewhere in aLIGO and similar detectors, is that of combining multiple sensor signals with a variety of noise levels and response functions to provide a controller which is effective in the control band while minimizing noise in the gravitational-wave detection band. The currently employed approach of classical controls requires experts to spend considerable time diagonalizing the system and constructing near-optimal (really just "good enough") filters for each degree of freedom of the system.

These technologies can be first investigated by simulation and then applied to prototype facilities. Once effectiveness of these advanced control is proved, it can be implemented to the aLIGO interferometers in order to accelerate the interferometer optimization.

Virtual Interferometer The flexibility of the Advanced LIGO CDS system allows, for the first time, the beginnings of the "Virtual Interferometer".

Basically, the future detectors should have a computer facility which enables us to login and run the control system for the test of operating and diagnosing tests without having the actual detector equipment. At the beginning this can only be a tool for the commissioning and development, as seen in the "Simulated Plant" concept being tested at the 40m proto-

type [34], but eventually can provide various realtime test of the interferometer behavior by cooperative interaction with the other simulation tools. This should include the test of the online data production for mock data challenges.

3.2.5 Interferometer modeling / simulations

Interferometric gravitational-wave detectors are sufficiently complicated optical systems that detailed modeling is required for design and performance studies. At present, a variety of simulation tools exist for addressing the various problems encountered in interferometric GW detectors.

As mentioned previously in section 3.2.3, simulations which use the FFT for propagating paraxial beams can be used to make detailed predictions about the impact of optical phase errors (surface roughness, phase distortions, etc.) and finite aperture sizes. FFT simulations are, however, too slow to simulation interferometer dynamics, and are therefore only used to find steady-state solutions.

For understanding interferometer dynamics over a wide range of conditions which don't allow for linearization (e.g., not only at the operating point), time-domain simulation is the most appropriate tool. This type of simulation is important for lock acquisition studies and existing tools fill the need for most optical configurations [35]. However, like FFT simulations, despite considerable optimization effort time-domain simulations are slow and able to simulation only the lowest transverse-spatial modes.

For control system development, where we can assume that we are at a stable operating point and linearize around that point, frequency domain simulations prove an invaluable tool. With the development of advanced detectors with more than 100 kW of power circulating in the arm cavities, radiation pressure effects have come to play an important role in interferometer dynamics (both for LSC and ASC, as mentioned above). Advanced LIGO control system development has depended on the Optickle simulation engine, which has been packaged for LSC design in Looptickle and later Lentickle, and for ASC design as Pickle.

In addition to control system development, frequency domain simulation tools like Optickle, are also used to compute limitations to interferometer sensitivity due to fundamental noise sources (e.g., quantum noise) and technical noises (e.g., auxiliary length degree of freedom control noise). Expansion of the current simulation code to include the non-linear optics used in squeezed light sources will allow for more complete modeling of advanced and future detectors.

The configuration level simulation, discussed in section 3.1, operates at a higher level in that the response of a given optical configuration is symbolically computed and parameterized [36]. These symbolic computations can be compared with the more detailed numerical results given by frequency domain codes. While inappropriate for detailed simulation of the optical plant, this approach is very effective for optimizing plant parameters and even selecting among a variety of optical configurations. Further development of the GWINC configuration level simulation to accommodate the variety of optical configurations under consideration for future detectors will aid in downselection and optimization.

To date these simulations have focused on the core of the interferometer, the optics, and

have largely neglected the surrounding mechanical systems. A missing piece in detector simulation is a comprehensive mechanical simulation tool for the vibration isolation and suspension design which includes the capability to handle a variety of mechanical systems and the ability to compute of thermal noise for any given configuration.

In addition development of the various of simulation tools, future detector design and study will benefit greatly from a dedicated effort to organize and document these tools. At present, each simulation tool has a different user interface and while there are many similarities in the parameters required, the format in which these parameters are presented differs from one tool to the next. This divergence of parameter formats and lack of high level organization in the simulation effort inevitably slows progress toward the development of future detectors.

Modelling thermal distortions and radiation pressure during commissioning Advanced LIGO and future detectors will operate at higher light power so that thermal distortions of the optics and the change of the mirror suspension response due to radiation pressure will play a dominant role. In particular the transfer functions of any displacement signal into the detection ports will show the optical spring effects and higher-order mode resonances. Thus to model noise coupling of auxiliary degrees of freedom or auxiliary optics system into the gravitational wave channel we require models that include thermal effects and radiation pressure at the same time. For the rapid development of the control systems and noise mitigation strategies during the detector commissioning it is desirable that such simulation software is a fast, flexible and easy to use tool. The frequency domain simulation FINESSE [37] has been used extensively by the commissioning teams of the first detectors generation, which also provided a thorough validation of the code, and is now used for the commissioning for Advanced LIGO. FINESSE is a frequency domain code and uses Hermite-Gauss expansion to describe the geometric properties of optical beams. It has been extended to allow the use of measured mirror surface maps which was successfully applied during the implementation of the Virgo thermal compensation system. Thus the software is able to fully describe thermal deformations and their effects. A general framework for implementing radiation pressure effects into the frequency domain models such as FINESSE has been described by Corbitt [38]. An effort is underway to implement this framework within FINESSE. This will provide the community with a frequency domain simulation tool that can model thermal and radiation pressure effects at the same time. FINESSE has been extensively tested over the last 10 years, with dedicate campaigns to validate the results against experimental data and independent numerical tools such as FFT based codes. In order to continue to provide a reliable simulation solution to the commissioning teams it will be necessary to perform a dedicated validation of the radiation pressure implementation including higher-order modes, ideally performed by a team included commissioning and simulation experts and especially scientists with a background in quantum optics calculations.

4 Quantum Noise Limits

The Quantum Noise Working Group (QNWG) covers research involving theoretical studies of squeezing/QND topologies; development of quantum radiation pressure dominated and QND apparatus; Experiments to prototype QND: filter cavities, variational readout, etc.; and development of squeezed light sources.

4.1 Introduction

The 2nd generation detectors, which are now being assembled (Advanced LIGO, Advanced Virgo, and KAGRA), are expected to be limited by quantum noise over nearly the entire GW band (10 - 10000 Hz). By quantum noise, we refer to the ground state fluctuations of the EM field which beat with the laser field to produce shot noise and radiation pressure noise.

To upgrade those detectors it is essential to reduce this quantum noise. There are several configurations that have been proposed within the community [39, 40]. They generally fall into the following four categories:

- injection of squeezed light with a phase shifting filter cavity;
- frequency dependent readout quadrature (a.k.a. variational readout);
- using coherent feedback to modify the dynamics of the test masses, e. g., the optical spring effect associated with the detuned signal recycling;
- injecting multiple carrier fields.

They all require, to a certain extent, introducing additional optics and increasing the complexity of the detectors. More specifically, the following configurations that are compatible to the topology of the aLIGO and can therefore be possible candidates for near-term upgrade:

1. *frequency dependent squeeze angle*—injecting squeezed light with an optical filter cavity [41];
2. *frequency dependent phase readout*—filtering the output with a cavity to measure appropriate quadratures at different frequencies [41, 42];
3. *speed-meter configurations*—measuring quantity that is proportional to the test mass speed at low frequencies [43, 44, 45, 46];
4. *long signal recycling cavity*—elongating the recycling cavity to have a frequency-dependent response in the signal-recycling cavity;
5. *dual-carrier scheme*—introducing an additional carrier light to gain another readout channel [47];

6. *local-readout scheme*—being a special case of the dual-carrier scheme in which the additional carrier is anti-resonant in the arm cavity and resonant in the power-recycling cavity [48].

These configurations are not excluded from each other and can be combined in different ways. In particular, we not only consider them standalone, but also combine (i) and (ii)—input and output filter cavities—with other schemes.

4.2 Optical Topologies

In this section, we will briefly describe the optical topologies that we mentioned in the introduction. The quantum noise spectral density of these topologies are evaluated by using the standard input-output formalism.

4.2.1 Frequency-dependent squeezing angle (input filtering)

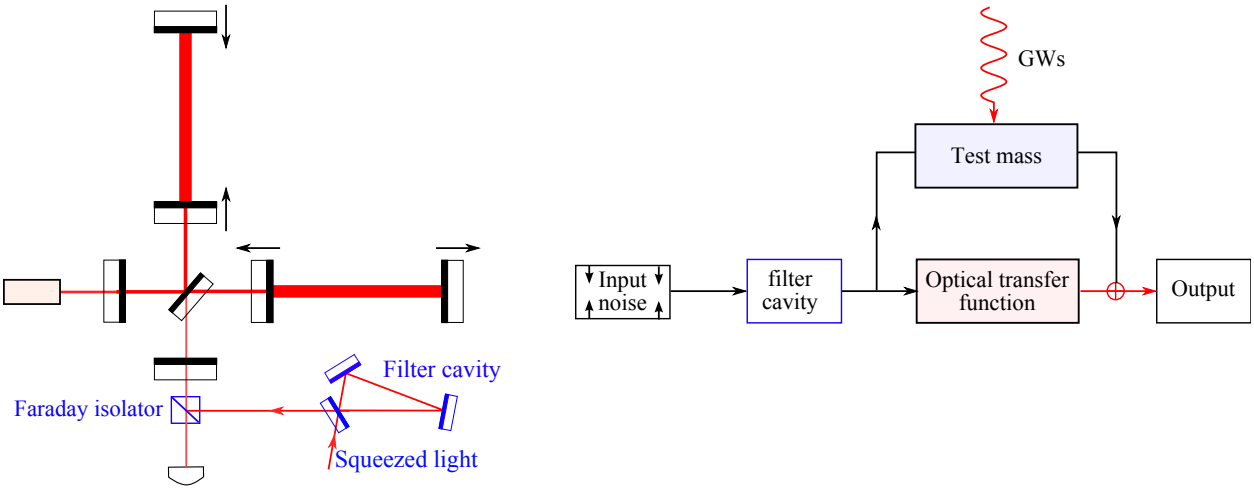

Figure 9: Schematics showing the frequency-dependent squeezing scheme (left) and its associated flow chart (right).

The first scheme is frequency-dependent squeezing. As shown schematically in Fig. 9, it utilizes an optical cavity to rotate the amplitude and phase quadratures, or equivalently the squeezing angle, in a frequency-dependent way. If the parameters of the filter cavity is appropriately specified, one can rotate the squeezing angle such that the quantum noise spectrum is reduced by an overall factor that is equal to squeezing factor.

For illustration, in Fig. 10, we show the resulting noise spectrum in *the ideal case without optical loss*. As we can see, the squeezing angle rotates in such a way that at low frequencies the fluctuation in the amplitude quadrature is squeezed—thus reducing the radiation-pressure noise, while at high frequencies the phase quadrature is squeezed—thus reducing the shot noise. In order to achieve the desired rotation of squeezing angle, the filter cavity needs to have a bandwidth that is comparable to the detection bandwidth—this indicates a high-finesse cavity is necessary if the cavity length is short. The specification for the filter cavity can almost be analytically calculated by using the method outlined in [45].

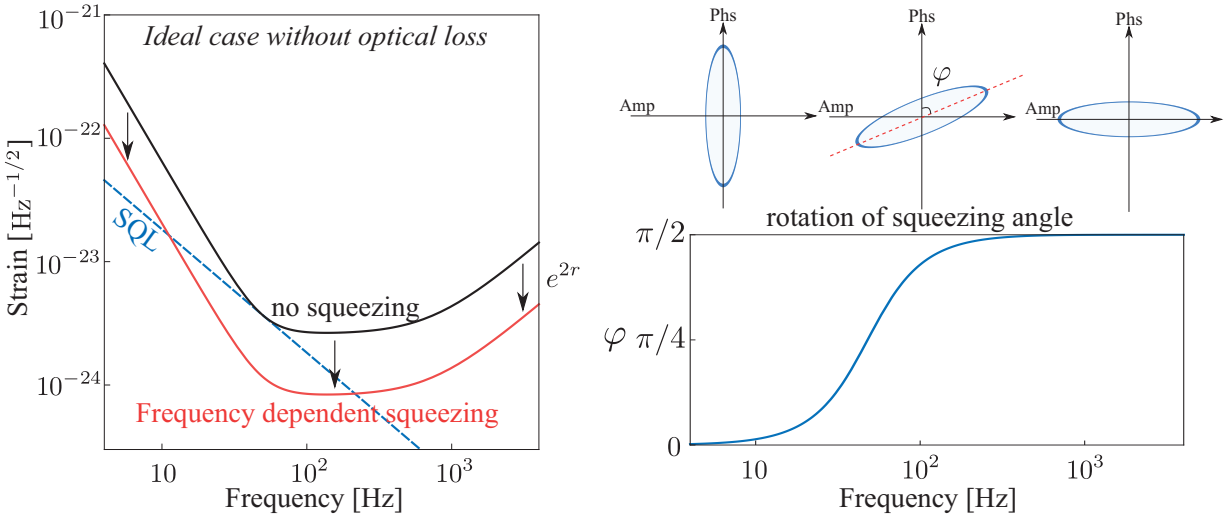

Figure 10: Noise spectrum for frequency-dependent squeezing (left) and rotation of the squeezing angle (right).

In reality, the optical loss will affect the performance of input filtering, as shown in the left panel of Fig. 11. Additionally, parameters of the filter cavity, in particular, the transmissivity of the mirrors and the detuning, cannot be exactly set to the optimal value, and their variation will influence the sensitivity in a similar manner to the optical loss, as illustrated in the right panel of Fig. 11.

4.2.2 Frequency dependent readout phase (output filtering)

A close related counterpart to the input filtering is the variational readout, and as shown schematically in Fig. 12, it uses an optical cavity to filter the detector output which allows one to measure different optical quadratures at different frequencies. The filter cavity has the same functionality as in the case of the frequency-dependent squeezing—the only difference is that it rotates the optical quadratures of the output instead of input. In the ideal case, this scheme can coherently cancel the radiation-pressure noise at low-frequencies, and give rise to a shot-noise only sensitivity [41]. In Fig. 13, we show the resulting noise spectrum in the ideal lossless case. In reality, due to the presence of optical loss and parameter variation of the filter cavity, such a cancelation cannot be perfect, as illustrated in Fig. 14.

4.2.3 Long signal-recycling cavity

In this subsection, we will discuss the long signal-recycling cavity scheme. As shown in Fig. 15, the signal recycling mirror is moved further away from the beam splitter compared with the aLIGO configuration. In the usual case when the beam splitter and the signal-recycling mirror are close to each other, the signal-recycling cavity is relatively short (order of 10 meters) and one can ignore the phase shift difference between different sidebands with frequency Ω ranging from 10 - 10000 Hz, namely $\Omega L_{\rm sr}/c \approx 0$ with $L_{\rm sr}$ being the signal-recycling cavity length. We can therefore treat the signal-recycling cavity as an effective

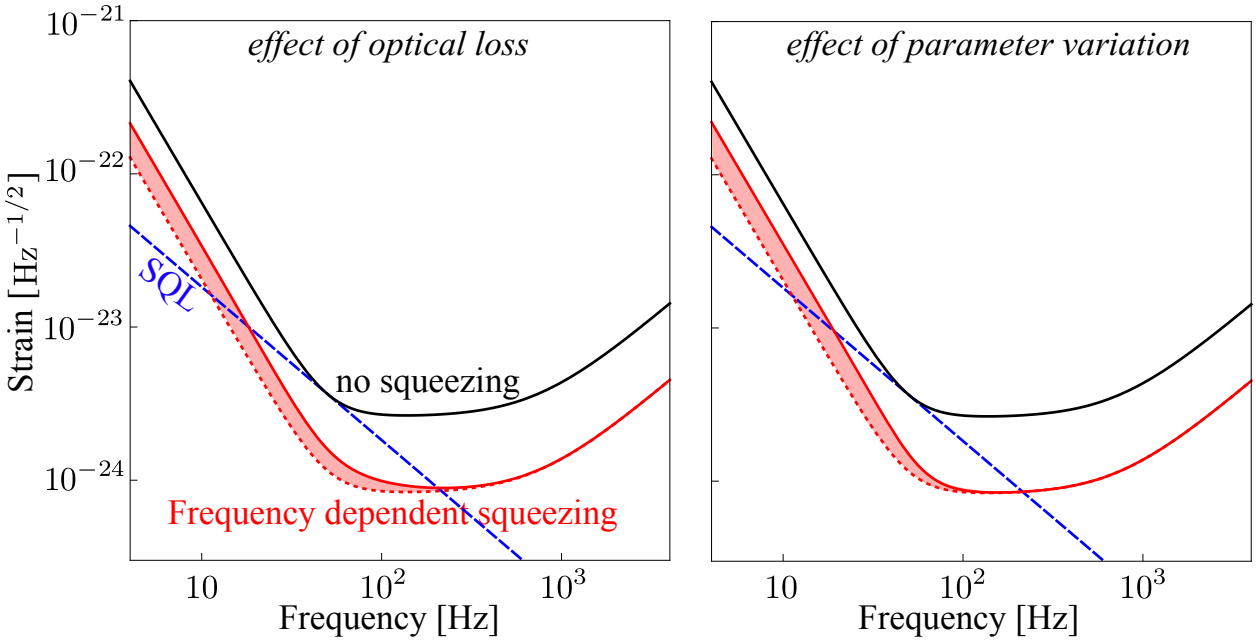

Figure 11: The effect of optical loss (left) and the parameter variation of the filter cavity (right) for input filtering. The shaded regions illustrate the degradation in sensitivity. Here we have assumed the total optical loss of 20% (round-trip loss multiplied by the number of bounces inside the cavity) and parameter variations of 10%.

compound mirror with complex transmissivity and reflectivity, which is the approach applied in Ref. [49]. With a long signal-recycling cavity, however, $\Omega L_{\rm sr}/c$ is not negligible and different sidebands pick up different phase shifts. After taking into account this fact, one can then apply the standard procedure to derive the input-output relation for this scheme. The final expression is quite lengthy and not illuminating, and we will not show it here. One can evaluate its noise spectrum numerically.

4.2.4 Speed meter

Here we describe the speed meter configuration. The motivation for it arises from the perspective of viewing the gravitational-wave detector as a quantum measurement device. Normally, we measure the test mass position at different times to infer the gravitational-wave signal. However, position is not a conserved dynamical quantity of the test mass which is treated as a free mass in the theoretical model. According to the quantum measurement theory [50], such a measurement process will inevitably introduce additional back action and perturb the test mass motion. In the context here, the back action is the radiation-pressure noise. In order to evade the back action, one needs to measure the conserved dynamical quantity of the test mass—the momentum or the energy. Since the momentum is proportional to the speed, that is why speed meter is ideal for measuring gravitational wave with no radiation-pressure noise [43].

There are several speed-meter configurations, e.g., the Sagnac interferometer [46] and a recent proposed scheme by using different polarizations [51]. In Fig. 16, we show one particular variant of them, which is proposed in Ref. [45]. It uses a sloshing cavity. We can gain a

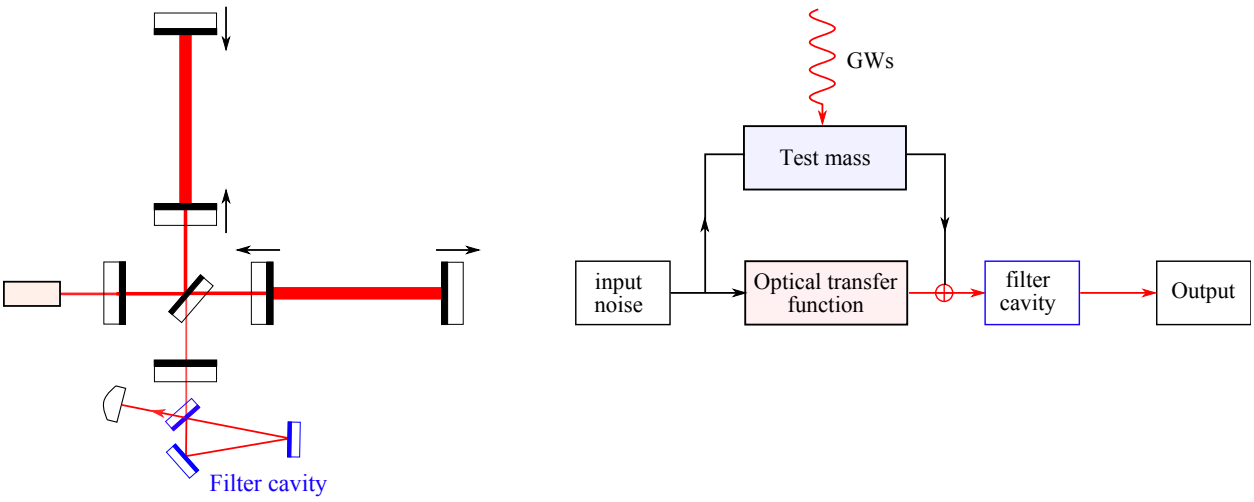

Figure 12: Schematics showing the frequency dependent (or variational) readout scheme (left) and its associated flow chart (right).

qualitative understanding of how such a scheme allows us to measure the speed of the test mass. Basically, the information of test mass position at an early moment is stored in the sloshing cavity, and it coherently superposes (but with a minus sign due to the phase shift in the tuned cavity) with the output of the interferometer which contains the current test mass position. The sloshing happens at a frequency that is comparable to the detection frequency, and the superposed output is, therefore, equal to the derivative of the test-mass position, i.e., the speed.

This corresponding noise spectrum is shown in Fig. 17. The low-frequency spectrum has the same slope as the standard quantum limit, which is a unique feature of speed meter. When the optical is high enough, we can surpass the standard quantum limit.

One important characteristic frequency for this type of speed meter is the sloshing frequency ω_s, and it is defined as

$$\omega_s = \frac{c}{2}\sqrt{\frac{T_s}{L\,L_s}}, \tag{1}$$

where T_s is the power transmissivity for the front mirror of the sloshing cavity and L_s is the cavity length. To achieve a speed response in the detection band, this sloshing frequency needs to be around 100Hz. For a 4km arm cavity—$L = 4000$ and 100m sloshing cavity—$L_s = 100$, it requires the transmittance of the sloshing mirror to be

$$T_s \approx 30\,\text{ppm}. \tag{2}$$

This puts a rather tight constraint on the optical loss of the sloshing cavity. To release such a constraint on the optical loss, we can use the fact that ω_s only depends on the ratio between the transmissivity of the sloshing mirror and the cavity length and we can therefore increase the cavity length.

In addition, it seems that no filter cavity is needed for speed meter configuration, as the radiation pressure noise at low frequencies is cancelled. However, such a cancellation is achieved by choosing the homodyne detection angle that is deviated from the phase quadrature, therefore decreasing sensitivity at high frequencies. The deviation is proportional to

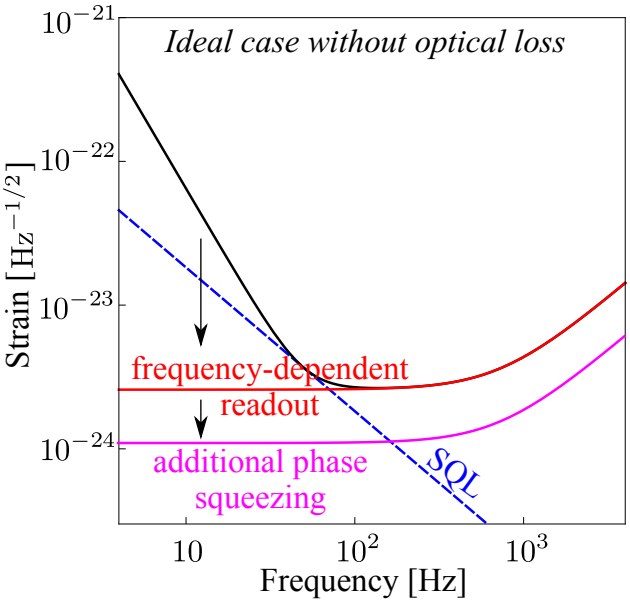

Figure 13: The noise spectrum for the frequency-dependent readout scheme.

the optical power. With frequency-dependent squeezing, we can reduce the effective optical power seen by the test mass, which allows us to measure the quadrature closer to the phase one, and thus enhance the high-frequency sensitivity. Similarly, the frequency dependent readout allows us to cancel the low-frequency radiation pressure noise without sacrificing the high-frequency sensitivity by rotating the readout quadrature to the phase one at high frequencies.

4.2.5 Multiple-Carrier Fields

In this section, we will introduce the multiple carrier light scheme, and in particular, we will focus on the dual-carrier case as shown schematically in Fig. 18. The additional carrier light provides us another readout channel. As these two carriers can have a very large frequency separation, we can in principle design the optics in such a way that they have different optical power and see different detune and bandwidth. In addition, they can be independently measured at the output. This allows us to gain a lot flexibilities and almost provides multiple interferometers but within the same set of optics.

These two optical fields are not completely independent, and they are coupled to each other as both act on the test masses via radiation pressure and sense the test-mass motion (shown pictorially by the flow chart in Fig. 18). Since the frequency separation between them is much lager than the detection band, these two fields can be measured independently. To achieve the optimal sensitivity, we need to combine them with the optimal filters. In [47], the authors have shown the procedure for obtaining the optimal sensitivity and the associated optimal filters in the general case with multiple carriers.

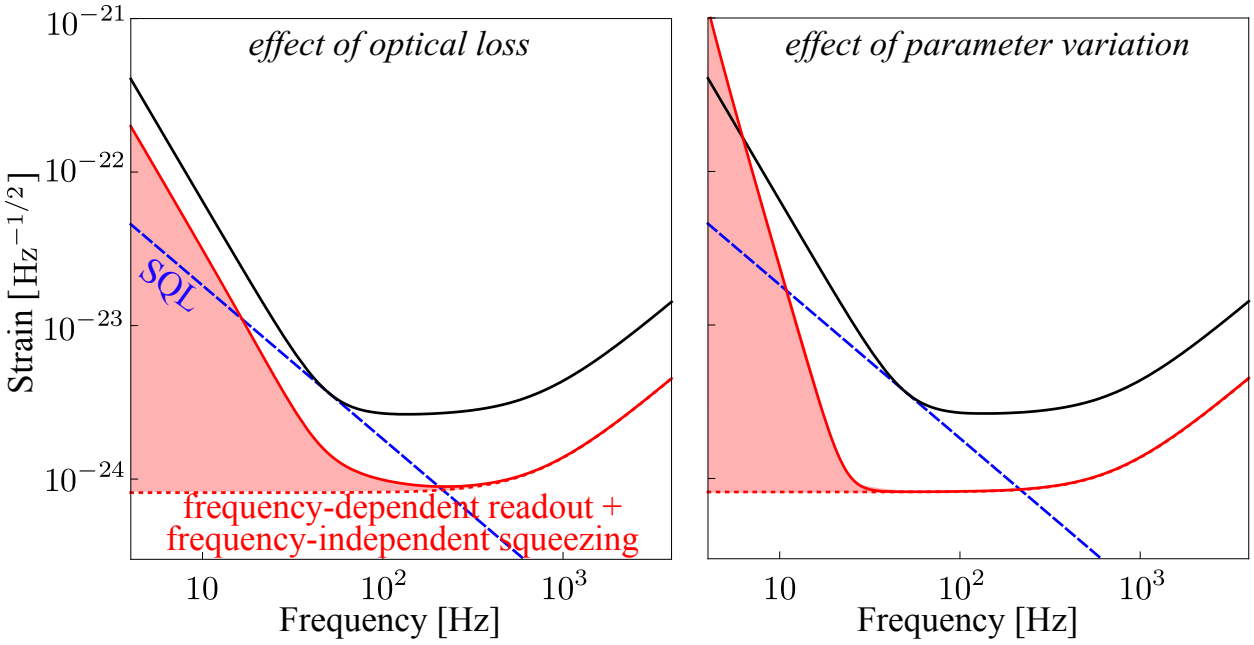

Figure 14: The effect of optical loss (left) and parameter variation of the filter cavity (right) for frequency-dependent readout (output filtering). Similar to Fig. 11, we have used a total optical loss of 20%. In contrast, the parameter variation is chosen to be only 10^{-4} in order to produce reasonable sensitivity, as it is much more sensitive than input filtering.

4.2.6 Local Readout

In this subsection, we will discuss the local-readout scheme, as shown schematically in Fig. 19. It is actually a special case of the dual-carrier scheme mentioned in the pervious subsection—the second carrier light is only resonant in the power-recycling cavity and is anti-resonant in arm cavity (barely enters the arm cavity). Why we single this scheme out of the general dual-carrier scheme and give it a special name is more or less due to a historic reason. This scheme was first proposed in Ref. [48] and was motivated by trying to enhance the low-frequency sensitivity of a detuned signal-recycling interferometer, which is not as good as the tuned signal-recycling due to the optical-spring effect. The name—"local readout"—originates from the fact that the second carrier only measures the motion of the input test mass (ITM) which is *local* motion in the proper frame of the beam splitter and does not contain gravitational-wave signal. One might ask: "how can we recover the detector sensitivity if the second carrier measures something that does not contain the signal?" Interestingly, even though no signal is measured by the second carrier, it measures the radiation-pressure noise of ITM introduced by the first carrier which has a much higher optical power due to the amplification of the arm cavity, as shown schematically by the flow chart of Fig. 19. By combining the outputs of two carriers optimally, we can cancel some part of the radiation-pressure noise and enhance the sensitivity—the local-readout scheme can therefore be viewed as a noise-cancelation scheme. The cancelation efficiency is only limited by the radiation-pressure noise of the second carrier.

To evaluate the sensitivity for this scheme rigorously, one has to treat the input test mass (ITM) and end test mass (ETM) individually, instead of assuming a single reduced mass as

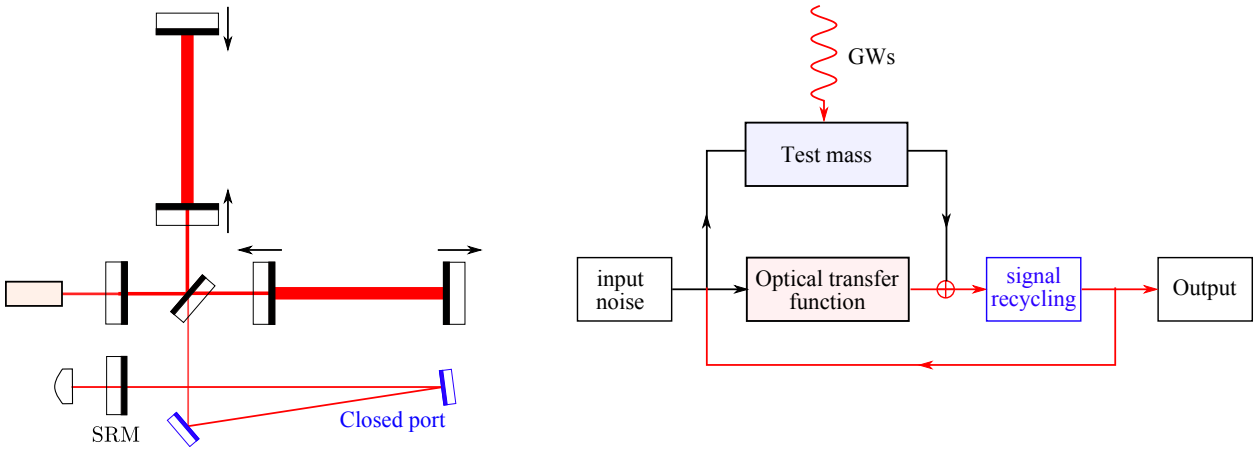

Figure 15: Schematics showing the long signal-recycling cavity scheme (left) and its associated flow chart (right). The signal-recycling mirror coherently reflects back the signal, forming a feedback loop as indicated in the flow chart.

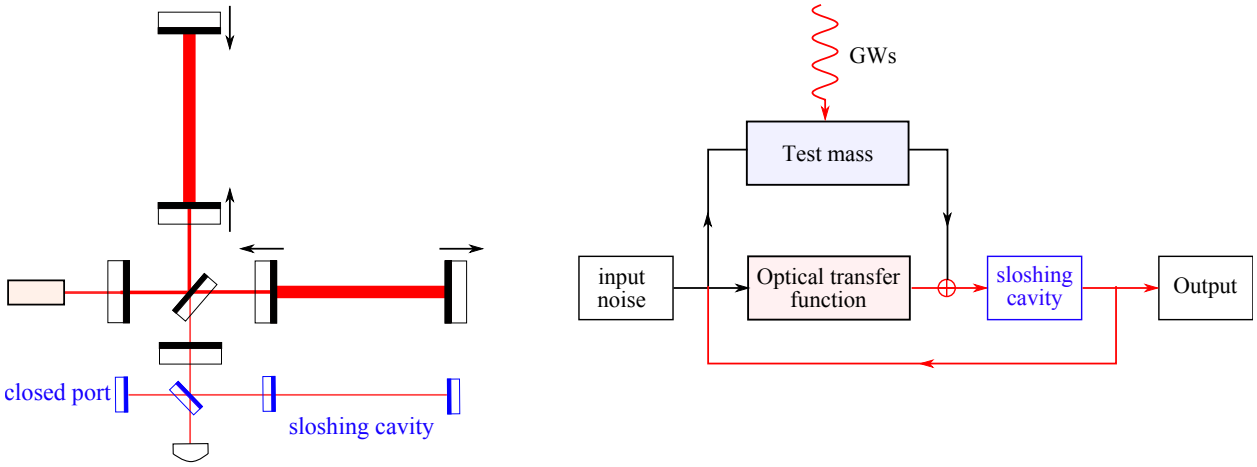

Figure 16: Schematics showing the speed-meter configuration (left) and its flow chart (right).

we usually do for those schemes mentioned earlier. One can refer to [48] for details.

4.3 Numerical Optimization and Comparison

To find out the possible candidate that is feasible for upgrading the sensitivity of aLIGO, we made a systematic comparison of those configurations mentioned in the previous section, and the results are reported in the LIGO document [52]. Here we will just show the main result and one can refer to the document for more detail.

The final optimization result critically depends on the cost function. In the literature, optimizations have been carried out by using a cost function that is source-oriented—trying to maximize the signal-to-noise ratio for particular astrophysical sources. Here we apply a rather different cost function that tries to maximize the *broadband* improvement over aLIGO. This follows the same philosophy of designing aLIGO which aims at a factor of 10 broadband

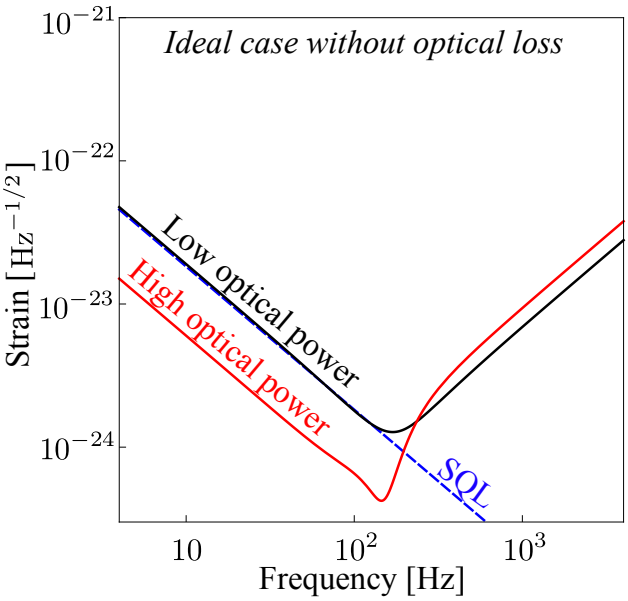

Figure 17: Plot showing the noise spectrum for the speed-meter configuration for two different optical powers.

improvement over initial LIGO.

For optimization, we also take into account the various classical noise sources (to be distinguished from the quantum noise). In particular, we consider Brownian thermal noise in the mirror suspensions [53, 54], seismic vibrations propagating to the mirror [55], terrestrial gravitational fluctuations [56, 57], and Brownian thermal fluctuations of the mirror (and mirror coating) surface [58, 59].

The results of the numerical optimization are shown in Figs. 20 and 21, where we plot the total noise spectra (the quantum noise + the classical noises) for different configurations with frequency dependent squeezing (input filtering) and frequency dependent readout (output filtering), respectively. In producing Fig. 20, we assume a moderate reduction in the thermal noise and the same mass and optical power as those for aLIGO. In producing Fig. 21, we assume a more optimistic reduction in the thermal noise, the mirror mass to be 150 kg and the maximum arm cavity power to be 3 MW.

As we can see, by adding just one filter cavity to the signal-recycled interferometer (aLIGO topology), we can already obtain a broadband improvement over aLIGO. Limited by thermal noise at low frequencies, the difference among these configurations is not very prominent. This leads us to the conclusion that adding one input filter cavity to aLIGO seems to be the most feasible approach for upgrading in the near term, due to its simplicity compared with other schemes. If the low-frequency thermal noise can be reduced in the future, the speed meter and the multiple-carrier scheme can provide significant low-frequency enhancement of the sensitivity. This extra enhancement will, for some low enough thermal noise, be enough to compensate for the extra complexity.

4.4 Time-Depdendent Interferometer Configurations

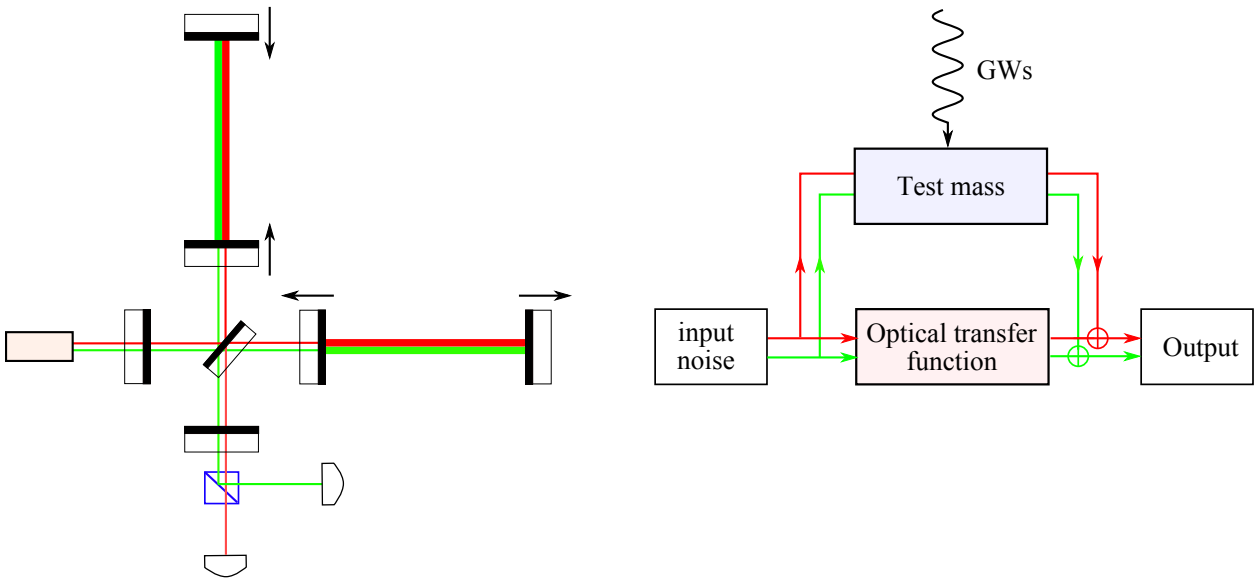

Figure 18: Schematics showing the dual-carrier scheme (left) and its flow chart (right).

4.4.1 Time allocations for steady-state operation with different configurations

LIGO aims at several distinct astrophysical populations. The above optimization works in general towards a baseline configuration that optimizes the overall sensitivity for all sources. However, if each particular population is targeted, one might obtain somewhat different optimizations. It would be interesting to ask: is it better to run the interferometer through a sequence of configurations, staying a certain fraction of the total observational time at each configuration, or to run the interferometer at a generic, "one-configuration-fits-all" mode.

The answer of course depends on how optimal one can gain for each particular source compared with the baseline, how much one loses for the other sources that are not optimized for — and how likely each particular source is present, in the first place.

As an example, compared with the baseline configuration, O, we have two alternative configurations A and B. Suppose for configuration A we have a relative sensitivity 1.5 for events of type a, but 1/1.5 for those of type b, while for configuration B, we have the opposite, 1/1.5 for a, but 1.5 for b. If we use A half the time and B half the time, assuming that the durations we keep our intereferometer running at each configuration is much longer than the durations of the signals of either type, the the mean event rate for both types of events can be estimated as 1.83 times the baseline event rate, a rather dramatic improvement — regardless of the intrinsic rates of a and b. If intrinsic rates for a and b could be estimated, we might further improve rate of detection — or bais towards the rarer type of events — by adjusting the fraction of time we assign to A and B.

This simple example teaches us that if sizable improvment of sensitivity is possible for a particular population, we might not want to keep a "one-configuration-fits-all" strategy, but instead should aggressively look for that type of sources by allocating preferences.

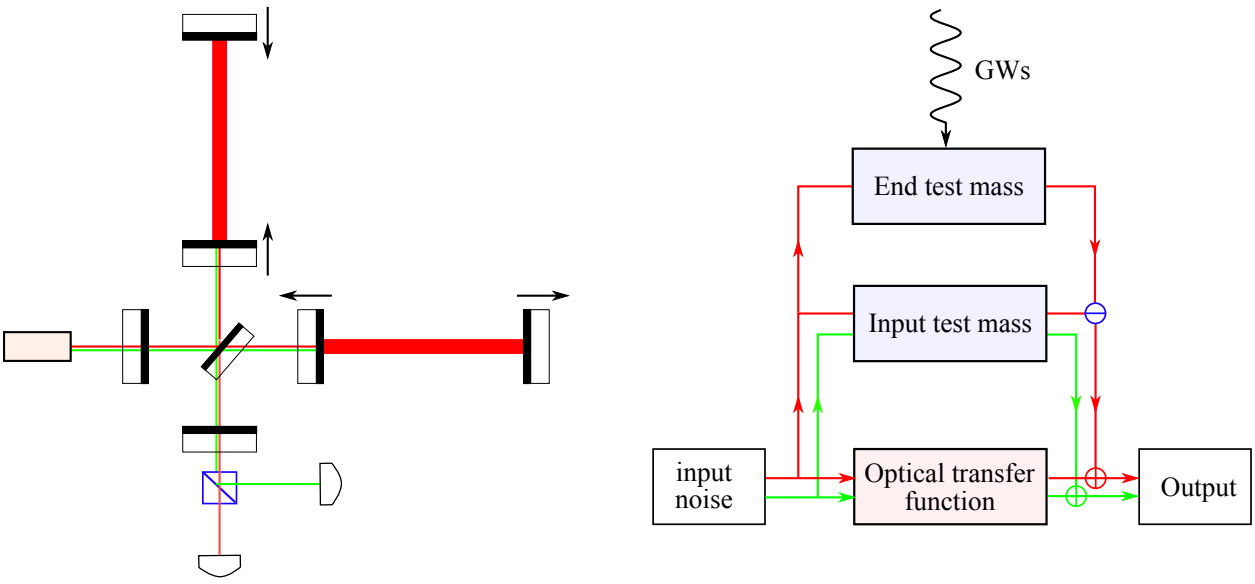

Figure 19: Diagram of the local-readout topology (left) and the resulting feedback loops (right).

4.4.2 Triggered switch of configurations

The interferometers may also switch between two configurations when triggered by the possible arrival of a particular signal. For example, if restricted to frequency-independent input squeezing, a trade-off is made between sensitivities at low and high frequencies by adjusting the angle of the squeezing ellipse.

Instead, it may be possible to set the low-frequency-enhanced configuration as the default configuration, which is most sensitive to the early stage of compact binary coalescence. If an event trigger is obtained from this configuration, the control system can promptly switch to the high-frequency-enhanced configuration to gather more statistics for the merger phase. Although this type of scheme makes sense in an intuitive, quasi-static sense, detailed modeling of the transient behavior of the interferometer is required to further estimate if this can be done in practice.

4.5 Other Configurations

Apart from these configurations that have been mentioned and compared in the previous sections, there are also other configurations that can also achieve lower quantum noise and need to be further considered both theoretically and experimentally. In this section, we list some that have been proposed by the GW community.

4.5.1 Time-dependent Interferometer Configurations

It may be interesting to consider time-dependent interferometer configurations. Here are several examples that show why this might be interesting.

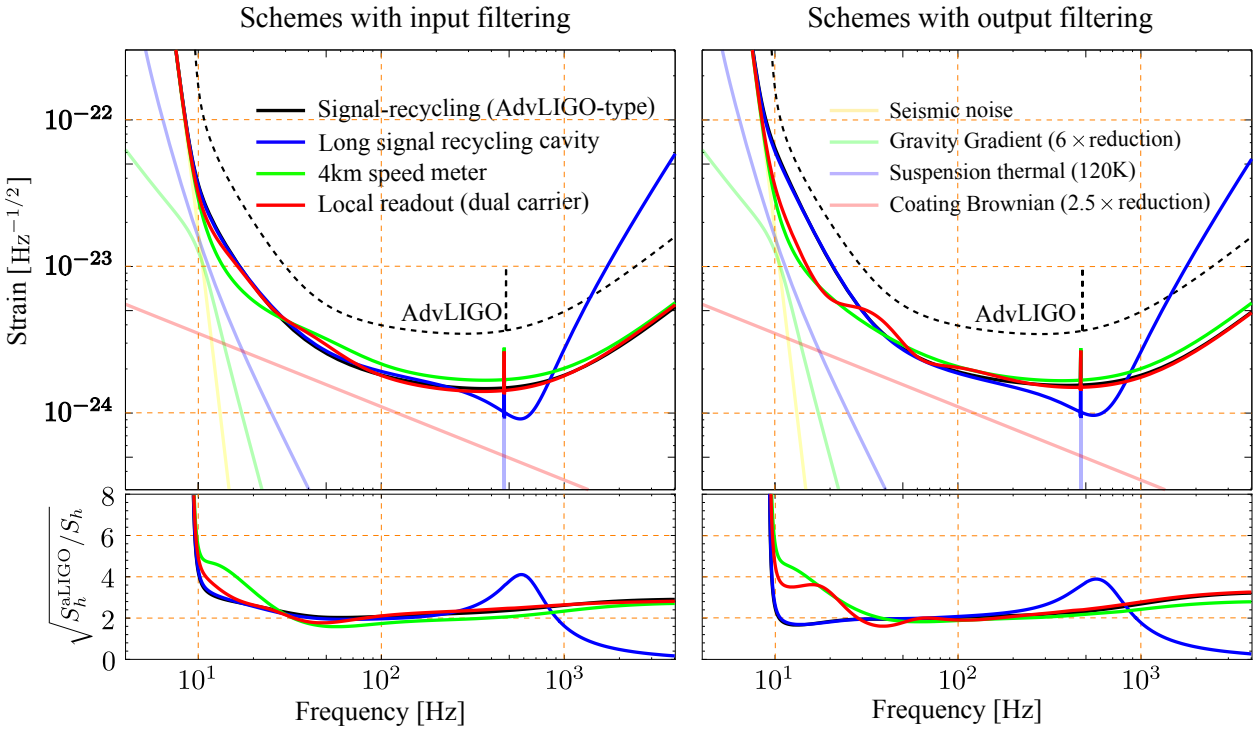

Figure 20: The optimized total noise spectrum for different schemes assuming a moderate improvement of the thermal noise compared with aLIGO baseline design. The lower panels show the linear strain sensitivity improvement over aLIGO.

4.5.2 Variable Reflectivity Signal Mirror

The signal recycling mirror can be replaced with a Fabry-Perot cavity. This tunable cavity will change the effective reflectivity of the signal mirror and allow for a tunable finesse for the signal cavity in addition to the usual signal cavity detuning phase. This can be realized either by an etalon, or by a Michelson interferometer, as has been demonstrated at the ANU [60]. This option is also naturally combined with the concept of a long signal recycling cavity.

4.5.3 Intracavity Readout scheme

This refers to configurations in which the gravitational wave signal is detected when a second carrier field (or some other sensing device) is used to measure the motion of a particular set of mirrors in their local inertial frames (see Ref. [61] and references therein). The word "intracavity" is used because it is assumed that the first carrier field does not generate useful output signals for readout.

The "local readout scheme" mentioned in the previous subsection can be regarded as an example of a mixture of intra- and extra-cavity readout. At high frequencies, the interferometer is dominated by extra-cavity readout, while at lower frequencies, it is dominated by intra-cavity readout. In the local readout example above, one may find it useful to use an alternate wavelength laser: the second wavelength can be made to have a very high finesse in the recycling cavities only, so as to maintain a high phase sensitivity for the ITM motion.

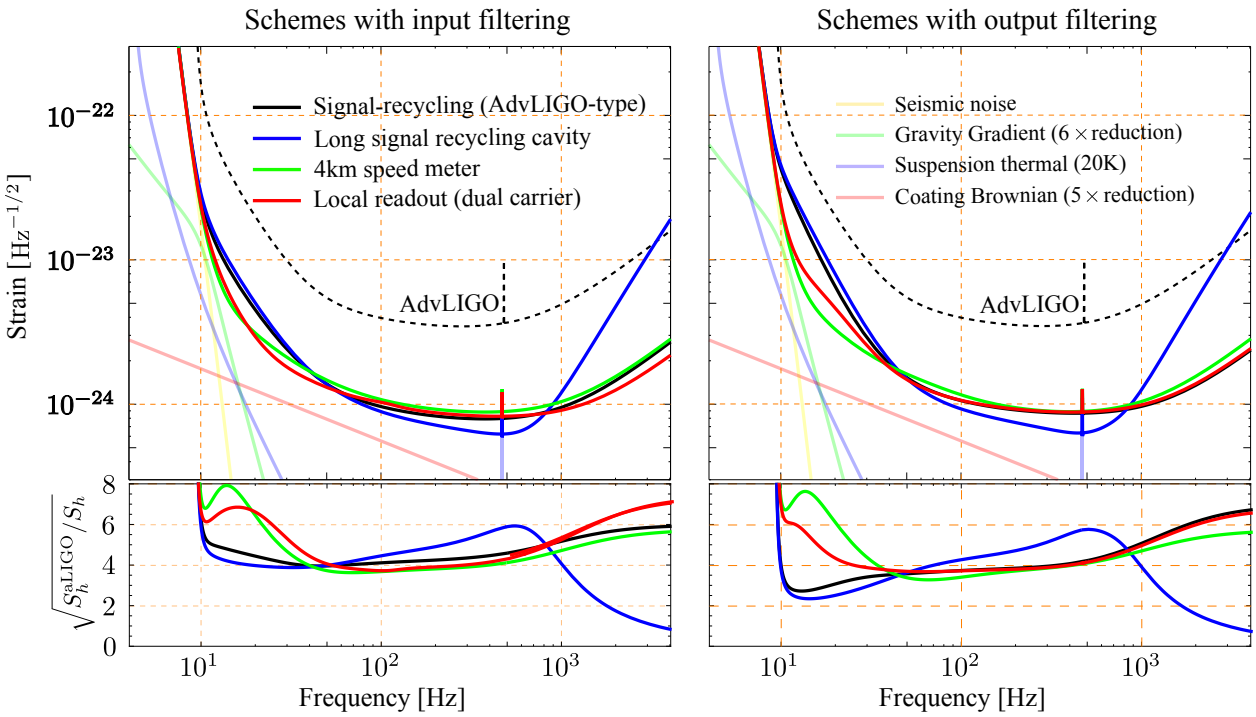

Figure 21: Optimization results for different schemes assuming more substantial thermal noise improvements, increasing the mirror mass from 40 to 150 kg, and increasing the arm cavity power from 800 to 3000 kW.

4.5.4 Ponderomotive Squeezing

Squeezing can be induced by mirror motion under radiation pressure — this is called ponderomotive squeezing. Although to date It has been more difficult than generating squeezing with nonlinear crystals, it may become more reliable and more flexible in the future. Currently a Ponderomotive Squeezing experiment is going on at MIT [62]. See Fig. 22 for a sample configuration.

a 3rd generation or beyond concept.

4.5.5 Internal squeezing and slow light

Previously, it was proposed [63] to use gratings to broaden the frequency response of the SRC. In principal, such a "white light" cavity would have the high sensitivity of narrowband, tuned signal recycling with the wide bandwidth of detuned recycling. While the grating based approach has its problems alternate dispersive media may be more successful. Two approaches currently being developed are to use a negative dispersion material [64] (such as an atomic vapor) and to use a photorefractive crystal [65].

In addition to its possible use in broadening the signal cavity, dispersive materials may have use in squeezing applications:

- Atomic clouds or substrate doping can be used as a form of intra-cavity squeezer in the SRC.

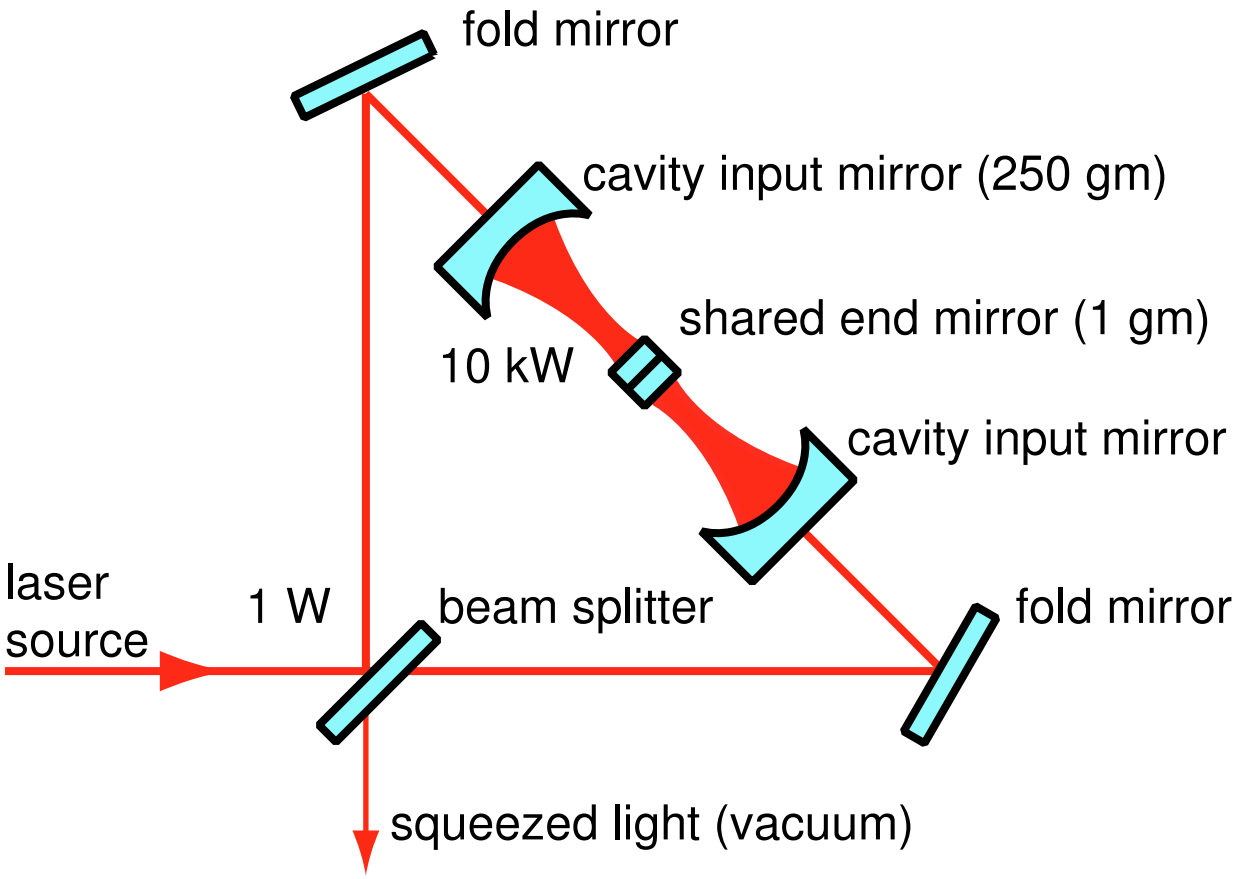

Figure 22: Ponderomotive Squeezer, taken from Corbitt et al. [**?**]

- Electromagnetically Induced Transparency in an atomic vapor can slow down light, possibly improving high finesse optical filters [66]. In fact, with enough slowing, one can almost eliminate the need for long filter cavities.

4.5.6 Significantly different configurations

For example, Displacement-Noise-Free Interferometry (DFI) [67]. Although DFI might turn out not to be suitable for ground-based detection, there might be new ideas in this vein.

Then there is the general question of whether atom interferometry offers a competitive topology for a third generation detector.

4.5.7 General Questions

Theoretically, advanced gravitational-wave detectors have two limitations, the *Standard Quantum Limit* and the *Energetic Quantum Limit*.

- *Is SQL-beating unavoidable?* The SQL arises from a trade-off between back-action and sensing noise — and more fundamentally it arises from the fact that light in the interferometer couple to the positions of free masses, which cannot be measured continuously without additional noise. The SQL sets the scale at which radiation-pressure noise and optical spring become important. The SQL can be avoided if we avoid sensing back-action, using back-action-evasion techniques. It can also be circumvented if we have optical springs. It can fundamentally be eliminated if we have mirrors with infinite mass. However, Will heavy mirrors be available? Which is easier, heavy mirrors vs. light mirrors with SQL-beating?

- *Can we surpass the Energetic Quantum Limit?* The Energetic Quantum Limit arises from Energy-Phase uncertainty relation (see, e.g., [68]) and basically describes the requirement for higher optical power when lower shot noise is desired. This can in principle be surpassed by optical springs. However, optical spring frequency is usually low, and does not reach frequencies in which shot noise dominate. However, can one do something to make it work? What about very light test masses coupled with heavy test masses, something like the optical-lever scheme?

4.6 Development of quantum radiation pressure dominated and QND apparatus

To date no experiment has observed quantum radiation pressure noise, let alone reached the 'naive' standard quantum limit. Such experiments are crucial to learn about problems which could mask such phenomena and how to beat such limits ahead of the operation of advanced generation detectors. To date there are major activities planned or underway at the AEI 10 m prototype; MIT; the University of Tokyo. The Glasgow 10m, the Gingin Facility and the ANU have embarked on testing optical spring dynamics. More effort is needed toward observing QRP noise.. As such experiments run up against excess noise sources and thermal noise they will inform activities across other working groups.

4.7 Experiments to prototype QND: filter cavities, variational readout, etc

Obviously, without QRP and SQL limited apparatus, no direct tests of these ideas can be performed. However, measuring transfer functions, demonstrating low loss manipulation of squeezed states an variational readouts can be performed with shot noise limited systems. Plans are underway for such an experiment at MIT and AEI. More effort is needed.

4.7.1 Loss Limitation

Optical losses might become more important when squeezing is used, or when internal ponderomotive squeezing is employed for sensitivity improvement (e.g. in schemes with output filtering).

The effect of losses is further amplified if back-action evasion is required, in which case the signal strength in the quadrature being detected is significantly less than conventional situations. A rule of thumb for this limitation is available from Kimble et al. [41], where we have

$$\sqrt{S_h/S_h^{\mathrm{SQL}}} \geq (e^{-2q}\mathcal{E})^{-1/4} \tag{3}$$

where $\mathcal{E}$ is the power loss, and e^{-2q} is the power squeezing factor. Assuming $\mathcal{E}$ to be 0.01, and 10 dB squeezing, we have a SQL-beating limit of 0.18.

For a given filter bandwidth γ_{filter} (to be determined by the needs of input/output filtering), when realized by a cavity of length L, the total loss $\mathcal{E}$ is determined by

$$\mathcal{E} = \frac{4\epsilon}{T} = \frac{\epsilon c}{\gamma_{\mathrm{filter}} L} \tag{4}$$

where T is the input-mirror power transmissivity [related to bandwidth by $\gamma_{\mathrm{filter}} = Tc/(4L)$] and ϵ is the loss per round-trip. It is therefore the ratio ϵ/L that determines the goodness of the filter. Since the per-round-trip loss ϵ depends on the beam spot size, which in turn depends on L, an optimization is need to find out the optimal length and design of filter cavities [69].

Practically speaking, ultra-low losses (around 1 ppm) have been achieved on the mirrors of fixed cavities [70, 71]. However, the lowest loss measured on the large, test-mass-sized beams are more usually in the 50-100 ppm range. FFT simulations have shown that the loss for large beams is dominated by the large scale figure error of the substrate, while the losses for small beams are dominated by point defects in the coatings. Since the low frequency performance of the QND schemes so strongly depends on the loss for intermediate sized ($\sim$mm) beams, it is vitally important to develop ultra-low loss mirrors for this beam size. The modern polishing technology is already good enough.

Excess Noise Associated with atoms If atoms are to be inserted into interferometers, we must consider the excess noise induced by them. Since the main concern is with excess phase noise produced by the scatter, we should design and simulate the excess phase noise associated with these materials. The next step would be to demonstrate a higher optical phase sensitivity (increased signal without increased noise) at the $\sim 10^{-9}$ rad/$\sqrt{Hz}$ level.

4.7.2 Optical Loss in Filter Cavities

The purpose of filter cavities is to rotate squeezing ellipses into optimal orientations over frequencies that include the low-frequency band subject to optomechanical effects to achieve a broadband reduction of quantum noise. Round-trip loss in addition to the finite input transmission of the cavity can degrade the squeezing and also lead to sub-optimal rotation of the squeezed light. Figure 23 shows the effect of round-trip loss on the degradation of squeezing for a filter cavity with 22 Hz detuning and bandwidth. The colors correspond to

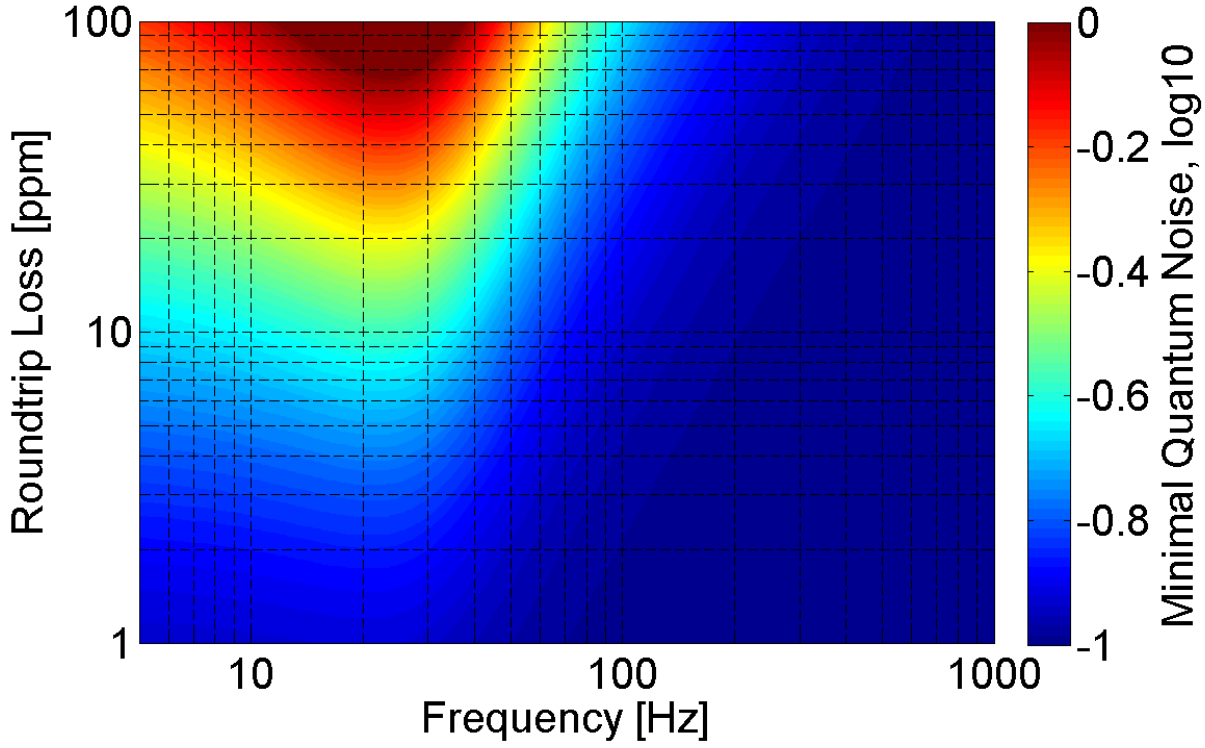

Figure 23: Degradation of 10 dB external squeezing reflected from a 300 m filter cavity as function of round-trip loss (in addition to input transmission) and frequency.

the quantum-noise spectral density along the minor axis of the noise ellipse relative to coherent vacuum noise. It can be seen that round-trip loss over 50 ppm degrades the squeezing to a level comparable to coherent vacuum around frequencies near the filter resonance. Here and in the following, round-trip loss are considered excluding the transmission of the input mirror. The input transmission is comparatively large (about 550 ppm for the filter calculation of Fig. 23) and does not directly contribute to squeezing degradation. Round-trip loss is dominated by optical scatter loss from imperfect mirrors in combination with finite aperture size. The goal is to minimize scatter loss.

Scatter loss in cavities is determined by properties of the individual mirrors such as mirror size, mirror curvature, mirror surface abberations and defects, and by the optical path length of the cavity. Scatter loss in cavities is not fully understood yet. A concerted effort of high-finesse cavity experiments, scattering measurements, numerical simulations and theoretical work is required to form a consistent picture between loss models and observations. Addi-

tional more specific problems that need to be investigated include small-angle scatter loss in cavities, coherent loss versus incoherent loss, and round-trip loss as a function of cavity aspect ratio.

Coherent scatter loss designates the effect when the spatial pattern of higher-order modes resonating inside the cavity matches the pattern of light scattered from a mirror. In this case scattered light can build up resonantly provided that the overall loss in these higher-order modes is not too high. In general, higher-order modes experience more loss since they describe a wider spatial intensity distribution that directs additional light power beyond the mirror aperture compared to the target mode of the cavity, which is usually the Gaussian shaped TEM_{00} mode. For this reason it is also necessary to understand how much round-trip loss is influenced by the cavity aperture, or better by the cavity aspect ratio, which is the aperture divided by the cavity length. Coherent scatter loss can potentially lead to a significant increase of the total scatter loss, and it is no more describable by simple perturbative scatter models.

4.8 Development of squeezed light sources

4.8.1 Crystal based squeezed light sources

Great progress has been made over the last 5 years in the generation of vacuum squeezed light.

1. Both ANU and AEI, using optical parametric oscillators (OPO) have measured squeezing of around 10 dB down to 10 Hz at 1064 nm. The AEI has observed greater than 12 dB at MHz frequencies at both 1064 nm and 1550 nm.

2. GEO 600 has been operated now for weeks at a time regularly observing more then 2.5 dB sensitivity improvement

3. An ANU designed squeezer was installed on the LIGO H1 detector operating in the S6 configuration. Sensitivity enhancement was observed above 200 Hz with 2.1 dB improvement above a few hundred Hertz. Importantly, no excess noise was seen below 200 Hz and no additional glitching was found.

4. Photodiodes with quantum efficiency in excess of 0.99 are now available.

Fig. 8 shows the predicted sensitivity curves for post aLIGO interferometers assuming 10 dB of quantum noise suppression at signal detection. Any absorption/scattering between the squeezed state generator and detection reduces the level of squeezing. Starting with a suitable source of squeezed light, Table 25 presents a comprehensive list of potential loss sources along with levels required to observe 6 dB, 10 dB and 15 dB of quantum noise reduction. The final column of the table presents the numbers achieved during the H1 squeezing test. The numbers are presented in terms of efficiencies (= (1 - minus) loss as a percentage).

From this table it is likely that 6 dB is achievable. Reaching the design performance of the aLIGO input Faradays and the aLIGO OMC, careful modematching and using now available

photodiodes with quantum efficiency (QE) > 99% should see 6 dB shot noise reduction using currently available squeezers.

10 dB and eventually 15 dB quantum noise suppression will require significant effort to reduce Faraday isolator loss (cf. Section 7.4.2), increase OMC transmission and tweak PD quantum efficiency. An escape efficiency of 99% is required. Currently the ANU squeezer operates with an escape efficiency of 98.5%.

A filter cavity will be needed to get broadband quantum noise suppression or to at least reduce the squeezing ellipse to a coherent state at frequencies where shot noise does not dominate.

The longer term goal of 15 dB observed quantum noise reduction is extremely ambitious. Loss tolerances on the isolators, OMC, modematching etc far exceed anything currently achieved. The most successful technique for generating high levels of low frequency, vacuum squeezed, light uses optical parametric oscillation (OPO). The current limitation arises from optical intra-cavity loss in the OPO cavity. Intra-cavity loss (separate from escape efficiency) is dominated by scattering from optical surfaces and absorption of the nonlinear crystal. Research and development into improved crystal fabrication technique, optical coatings and polishing, as well as particulate minimisation is needed. Further, improved temperature stability (preferably optically sensed) and positioning of the crystal interaction region is needed for phase matching and dual-wavelength dispersion compensation respectively. This will aid in accessing greater levels of squeezing. Finally, pump intensity stabilization will be needed.

Scattering in passive filter cavities will need to be reduced or km scale longer filter cavities employed. Alternative techniques such as electromagnetically induced transparency or optomechanically induced transparency should be explored.

As the level of squeezing is increased the requirement on stability of the squeeze phase angle is increased. As the phase angle rotates away from the optimum squeezing quadrature the level of squeezing available for quantum noise reduction is reduced. In the presence of phase fluctuations in the squeeze angle the average squeezing level is reduced. The effect gets worse as the ratio of the major to minor axes of the squeezed ellipse increases ie as the level of squeezing increases. The tolerance on phase noise will therefore decrease as total losses decrease. This is depicted in Fig. 24 where measured squeezing loci are plotted for different values of total loss and total phase noise.

From Table 25 we see that 6 dB noise reduction with a total loss of 76.7% requires phase noise to be controlled to better than 17 mrad. This requirement reduces to 4.4 mrad for 10 dB and 2.5 mrad for 15 dB. Achieving the levels of stability required for 10 dB or higher will likely require operating the squeezer inside the vacuum envelope. In vacuum operation has yet to be demonstrated.

An additional issue is backscattering. In the sub-100 Hz frequency range, interferometers and squeezers are particularly sensitive to scattered light. If scattered light from the interferometer seeds the squeezer noise will be generated. Scattered light reflected back off the squeezer which re-enters the made mode of the interferometer will add noise to the measurement. Effects can be mitigated by adding Faraday isolators or by using a squeezing geometry which has a level of immunity to backscatter.

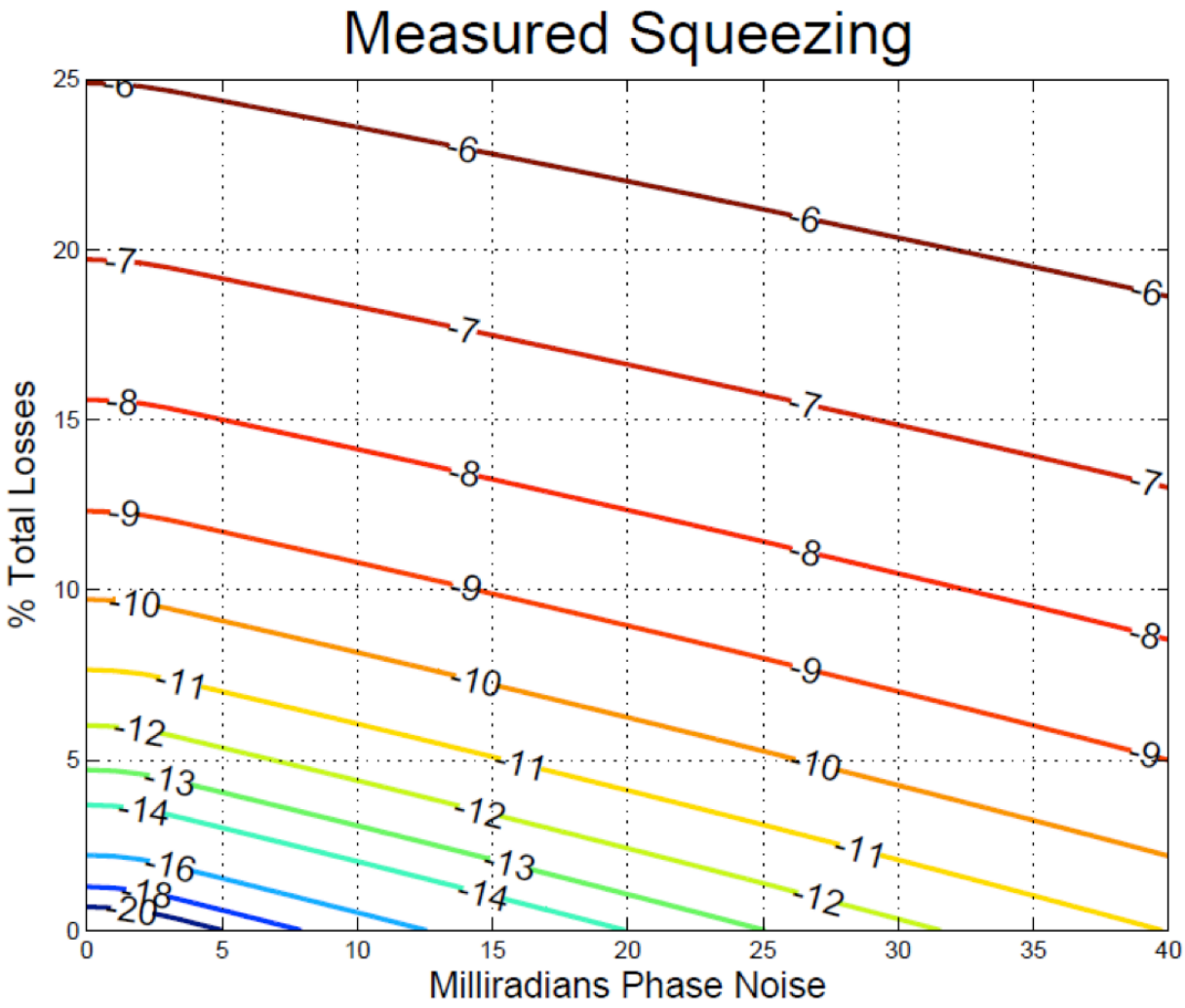

Figure 24: Measured squeezing for different values of total losses (the product of escape efficiency and detection efficiency) and total phase noise. For each value of phase noise, the non linear gain in the OPO is optimized to maximize the measured squeezing, but the nonlinear gain is capped at 90, (pump power at 80% of threshold). Operating the OPO closer to threshold doesnt improve the measured squeezing very much, but could make stable operation of the squeezer difficult. From Dwyer [72]

	Loss source	H1 experiment		Near term goal (6dB)	Longer term goal (10 dB)	Dreaming(15dB)
1	OPO escape efficiency	96%		98%	99%	99.8%
2	Injection path optics		80%	99.7%	99.7%	99.99%
3	viewport	99.8%		99.8%	99.8%	99.99%
4	3 faraday passes	94%, 94%, unknown		97% each (aLIGO input Faradays)	99% each	99.7 % each
7	RF pick off beamsplitter (beam for ISCT4)	98.8%		99%	99.5%	99.8%
5	Reflection off of Signal recycling cavity@100 Hz	arm cavity and michelson =98%		97.5%(Tsrm=35%)	99.2% (Tsrm=50%)	99.5%
6	Circulator for filter cavity	NA		98%	99.5%	99.8%
8	Squeezer mode matching to OMC	71% (inferred from total)		96%	98%	99.7%
10	OMC transmission	82%		97%	99.5%	99.7%
11	QE of PDs			99%	99.7%	99.99%
	Total efficiency (escape * detection)	40-45%		77.6%	91.3%	97.4%
	Total phase noise allowable			17mrad	7 mrad	2.5 mrad
	Measured squeezing (dB)			6	10	15.25

For numbers in the H1 column- red numbers were measured during the experiment, numbers in black were made before installing components or estimates of losses that were too small compared to the total to measure accurately with the uncertainty in our measurements.

Figure 25: Maximum acceptable losses to achieve 6 dB, 10 dB and 15 dB of observed quantum enhancement. From Dwyer [72]

4.8.2 Atomic media

Recently, Four Wave Mixing in an atomic medium has been shown to generate a small amount of squeezing (less than 1 dB) down to 100 Hz [73, 74]. Using the same nonlinearity, squeezed ellipse rotation has also been demonstrated. This technique is very far from producing the squeezing levels required in advanced detectors. A thorough examination of its potential is worth conducting.

4.8.3 Ponderomotive Squeezers

Ponderomotive squeezers use the non-linear phase dependent coupling between amplitude and phase arising from radiation pressure incident on a suspended cavity mirror. The only reported effort in this area is by MIT.

5 Optics

The Optics Working Group (OWG) of the LSC pursues research related to the development and implementation of optical components for ground-based gravitational wave detectors. This includes work on optical components being installed in Advanced LIGO, to better understand their behavior during commissioning and operation, possible upgrades to subsystems of Advanced LIGO including core optics, input optics, and auxiliary optics, and longer term research into ways around significant limitations in current detectors to be implemented in the third and fourth generation interferometers.

5.1 Mirror Coating Research

The high-reflection (HR) coatings on the Advanced LIGO test masses must satisfy a number of performance criteria including low absorption, low scatter, high uniformity, designed reflectivity at both 1064 and 532 nm, low mechanical loss, and low thermo-optic noise. Of these, mechanical loss and optical absorption provide the greatest sensitivity limits, and thus the most significant opportunity to improve performance. In general, coating research, especially research aimed at improving thermal noise and optical absorption, is of the highest priority within the OWG.

The majority of coating research is focused on understanding and reducing the thermal noise arising from the HR coatings because it is a leading noise source in Advanced LIGO's central frequency range and a major design hurdle for the 3rd generation detectors. However the anti-reflective (AR) coatings also present some challenges. Some of the AR coatings for Advanced LIGO test masses has shown anomalously high absorption. While an absorption method has been developed to reduce absorption, the mechanism producing the excess absorption is not well understood and deserves further research. There are also recent issues with monolayers on top of AR coatings changing transmission significantly in Advanced LIGO optics that deserves follow up research. These are important, but not crucial, research directions.

Coating research encompasses the following areas:

- **Materials Investigations:** Measurements of the physical characteristics (Mechanical loss, Thermo-optic loss, Young's modulus, etc) for coating material candidates for the 2+ generation of interferometers. This research includes investigations of how these characteristics change through processing, composition, temperature, etc. Specifically, cryogenic measurements of the mechanical loss vs temperature are used to determine the activation energy of the loss mechanism.

- **Structural Measurements and Modeling:** Research to determine the coating structure by measuring distribution of atoms and bond configuration. This knowledge informs a computational effort to model the coating structure. By successfully modeling the coating, it is hoped that a coating could be designed to meet the stringent requirements of future detectors.

- **Direct Thermal Noise Measurements:** Use of precision interferometry to directly measure thermal noise from coatings made from new materials, techniques, designs,

etc. to verify predictions coming out of material investigations. This is an important step to both test predictions and prove as much as possible coatings before use in actual gravitational wave detectors.

5.1.1 Materials Investigations

For room temperature mirrors at 1064 nm, the coatings with highest optical quality are ion beam sputtered (IBS) amorphous coatings, where the high index material is typically a metal oxide (ie. Ta_2O_5 or TiO_2) and the low index is usually silica. To achieve mirrors of high optical and mechanical quality, one avenue of research is to develop an amorphous coating of high mechanical quality. Alternatively, there are small scale, crystalline mirror coatings that have been developed with low mechanical loss. A second research track is exploring whether these coatings can achieve high optical quality and maintain their low mechanical loss when scaled to LIGO mirror sizes.

The thermal noise of a system depends on the level of thermal energy and the amount of dissipation. For many optical coating materials, the mechanical loss actually increases at cryogenic temperatures. Thus using coatings designed for room temperature at cryogenic temperatures will see less improvement in the thermal noise than one might naïvely assume. Thus the shift to cryogenics will require the development of new mirror coatings.

For third generation cryogenic mirrors, amorphous silicon and silica are being explored for the high and low index materials respectively. In addition, etched gratings, which form layers of variable effective density, would allow a reflective layer formed entirely of crystalline silicon.

Amorphous Coatings

Mechanical Loss Measurements The thermal noise due to the mirror coatings can be calculated from the coating mechanical loss using the Levin method [75]. Two methods are currently employed to measured the mechanical loss. The first method measures the loss via ringdown of small coated cantilever samples over the temperature range of 0 – 300 K. These measurements map out the Debye loss peaks and determine the activation energy of the loss mechanism. This knowledge can then be used as a constraint in models of the coating structure (see Section 5.1.2) By accurately modeling the coating structure, one may be able to identify the microscopic causes of internal friction and design coatings with minimal loss.

The second method measures the mechanical loss of coated thin silica disks at room temperature over a wide frequency range (typically 3 – 20 kHz). The frequency dependence allows separation of the bulk, surface and thermoelastic losses. Characterizing the mechanical loss at a wide range of frequencies and temperatures is valuable both as a search for new materials and to better understand the causes of thermal noise in amorphous thin film oxides.

For the room temperature interferometer, the high index materials that have been explored include: tantala, titania, niobia, hafnia, and zirconia. Silicon nitride, S_3N_4, also may be promising. Low index materials include silica and alumina. As applied, the high index materials have losses ranging from $3 - 7 \times 10^{-4}$. While any reduction in loss is important, a reduction by 10 is the goal for the third generation detectors.

The loss in the silica coating layers, while several times less than the high-index layer, is not negligible. For coating geometries, the loss in silica is dominated by surface and stress-induced losses. The latter loss can be minimized through a slow annealing process. However, this process typically destroys a multilayer coating by either crystallization of the high index material or adhesion failure due to differential thermal expansion. Thus the loss in the silica layers will depend on the geometry and thermal history of the multilayer coating. The loss in alumina is dominated by thermoelastic loss and is not currently suitable for room temperature coatings.

The most commonly used model for loss in these glassy materials [76] assumes an asymmetric, double-well bond potential formed by two nearly degenerate bond states. In silica, for example, the O bond potential has an angular dependence that is described by nested, asymmetric potentials [**?**], where the activation energy depends on the atomic distribution. In this model, one may minimize the loss by either removing the potential's double-well (ie. doping to change the bond potential) or by removing the asymmetry (ie. annealing to allow assume its lowest energy state).

Amorphous materials, including fused silica, tantala, titania doped tantala, and other oxides under consideration as coating materials have two independent elastic moduli, and thus two independent loss angles. Recent work at Caltech by Yanbei Chen's group suggests that it should be possible to design coatings with reduced Brownian thermal noise by having the thermal noise generated by different loss angles partially cancel out. Whether this is practical or significant depends on the values of the loss angles for the coating materials, which can only be determined experimentally. Measurement of torsional and bulk mechanical losses of coating materials will provide necessary input for these designs.

Doping Doping can reduce the mechanical loss by favorably changing the bond potential and by stabilizing the matrix against crystallization. For example, doping the tantala layers with titania has been shown to reduce mechanical loss by about 40%. This reduction allowed titania-doped tantala/silica to be selected for the Advanced LIGO coatings. Silica-doped titania has shown promise for reduced thermal noise, and was considered a fallback coating for Advanced LIGO. A trinary alloy of titania/tantala/silica as the high index material may allow for benefits from each material. Silica, while effective at stabilizing high-index materials and thus allowing for higher annealing temperatures, also reduces the index of refraction, thus requiring thicker coating layers. Effective medium theory may be of use in modeling alloys and doping, and comparing Q measurements to predictions of effective medium theory are an important next step in verifying this approach.

The use of dopants in tantala, titania and zirconia are being explored as a means of understanding and reducing the mechanical dissipation. While it is crucial that any new material also satisfy the stringent optical requirements of LIGO interferometers, there are advantages of initially just pursuing lower mechanical loss.

For cryogenic coatings, amorphous silicon is the leading candidate for a high index material. It has been shown that infusing hydrogen in the silicon coating can significantly reduce the loss, presumably by filling defects within the matrix. However, since the hydrogen does not remain bound, when it diffuses out of the silicon, the effect is reversed. Nevertheless, the

usefulness of dopants to improve the mechanical loss is clear.

Annealing Ion beam sputtering forms coatings with high compressive stress, and comparatively high mechanical loss and absorption. Annealing these coatings will reduce the stress and correspondingly reduce the absorption and mechanical loss. Typically the annealing temperature is limited by either the crystallization temperature for the high index material or shear failure from the differential expansion of the coating layers. If these failure mechanisms can be avoided, annealing could potentially provide significant improvements in mechanical loss and absorption.

The mechanical loss in silica coatings have be reduce by about 8× through high temperature annealing. In addition a zirconia/silica coating has been demonstrated to survive a 1000° C annealing without shear failure. Annealing has also been shown to reduce the absorption in zirconia coatings by a factor of several. Work is currently underway to use doping to stabilize the coatings against crystallization, which leads to unacceptable scatter. Coatings designs to withstand high temperature annealing could see significant improvements in their absorption and their mechanical loss.

Interface Effects Early experiments on loss in Initial LIGO's tantala/silica mirror coatings [77] demonstrated that the loss was primarily due to the tantala layers. No significant loss could be attributed to the coating interfaces. However, more recent measurements have been conducted at LMA on the Advanced LIGO coating of titania-doped tantala/silica. These new measurements suggest that there may be some excess loss associated with the coating interfaces. This may be related to mixing of materials and would allow for thermal noise to scale with the number of interfaces rather than material thickness. Given the change in material, the improvements in measuring techniques, and the importance of understanding this coating, the issue of mechanical loss at the coating interfaces deserves continued study.

Optical Absorption Absorption of light in the coatings will result in thermoelastic distortion of the optics and will ultimately limit the circulating light power in the interferometer. When coupled to the bulk absorption in the input test masses, this leads to significant surface deformation of the test masses and bulk thermal lensing in the input test masses. Coating absorptions as low as 0.3 ppm have been reported in undoped silica/tantala coatings, which titania-doped tantala and silica-doped titania coatings have been shown to have absorption at or below 0.5 ppm. Further improvements beyond this level will make thermal compensation easier for enhancements to Advanced LIGO and likely are necessary just to make compensation possible in higher power detectors envisioned beyond Advanced LIGO.

Detailed studies of absorption in other possible coating materials will be important when considering their use in any future detectors or enhancements to the Advanced LIGO detectors. Measurement of absorption at cryogenic temperatures is of increasing importance for future detectors. Initial measurements of the temperature dependence of the absorption of amorphous silicon coatings have been carried out, and these should be extended to other potential coating materials. Further studies of the effects of coating treatments such as dop-

ing and annealing on both the cryogenic loss and the optical absorption will be valuable, particularly if optimum treatment regimes can be developed to minimize both mechanical loss and optical absorption.

Studies aimed at understanding and improving coating mechanical loss may involve working with coatings with relatively high absorption during a research phase e.g. to understand why a particular dopant affects the mechanical loss. Further research into the absorption of anti-reflection coatings is also required, as these coatings consistently have a higher absorption (up to 10 ppm) than high-reflectivity coatings (typically below 1 ppm).

Optical Loss from Scattering Experience with scattered light in first generation interferometers suggests there may a need to develop coatings with lower intrinsic scatter. Examination of coatings with a scatterometer is valuable to determine the level of the scatter, to test the scattering properties of new coating materials and to test whether coatings provided by different vendors have different scattering characteristics. Lower scatter is necessary to maintain high optical power which will likely prove important in enhancements to Advanced LIGO and future detectors.

Realizing more sophisticated quantum non-demolition (QND) topologies also requires extreme low-loss optical systems as is explained in section 4.7.2 for the case of filter cavities. One of the important sources of optical loss is scattering from mirror-surface abberations. These are traditionally investigated by measuring the angular distribution of scattered light (i.e. measurements of the bidirectional scattering distribution function (BSDF)), or scanning the surface with lasers and integrating the scattered light in spheres. As much as these measurements are important to link scattering from mirrors with losses in optical systems like cavities, they do not give direct information about the cause of scattering.

Scatter loss in (future) optical systems with sizes up to a few hundreds of meters will likely be dominated by point-defect scattering as the quality of substrate polishing has advanced to a level that makes residual surface-roughness scatter loss negligible in most cases. These conclusions are based on numerous simulations and partially on scattering measurements in first-generation GW detectors. Even though it is believed that very low-loss systems can be realized in the near future with scatter loss around 10 ppm per mirror, the question is how much further loss can be decreased. Loss estimates play a major role when deciding between the various candidate QND configurations for future GW detectors. Whereas input filters (see section 4.2.1) are relatively robust against optical loss, output filters (see section 4.2.2) that can potentially eliminate all back-action quantum noise are known to be highly susceptible to loss. A few ppm loss per mirror typically destroys the entire advantage that output filters have over input filters (eventually making them even worse in performance). Similar problems are encountered with alternative QND schemes.

Assuming that point-like defects residing in the mirror coatings are the dominant source of scatter loss, one has to investigate individual defects for their material compositions, morphologies, and structures. The answers can be used to understand the origin of the defects with the goal to improve the coating process. Various analysis methods are available. Defect morphology can be studied optically or with force microscopy depending on defect size. Defect materials can be investigated spectroscopically. The analyses should progress

from larger to smaller defects since the larger defects dominate the point-defect scatter even if they are significantly less numerous.

Uniformity It has also proved challenging to maintain coating thickness uniformity across the large face of Advanced LIGO optics. Non-uniformity in thicknesses leads to non-uniformity of transmission and scatter of light out of the cavity mode to other optical modes. This also leads to limits on optical power and squeezing, as the higher spatial frequency scatter discussed in the previous paragraph. Even larger optics are possible in future detectors, making maintaining coating uniformity even more challenging and thus an important research topic. The limitation on obtainable uniformity can come from metrology limitations, so improved metrology is an important research direction. And additional research direction is to explore corrective coatings, which place additional coating material onto a coated optic after uniformity measurements have been made.

Thermo-optic Noise Thermo-refractive (dn/dT) and thermo-elastic (dL/dT) effects in coatings are noise sources that are driven by the same temperature fluctuations. These two noise sources are together referred to as thermo-optic noise. Analysis has shown that there is partial cancelation between thermo-refractive and thermo-elastic effects in tantala/silica coatings, so the total noise in Advanced LIGO is not expected to be as high as previously estimated. However, measurements of dn/dT for coating materials are important to allow thermo-refractive noise to be quantified for Advanced LIGO, when considering new materials that may have significant thermo-optic noise, and to allow for the design of coatings which can minimize the total (both Brownian and thermo-optic) noise.

Measurement of the thermal expansion coefficient of coating materials is also essential to allow the level of thermo-elastic noise to be predicted and, if possible, partially canceled with thermo-refractive noise through careful coating design. Measurement of thermal expansion coefficients at cryogenic temperatures is also valuable for future low temperature detectors.

Young's Modulus and Stress The Young's modulus of a coating is required both for the analysis of mechanical loss measurements and for calculations of the level of coating thermal noise. It is therefore important to obtain accurate values of Young's modulus for every coating, and post-deposition coating treatment, studied. Residual stress in coatings is likely to be an important property, and there is interesting evidence suggesting that stress can alter mechanical loss of coatings, particularly in silicon nitride. Therefore studies of the effects of residual stress on the loss and of methods of altering the stress in particular coatings are of interest. The use of several measurement techniques can be beneficial in these studies, as each technique has different systematic errors and, for example, different sensitivity to the properties of the coating substrate material. In addition to measuring these properties at room temperature, where possible the capability to measure the temperature dependence of these properties should be developed.

A Young's modulus and dissipation measurement method with sub nanometer spatial and depth resolution developed by Konrad Samwer shows that the Young' modulus in glasses has a position dependent spread as wide as 30% (and the local loss factor is also poorly

defined), that the spread is reduced with annealing, while crystals have constant Young's modulus everywhere. It has also been shown that fused silica, which is the glass with the lowest known mechanical loss, has a substantially narrower Young's modulus spread than other glasses. The method can either explore small shallow volumes, or wider and deeper volumes, up to several hundreds of atomic spacings in dimension. The capability of this method to scan the Young's modulus with sub nanometric resolution offers a new way to explore the uniformity of our coatings, as a function of annealing, and perhaps shine some light on some loss mechanisms.

Production Variables Variations in the loss of nominally identical coatings from different vendors have been observed, suggesting that the precise deposition parameters may be important in determining the loss. Thus more detailed measurements of the effects of parameters such as ion energy, sputtering ion, oxygen pressure and thermal treatment may be valuable. While ion beam sputtering produces the lowest optical loss coatings, the mechanical loss of coatings deposited by other techniques has not been extensively studied. Studies of coatings deposited by different techniques (e.g. magnetron sputtering, e-beam evaporation, atomic layer deposition) may enhance understanding of the relationship between loss and structure in these materials.

Coating layer thickness may also prove an important variable in determining amorphous material properties, especially mechanical loss. There are suggestions that very thin, much less than a wavelength, layers may have improved mechanical loss. This may be related to stress and/or annealing properties of thin coatings. If this effect can be confirmed and understood, it is possible to design high reflective coatings with much lower thermal noise using known materials like tantala and silica.

Crystalline Coatings Single-crystalline coatings grown by molecular beam epitaxy are of interest as a possible alternative to current amorphous coatings. This is likely to be of particular relevance for low-temperature detectors, as the cryogenic dissipation peaks observed in current silica and tantala coatings are thought to be related to the amorphous structure of the materials. There are multiple crystalline coatings under investigation within the LSC; among them are aluminum gallium arsenide, AlGaAs, and aluminum gallium phosphide, AlGaP. General factors which require investigation for crystalline coatings include adhesion to substrates at cryogenic temperatures, scattering, and fabrication on curved mirror substrates. Crystal coatings show great promise for future detectors and are a high priority research topic for the OWG.

Aluminum Gallium Arsenide, AlGaAs GaAs:AlGaAs coatings[78] have been studied as free-standing micromechanical resonators for use in quantum optomechanical experiments, and have been shown to have very low mechanical losses (as low as 4.5×10^{-6}) at cryogenic temperature. In addition, good optical properties have been demonstrated, with the lowest optical absorption measured to be approximately 10 ppm. However, these coatings are grown on GaAs substrates, and would require to be transferred and bonded onto appropriate mirror substrates for use in gravitational wave detectors. The method of epitaxial lift-off is well established, and has been demonstrated for AlGaAs coatings on flat substrates up to 150 mm

in diameter. The application of this technique to curved mirrors requires some development, and it is essential to study these coatings after transfer to appropriate substrates to evaluate any additional mechanical loss and scatter which may be associated with the bonding process.

Aluminum Gallium Phosphide, AlGaP AlGaP and GaP are lattice-matched to silicon, allowing a reflective coating to be grown directly on to a silicon mirror substrate, eliminating the need for coating transfer and bonding. Initial measurements of the mechanical loss at room temperature were limited by thermoelastic damping in the silicon substrate: however, these measurements did allow an upper limit of approximately $< 2 \times 10^{-4}$ to be placed on the coating loss at room temperature. Continuing to characterize the loss and optical properties of these coatings at cryogenic temperatures is also of very high priority. These coatings are more typically grown on GaP substrates, and thus further development of the techniques for growing these coatings on silicon substrates is desirable [79].

Coatings at cryogenic temperatures Planned future detectors such as the Einstein Telescope in Europe and KAGRA in Japan will operate at cryogenic temperature to reduce thermal noise. In addition, it is possible that an upgrade to improve the sensitivity of Advanced LIGO may be cooled to at least 120 K. It is therefore essential to fully characterize the performance of coating materials at cryogenic temperatures. In particular, the mechanical loss can be a strong function of temperature and low temperature loss peaks have been observed in silica, tantala and titania-doped tantala coatings. While these loss peaks will lessen the potential reduction in thermal noise obtained from cooling, there is still some benefit to operating these coatings at cryogenic temperature. For example cooling to 20 K would provide a reduction in coating thermal noise by a factor of about 2, rather than the factor of 4 improvement which would be expected if the coating loss was constant with temperature.

Cryogenic mechanical loss measurements of coating materials are also a valuable tool for exploring the microscopic processes responsible for energy dissipation. Identification and analysis of Debye-like loss peaks allows key parameters of the dissipation mechanisms to be calculated and, coupled with atomic modelling and structural measurements, may allow the association of loss peaks with particular types of atomic motion within the coating structure.

To enable further reductions in coating thermal noise there is an ongoing effort to identify coatings with a lower mechanical loss at cryogenic temperatures. A number of research paths are being pursued including further improvement of current silica/tantala coating, the use of alternative coating materials, particularly amorphous silicon high-index layers, and the use of single-crystalline coatings.

There has recently been significant progress in understanding the loss mechanisms in tantala coatings, with analysis of cryogenic loss peaks providing information about the dissipation mechanisms, and structural studies and atomic modeling revealing correlations between structure, doping level and loss. The level of loss in tantala below 100 K is strongly dependent on heat-treatment and doping level, and continued studies to optimize coating composition and post-deposition annealing may yield further improvements in coating thermal noise. The results are consistent with a model in which transitions of atoms between energetically stable

positions are responsible for the loss, and suggest that the atomic structure of the coating is a key factor in determining the loss.

Amorphous silicon ($\alpha - Si$)coatings can have a particularly low mechanical loss, with recent measurements placing a conservative upper limit of 5×10^{-5} on the loss angle of ion-beam sputtered $\alpha - Si$ below 50 K. In addition, the high refractive index of silicon allows thinner coatings with fewer layer pairs. The use of a silicon/silica coating could potentially reduce coating thermal noise by a factor of 2.4 at 20 K compared to a silica/tantala coating. However, the first measurements of optical absorption in these coatings suggest that significant efforts to understand and reduce the absorption may be required. There is evidence in the literature that hydrogenation of amorphous silicon deposited by e-beam evaporation and chemical vapor deposition can reduce the mechanical loss by up to a factor of ten. Studies to test this for ion-beam sputtered coatings and to evaluate the effect of hydrogenation of the optical absorption should therefore be carried out.

Measurements of hafnia coatings indicate that, even when in a partially poly-crystalline form, this material has a lower loss than tantala at temperatures below 50 K. Experience with tantala suggests that poly-crystalline structure may significantly increase the loss. One method of preventing crystallization of hafnia films is doping with silica and it has been shown that this does not significantly increase the loss at room temperature. Low temperature loss measurements of silica-doped hafnia coatings are underway.

Diamond-like carbon (DLC) coatings may also be of interest for further study, as there is evidence in the literature that the loss of this material is very low, with some films having a lower loss than amorphous silicon.

Studies of other possible alternative amorphous coating materials should continue, and where possible the choice of material (or treatment regime e.g. dopant, doping level, heat-treatment) will be informed by the results of structural measurements and modeling. While most of the effort to date has focussed on developing alternative high-index coating materials for use at low temperature, it should be noted that silica coatings also have a cryogenic loss peak of a similar magnitude to that observed in tantala. Thus more studies of possible alternative low-index materials are required.

5.1.2 Structural Measurements and Modeling of Coating Materials

There is currently little theoretical understanding of the mechanical loss mechanisms in amorphous coating materials, although it seems likely that the loss mechanism is related to the local atomic structure and may involve transitions of two-level systems as is believed to be the case in fused silica. The mechanical loss of tantala in particular has been found to be strongly affected by treatments such as doping and annealing which cause both structural and chemical changes to occur in the material. Identifying the causes of mechanical loss in coatings is a crucial step in developing improved techniques for reducing coating loss and studies of the structure of coating materials using both experimental measurements and atomic modeling techniques are an important part of the coating research plan.

There is an effort underway to produce theoretical atomic level models of amorphous dielectric oxides to develop an understanding of mechanical loss processes. For these purposes,

silica is thought to be the best material to begin with, as there is fairly extensive literature on atomic modeling of silica and the cause of the mechanical loss is fairly well understood. Developing models of tantala is also a high priority, as between XX K and room temperature the loss of multilayer coatings is dominated by the tantala component.

In addition, direct structural measurements of coating materials are being carried out using electron diffraction and Reduced Density Function analysis. These measurements have identified the first correlation between changes in the mechanical loss of doped tantala coatings and changes in structural properties resulting from changes in the level of titania doping. Semi-empirical structural modeling is being carried out based on these measurements using a combination of Reverse Monte Carlo methods and Density Functional Theory, resulting in detailed models of the coating structure in which the distribution of parameters such as bond angles and nearest neighbor distances can be analyzed.

There are some indications that some changes in mechanical loss may be related to longer-range structural changes in coating materials. In particular, heat-treatment of tantala coatings can result in significant increases in the mechanical loss at low temperature with minimal changes observed in the average local atomic structure as measured by current electron microscopy techniques. Thus methods of studying medium range order in coating materials, such as fluctuation microscopy, should be used to establish if there are correlations with mechanical loss.

The use of complementary techniques which can provide additional information is likely to be required to fully understand the links between structure, loss and other relevant material properties. In particular, nuclear magnetic resonance can be used as an alternative probe of the local atomic structure, while x-ray techniques such as XAS, EXAFS, XANES, X-ray reflectometry and absorption may be used to obtain direct measurements of the short range order around specific atomic species in the coating structure. Electron parametric resonance (EPR) spectroscopy can show unpaired electrons in tantala, which can be a marker for oxygen deficiency. Electron energy loss spectroscopy (EELS) can also give information about stoichiometry. In addition, measurements at facilities such as SSRL may allow direct measurement of the temperature dependent phonon spectrum in coatings.

5.1.3 Coating Design

Optimized Coatings Since the thermal noise in the coatings typically scales as the total thickness of the more lossy material (although there are recent reports of mechanical loss being different in tantala with different thicknesses), reducing this thickness while maintaining the optical properties will reduce thermal noise. Constrained numerical optimization codes have been shown to produce high reflectivity coatings while reducing the volume of high index materials by as much as 20%. Thermo-optic noise from thermoelastic and thermorefractive effects is included in this optimization. The mechanical loss of the low index (silica) material takes on a larger role for thickness optimized coatings, as optimization typically makes the high index (titania- tantala) contribution equal to the low index. Such an optimized design is used in Advanced LIGO. Greater understanding of mechanical loss in thin film silica and/or other low index materials is crucial to exploiting the full potential of this optimization.

Designing coatings that take advantage of different loss angles for bulk and torsional motion will be important once numerical values are found. This optimization will need to be done while including thickness effects on Brownian thermal noise as well as thermo-optic noise.

Diffraction gratings All-reflective interferometers using diffraction gratings as optics avoid problems associated with the transmission of large laser powers through optical substrates. Moderately high finesse optical cavities have been demonstrated using small gratings. The challenge will be to scale up the optical aperture to what is required for a large detector. In addition, absorption by the grating surface can distort its surface profile, possibly resulting in changes in the beam profile as well as power-dependent changes in the diffracted beam shape and efficiency. Modeling has been done along with sample produced, but these effects need to be investigated more in depth. Investigations of mechanical loss in gratings are needed to verify thermal noise levels as are direct thermal noise measurements. Demonstration of high reflectance values is also important.

Coating-less or coating-reduced optics A few ideas have been proposed to reduce the mirror thermal noise by reducing or removing the coating, including:

- Corner cube style retro reflectors
- Brewster angle prism retroreflectors
- Khalili cavities as end mirrors

Corner reflectors and Brewster angle mirrors would allow for no coatings to be needed and Khalili cavities would allow for much thinner coatings than conventional mirrors. Experimental work is needed to test some of these concepts for practical limitations. A bench experiment has been done forming a cavity with one Brewster angle mirror and one conventional mirror on fixed suspensions to see if a high finesse cavity can be formed. Follow on work with suspended mirrors will be necessary to evaluate the mechanical stability of such a system. The new prototype interferometer at the AEI in Hannover is slated to test Khalili cavities as a way of reducing coating thermal noise.

5.1.4 Direct Coating Noise Measurements

Direct measurements of thermal noise are of interest to compare with the predictions obtained from mechanical loss measurements and to test the improving theories of coating thermal noise. In the cases (e.g. crystalline coatings) where thermo-optic noise cancellation is required to get the thermo-elastic or thermo-refractive noise below the Brownian noise, Q measurements alone cannot truly probe the thermal noise limits.

Fixed Spacer Cavities Coating thermal noise measurements are now being carried out using fixed spacer cavities, which are limited by coating thermal noise over a wide frequency band and are significantly easier to operate than a suspended mirror system. These systems

will use standard size (1 inch diameter) substrates and can provide a convenient test-bed for the development of low thermal noise optics.

AEI 10 meter prototype The 10 meter prototype interferometer at the Albert Einstein Institute in Hannover Germany will be able to directly measure coating thermal noise. In addition to testing Khalili cavities as a means of reducing coating thermal noise, it will have the ability to change the size of the laser spot on the mirrors. This will allow for a direct test of spot size dependence, which is an important driver of the desire for larger optics in future detectors.

5.2 Substrate Research

5.2.1 Fused Silica

Experiments to measure mechanical loss in silica versus annealing parameters, including ramp down and dwell times have lead to improvements in the substrate thermal noise. In order for the fused silica thermal noise to pose a problem in the future, the thermal noise of the coating would have to be reduced by more than an order of magnitude. This makes silica substrate mechanical loss studies a lower priority than coating mechanical loss.

5.2.2 Silicon

The OWG is investigating alternative materials to fused silica for use as test mass substrates for use in low temperature detectors. Both silicon and sapphire potentially offer superior performance at cryogenic temperatures and/or at particular frequency bands. Different substrate materials, operating temperatures, and laser wavelengths may also require and/or allow for different coatings and suspension connection techniques that must also be studied.

Research efforts on silicon have focused on acquiring and fabricating cylindrical test specimens and investigating their mechanical properties as a function of doping. Studies of silicon properties, including mechanical loss for predicting thermal noise, of different crystal orientations are valuable. In addition, silicon cantilever micro-resonators with resonant frequencies in the sub-kHz range have been fabricated to explore dissipation mechanisms in a regime where thermoelastic effects are significant. Surface loss effects are also emphasized by the large surface-area to volume ratio of the micro-resonators. Preliminary experiments measuring the dissipation have been carried out and reveal disagreement with theoretically predicted loss. Silicon is also a potential coating material at 1550 nm and will need to be studied as a thin film.

Understanding the optical loss of silicon if used as a transmissive optic at 1550 nm is also a useful area of research. The high thermal conductivity of silicon could significantly reduce the effects of thermal loading of transmissive components if the optical loss is low enough. Understanding the temperature dependence of light absorption along with all other thermo-optic and thermophysical properties is important. Silicon might also be used as the high index material in coatings. Research will be required to develop suitable components if a change in wavelength is considered. Silicon mirrors and suspension elements have an

advantage of being conductive thus control of charging effects may be easier to implement. Nonetheless, charging will need to be investigated since doping and especially coatings can influence the charging dynamics.

5.2.3 Sapphire

Recent efforts have yielded information about the mechanical and optical properties of sapphire, methods for growing and processing large sapphire blanks, and ways to achieve high homogeneity, low absorption sapphire. Studies on annealing for improved optical absorption have been extended to elucidate further details of the kinetics of the out- diffusion process. Gathering experimental data at low temperature is important to predict the performance of cryogenic sapphire test masses. Room temperature sapphire is also a potential mirror substrate for detectors optimized at higher frequencies. Measurements of mechanical properties including mechanical loss as a function of crystal orientation are also important for predicting substrate and coating thermal noise.

5.2.4 Composite Masses

Increasing the mass of the test masses reduces the influence of both classical and quantum radiation pressure noise. Beyond a certain size, however, it is impractical to fabricate monolithic masses. Using large masses made as a composite of multiple, smaller pieces can circumvent this problem. Non-cylindrical mass distributions could also be used to increase the total mass and total angular moment of inertia without increasing the optical pathlengths within the substrate. The larger translational and angular moments of inertia would reduce the radiation pressure noise and the influence of the Sidles-Sigg instability. Thermal noise issues related to mechanical loss from the interfaces will have to be resolved. This research is longer term in nature, and thus is of lower priority compared to more immediate needs.

5.2.5 Parametric Instabilities

The build-up of parametric instabilities in the arm cavities related to the high laser power levels are a potential problem from high optical power in Advanced LIGO and beyond. These undesirable effects result from exchange of energy between light stored in cavities and acoustic modes of the mirror which define the cavities. At high optical powers, the radiation pressure force of scattered high order optical cavity modes can couple strongly to the mechanical modes of the test masses, resulting in a parametric instability. High excitation of the mirrors acoustic modes can result in difficulties in the controls engineering and at very high amplitudes can lead to loss of lock. Unfortunately, the requirements for high sensitivity are commensurate with the conditions under which parametric instability occurs. These include high optical power and low mechanical loss materials in the mirrors.

Using finite element methods, it is possible to start developing a quantitative understanding of this problem by modeling the modes and parametric gain for different test mass configurations, as well as investigate methods for mitigating the instabilities. In order to make a realistic estimate for the parametric gain, it is necessary to also include the full field calculations of the dual-recycled interferometer [80].

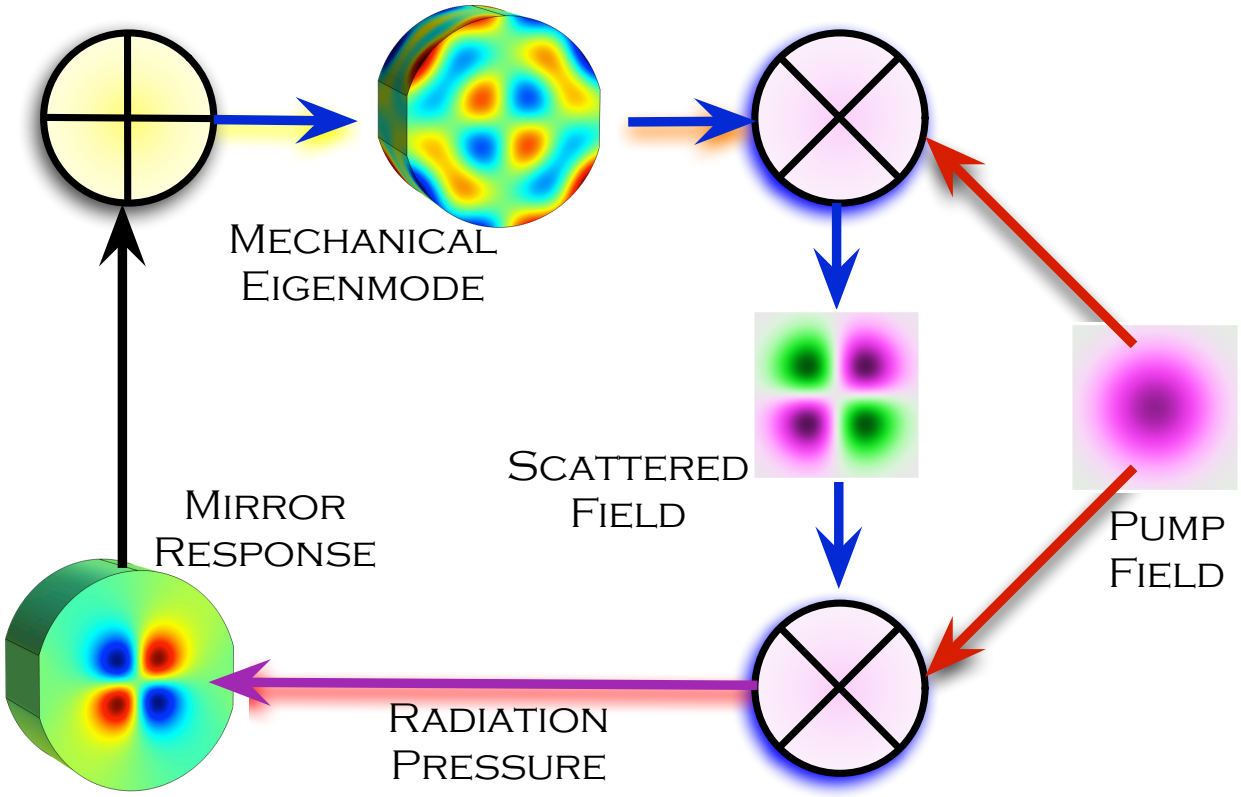

Figure 26: Schematic diagram of the parametric instability mechanism [81]

Measurements on suspended test masses are needed to obtain realistic, as-built, test mass Q values to establish the net gain for the instabilities. Adding tuned mass dampers to the barrel of the test masses (LASTI-MIT) and/or using feedback to the electro-static drive also show promise for controlling parametric instability. In addition, spatially-resolved radiation pressure feedback on the mirror surfaces is being contemplated (Gingin-UWA). Outstanding questions include whether these approaches are compatible with high sensitivity, including low shot noise, low thermal noise, and realizable controls.

Small scale suspended test mass experiments are also underway to study parametric instability. The larger scale experiments will be useful in testing noise performance of various parametric instability suppression schemes, the small scale experiments will be useful to validate the theory of parametric instability and for proof-of-principle test of suppression schemes. The small scale experiments using millimeter scale test masses in a tabletop configuration using coupled cavities and/or specially designed near-concentric cavities can be done using a standard NPRO laser and s tandard 1 inch optics. The small scale resonator experiment at UWA has reached the threshold of parametric instability. These experiments are valuable but because of its applicability to Advanced LIGO, the emphasis of parametric instability research should be on suppression schemes.

5.2.6 Charging

Surface charge may build up on the test masses through a variety of mechanisms, including contact with dust (particularly during pump down) and/or the earthquake limit stops, removal of First Contact used to keep the optic clean during transport and handling, as well as cosmic ray showers. There is evidence from initial LIGO that charging of the optics has occurred and noise has visibly increased from hitting earthquake stops. There are several mechanisms by which the interaction between changes on the optic and charges on nearby surfaces can generate force noise on the optic. One noise mechanism is that a static charge distribution on either the optic or the earthquake stop will couple motion of the earthquake stop into forces on the optic [T080214].

Another mechanism is the noise caused by time-varying charge distributions on the optic (or the earthquake stop) resulting in time-varying forces on the optic. Gaussian noise from this mechanism can be described by a Markov process [T960137]. The result depends on the magnitude of the deposited charge and the correlation time of the deposited charge, with a smaller actuating noise for correlation times far from the reciprocal of the frequency at which the noise is being measured. These correlation times are being measured using scanning Kelvin probes operated in vacuum which measure the magnitude and distribution of surface charges and their rate of motion across a sample. Current results indicate that the correlation times depend on the type of silica, but can be very long for very clean samples, leading to current estimates that this need not be a significant noise source for Advanced LIGO. Continuing work will focus on examining a variety of silica types, different cleaning and handling methods (including ways of applying and removing First Contact), and optics with coatings. Various coatings will be characterized as they are developed in the coating research program. Understanding what sensitivity limits might come from charging and how this may depend on cleaning and handling is crucial for Advanced LIGO. Depending on results, it may prove an important area of research for upgrades.

Charge may also interact with the electro-static drive to be used in Advanced LIGO causing noise or reduced effectiveness of the drive. Modeling has been started to study this, and experimental work at LASTI at MIT has begun to better understand the role of charge with the electro-static drive. There have also been two experimental verifications of a charging contribution from dielectric polarization of the fused silica [G1200853, P1000077]. Further experimental and theoretical work is planned on polarization noise. Calculations have also been carried out to estimate the force noise that might be expected from Coulomb interactions between charge accumulations on the test mass and various components in the suspension system. The earthquake stops being the closest to the test mass surfaces are of greatest concern for most issues with charge on the optic [T080214].

The leading solution to mitigating charge in the advanced detectors involves blowing nitrogen gas across needles at 4kV AC, which ionizes the gas externally to the vacuum chamber [G1000383, T1000135, T1100332]. The nitrogen ions, which comprise both polarities, travel through an aperture and into the vacuum tank. As this is essentially a thermally driven process, with charge on the optic attracting the appropriate polarity of ion to provide neutralization, it is unlikely that any damage to the HR coatings will occur, although tests are currently underway to assess this issue. A prototype system has been demonstrated at MIT and work is ongoing to test this technique on the monolithic noise prototype at LASTI. The

discharge procedure would require approximately 1 day of downtime for the detector. In addition to the above technique, alternative discharge strategies are also being developed.

Shining UV light on in situ optics has been investigated as a way to mitigate charge buildup. This involves testing UV LEDs, developing AC driver electronics, and performing experiments to determine if the UV can cause harm to the optics or their coatings. Coated optics are tested by subjecting them to UV light for days to weeks at a time, then are re-measured for optical absorption and mechanical loss. Results on tantala/silica optics indicate that UV can cause increased optical absorption and thus this method is not deemed suitable for aLIGO. An interesting variation of this technique utilizes the fact that charging events arising from contact with earthquake stops will deposit charge in this local region. Work at Stanford is currently underway to develop a composite earthquake stop/UV-LED package. The benefit of this approach is that the discharge can be performed without the danger of illuminating the optic surface with UV radiation. Furthermore, there are a number of interesting coating materials for future upgrades to aLIGO and 3rd generation detectors, including AlGaP, AlGaAs, hafnia, zirconia, and others, that might allow for UV charge control, and this line of research is currently being considered. This work is being pursued by a number of groups including American University, Caltech, Glasgow, Hobbart-William-Smith, Stanford and University of West of Scotland.

Experimental work on low energy ions as a way to mitigate charge without the need for UV exposure has also been extensively studied. These ions can be brought into contact with the charged optic through either a partially directional gun or from a low pressure vent of the entire vacuum chamber. UV light is also being explored as a way to generate low energy ions, somewhat combining these two approaches. Work on utilizing a DC glow discharge to generate both polarities of charge carriers in Argon has also been shown to mitigate charge on the surface of fused silica [P1100033]. The technique uses a Faraday cup to maintain a neutral flow of ions which can be used to flow over the surface of the optic. Although tests do not show any absorption change at the level 50 ppm, the possibility of performing further tests in the Stanford photothermal common path interferometer are being considered to verify this approach. Any DC glow discharge technique is likely to be considered a backup to the above ionisation technique. There are other ideas being developed to measure charge and eliminate it as a problem for LIGO optics. Developing and testing finite conductivity coatings for the substrate of the surface of the test masses in order to: a) distribute the charge uniformly with a time constant of less than a few hours and b) allow discharging by "UV electron photoemission wireless" conduction. Work is progressing on conductive layers composed of either zinc oxide, tin oxide [P1100018] or slightly reduced (i.e. oxygen deficient) tantalum pentoxide, and measuring the relationship between electrical conductivity, optical absorption, and mechanical loss. A "UV electron photoemission wireless conduction" system has been developed, and tests verify that it can ground the test mass to less than a 10 V potential. The UV source will consist of UV GaAs LED's and photoelectrons will be generated from the earthquake stops and from the facing surfaces on the side of the test masses. To reduce potential disturbances, no bias and or active controls will be used. Similarly, we have developed an electric field measurement system that meets following requirements: a) compatible with integration into the earthquake stops b) capable of measuring the potential of the test mass opposite the earthquake stops to an accuracy of equal to or better than 10 V. Further tests on the prototype aLIGO suspension

will be pursued.

It would also be useful to directly measure noise from charging, to confirm both the Weiss Markov-process noise model and the parameters found from the Kelvin probe work. Torsion balances, which have been used for laboratory gravity experiments and to test noise models of LISA, offer another possibility to verify Markov noise from charges. Torsion balances are well suited to this since they reach their highest sensitivity at frequencies where Markov charge noise is expected to be large. For charge studies, the torsion pendulum will need to be made entirely of an insulator, likely fused silica, which is a departure from previous experience. The LSC group at the University of Washington, which has experience with torsion pendulums through LISA and other research programs, has performed studies of charging noise [G1000367]. Additional torsion balance experiments are also being developed at University of Glasgow [G1100714] and Moscow State University. In Glasgow, a torsion bob comprising fused silica discs is being utilized to study charge motion on the surface of fused silica and the level of charge deposition when fused silica surfaces come into contact. A Kelvin probe located within the vacuum tank also allows the correlation time to be measured. Initial results suggest that the Weiss theory does give an accurate estimation to the level of charge noise [G1300213, P1300078]. Further tests are planned with zinc oxide coatings which have the possibility of providing well defined characteristic correlation times, thus allowing the level of charge noise to be varied in a reproducible way. Research at Moscow State University is focusing on the exploration of noise associated with dielectric polarization induced when an electrostatic drive (ESD) is operated near a fused silica test mass [G1200166]. The experimental setup includes a monolithic torsion oscillator with frequency of 63 Hz fabricated entirely from fused silica.

There is a wide range of charging research currently underway in the LSC groups. A viable solution to the charging problem for Advanced LIGO exists and additional backup scenarios are under further development. This work is performed in conjunction with the Suspensions Working Group.

5.3 Optics Research and Development for Fourth Generation Detectors

The OWG also conducts directed research for future gravitational wave detectors beyond the third generation. While this research is more speculative and long term, it is clear that research on optical components for future ground-based interferometers must begin well in advance of any complete conceptual design.

6 Suspensions and Vibration Isolation Systems

The research of the Suspension and Isolation Working Group (SWG) is aimed at providing the necessary isolation, alignment, and control of the interferometer optics from seismic and mechanical disturbances while simultaneously ensuring that the displacement due to thermal noise of the suspended systems is at a suitably low level. To first order we can divide the research into two broad subdivisions, suspensions and isolation, both of which involve mechanical and control aspects. Suspension research involves study of the mechanical design of the suspensions, the thermo-mechanical properties of the suspension materials and suitable techniques for damping suspension resonances and applying signals for interferometer control. Isolation system research involves mechanical design and active control for isolation and alignment. The overall isolation of the optics comes from the product of the two systems.

The isolation and suspension system for the most sensitive optics in Advanced LIGO is comprised of three sub-systems: the hydraulic external pre-isolator (HEPI) for low frequency alignment and control, a two-stage hybrid active & passive isolation platform designed to give a factor of 1000 attenuation at 10 Hz, and a quadruple pendulum suspension system that provides passive isolation above a few Hz. The final stage of the suspension consists of a 40 kg silica mirror suspended on fused silica fibers to reduce suspension thermal noise.

The R&D for baseline Advanced LIGO isolation and suspension sub-systems is complete, and assembly and installation and commissioning are now underway. There is ongoing R&D work to provide incremental improvements to Advanced LIGO which could reduce risk, reducing commissioning time, improve performance, enhance robustness, and improve the duty cycle of the aLIGO vibration isolation and suspension. This work is discussed in Sections 6.1 and 6.2.

The LSC has recently set forth a few possible upgrade paths for the Advanced LIGO Interferometers, which are summarized in Section 3.1.

These efforts focus on incorporating Third Generation (3G) technologies into the existing observatories. In this way there will be a continuous transition from the baseline Advanced LIGO configuration to the 3G LIGO detectors. Upgrades to the existing seismic isolation platforms and replacement of the current pendulum suspensions will be necessary to accomplish many of the desired enhancements such as novel mirror coatings, new mirror substrate materials, cryogenic suspensions and optics, and heavy, possibly composite test masses. Additional seismic isolation will be necessary to take advantage of the improved thermal noise of large, cryogenic optics. These upgrades will be installed when Advanced LIGO has made the first detections and completed its science runs, sometime after 2018, according to the schedule described in the Introduction (Section 1).

The R&D for the 4th generation detectors is discussed in section 6.4.

6.1 Vibration Isolation R&D for aLIGO incremental upgrades

6.1.1 Current status and ongoing work

The hydraulic pre-isolation stage (HEPI) is in place at LLO and is being installed at LHO. LIGO requires two variations of the in-vacuum platform, a two-stage active platform for

the BSC and a single-stage platform for the HAM. Both types of platforms are now being installed at LLO and LHO. In addition to the Observatory systems, several prototype platforms are still in operation at the LASTI facility at MIT and the Engineering Test Facility at Stanford and used extensively for development.

6.1.2 Control System Enhancements

Advanced LIGO has an impressive array of sensors and a flexible control system. Most of the baseline Advanced LIGO control schemes use local information to control the seismic platforms and Interferometer readouts to control the interferometer lengths and angles. As system integration proceeds, studies need to be conducted to investigate optimal ways to combine all the sensor information to achieve the best interferometer performance. For example, using feedforward to directly cancel the contribution of ground motion signals which appear in the interferometer signal was demonstrated in Enhanced LIGO [82]. Studies on the coherence between various channels from the ground, up through the seismic platforms and suspension systems to the various interferometer readouts should be conducted. When coherent contributions are found, they could be used to inform the development of advanced control techniques to be layered onto the existing controls. Other control improvements have also been suggested such as optimally distributing the control authority between the isolation stages [33] to improve system locking and robustness, and changing the control laws in real time in response to changing environmental conditions [33, 83]. Another question which needs to be answered is what in particular limits the upper unity gain frequencies of the isolation control loops for the Advanced LIGO seismic isolation platforms? A clear understanding of the practical limits could be used to inform a campaign to modify the platforms to achieve better isolation performance, particularly in the 5 Hz to 40 Hz band.

An interesting risk reduction idea would be to develop a fail-operate control system for the seismic isolation platforms. These systems use position sensors, geophones and seismometers in their control loops. While these instruments have very low failure rates, we cannot exclude the possibility that one of them could stop working during operations, thus compromising the functioning of the platform and the interferometer. It is therefore important to study methods to monitor performance of the sensors, actuators, and the mechanical plant to help mark when the behavior of a component begins to degrade, and to identify which component is malfunctioning. A set of basic matlab scripts have been developed to perform this task [84] but those functions are difficult to use in the observatory environment and can only be used while the interferometer is offline. A realtime estimator system could be developed to continuous compare the expected and actual performance of the system so that diagnostics could be run continuously in the background. In the event of a problem, it is also important to study "emergency control schemes" that would allow the platform to keep operating with a malfunctioning sensor. Feedforward techniques to either compensate for the loss of performance, or possibly reconstruct the lost signal are good candidates. Control schemes accounting for the failure of each type of sensors should be proposed and studied.

6.1.3 Tilt/horizontal coupling and advanced seismometers

One of the limits to the performance of seismic isolation systems is the coupling between ground tilt and horizontal motion of the isolation platforms. This is fundamentally caused by the inability of a horizontal sensor (or a passive horizontal isolation stage) to distinguish between horizontal accelerations and tilts in a gravitational field.

This tilt-horizontal coupling causes a variety of problems and is a basic limit to the performance of the isolation systems at low frequencies (below ∼0.3 Hz) [85]. The aLIGO HEPI and ISI systems are now limited by this coupling at low frequencies, and an external sensor could be easily integrated into the system to reduce amplification of low frequency noise.

Several methods of addressing tilt issues are being pursued. We are developing sensors to measure the rotational acceleration of the ground or of stages of the seismic isolation system in vacuum, which could be used to remove the rotational component, creating a purely translational horizontal sensor. Several rotational sensors are being investigated:

1. pairs of differential vertical seismometers, whose spatial separation would allow us to measure ground tilt [85].
2. Suspended bar tiltmeters are being investigated and these may also yield results on losses in different materials [86, 87].
3. A laser gyroscope operating on the Sagnac principle is being developed. Unlike a traditional ring laser this gyroscope will use a passive cavity to avoid the effects of fluctuations in gas pressure [88].
4. Suspending a horizontal seismometer. This approach is distinct from the others in that the seismometer is made to passively reject tilt noise, thus producing a tilt-free horizontal sensor [89].

When development of these various techniques for addressing tilt-horizontal coupling issues is further advanced a comparison of their relative merits for application to future detectors can be made.

6.1.4 Seismic Platform Interferometer

It is also possible to improve the performance below 1 Hz with an auxiliary system which reduces the differential motion and tilt of the various optical tables in the detector. This type of approach has been discussed for many years, and is traditionally called a 'Suspension Point Interferometer' (SPI), i.e., an interferometric sensor which measures between the points which suspend the arm mirrors [5].

The systems under investigation are slightly different; the method involves controlling the relative motion of the optical tables, and hence an alternative name is Seismic Platform Interferometer. The relative motion of the tables for this system will need to be measured in at least 3 degrees of freedom, namely length, pitch, and yaw. This will allow the detectors to be mounted securely to the table, and will also allow the benefits to be shared by multiple suspensions on the same table, a common situation on the HAM optical tables.

A prototype system has been demonstrated at Stanford [90, 91] using a fiber coupled 1.5 micron laser, which uses a Mach-Zender interferometer to measure the inter-platform length motion and an optical lever to measure differential angles. At the AEI 10m prototype, another SPI prototype is under development. It is based on a set of Mach-Zender interferometers, and use a LISA style phasemeter for readout [92]. The rotational degrees of freedom (DOFs) are sensed via differential wave-front sensing. The target sensitivity is 100 pm/$\sqrt{\text{Hz}}$ and 1 nrad/$\sqrt{\text{Hz}}$ at 10 mHz for displacement and rotational DOFs respectively.

Considerable work remains to adapt either of these systems for use with Advanced LIGO (e.g. stable mechanical coupling to stage 1 of the HAM-ISI or stage 0 of the BSC-ISI, reliable UHV compatible fiber coupling, control integration). In addition, were this system to be used for the 4 km arms, then considerable work would be required to achieve the necessary laser frequency stability required to realize a beneficial system.

It should be noted that improved rotational sensing described in Section 6.1.3 and the SPI are complementary approaches to the low-frequency noise issue. It is also important to realize that since the optical tables for Advanced LIGO are controlled in all 6 degrees of freedom, once new SPI or tilt sensors become available, they can be incorporated into the existing control system easily, because the seismic tables will not require modification.

6.1.5 Pier Motion Control

The motion at the top of the HEPI piers is significantly higher than the ground motion, especially in the horizontal direction. The amplification is due to both pier modes and couplings between the floor and the chamber. Solutions to mitigate this motion amplification should be proposed and studied. Both passive (reinforcement, truss, cross beams, cables) and active solutions (feedback shaker on the chamber, active tendons) should be considered.

6.1.6 Improved Seismic Sensors

Future improvement of the seismic isolation performance will require the use of a very-low-noise inertial instrument, with noise performance roughly a factor of 100 better than today's GS-13. Such an instrument remains to be designed, built and tested. The requirements for the design of this instrument will include: very low sensitivity to temperature gradients, very low thermal noise, very low sensitivity to environmental and actuator electromagnetic fields, and very low readout sensor noise. Both horizontal and vertical instruments will be necessary for future seismic isolation upgrades.

6.2 Suspension R&D for aLIGO Incremental Upgrades

6.2.1 Multiple pendulum suspensions - mechanical and control aspects

The quadruple suspension design for the test masses in Advanced LIGO [93] is based on the triple pendulum suspensions developed for GEO 600. The suspensions for the most sensitive mirrors (those hanging in the BSC chambers) have been designed and fabricated by a team in the UK. Other optics suspensions are the responsibility of the US part of the suspension

team, and consist of triple and double pendulums. Assembly, testing, and installation of the suspensions is now underway at LLO and LHO [94].

Testing of adaptive control schemes have be done [33] to automatically adjust the trade-off between damping strength and feedthrough of sensor noise in the GW band. Tests are also planned to study damping methods of the bounce and roll modes within the monolithic section. As described in section 6.1.2, studies of how to distribute the control authority (hierarchical control) are underway, both for control of a pendulum chain, and also for offloading pendulum control to the seismic isolation system.

Vibration absorbers have been developed to use viton to damp resonances of the support structures of the suspensions. Some risk-reduction characterization, with potential for incremental design improvements, will continue.

Upgrades to specific suspension designs are being considered for future application in Advanced LIGO. The LIGO Lab identifies many of these of potential near-term upgrades in LIGO-T1300176 [95]. Firstly the current size of the beamsplitter (BS) optic (37 cm diameter) was established early in the Advanced LIGO design, and is the limiting optical aperture. We may wish to retrofit a larger beamsplitter optic to enhance optical performance. This will require design changes to the beamsplitter triple suspension itself and its supporting structure. Secondly, noise in the signal recycling cavity (SRC) length coupling into the GW readout may be a greater noise source than we would like. In particular the highest vertical modes (around 28 Hz) in the small and large HAM triple suspensions (HSTS and HLTS) add noise in the GW band. This noise could be addressed by adding a third stage of cantilever springs at the middle masses of the HSTS and HLTSs, taking the vertical mode below 10 Hz and increasing the overall vertical isolation. Work has begun on revised BS and HXTS designs. A third area involving suspension design is the possible redesign of the end reaction masses for lower squeezed film damping, currently discussed under 3rd generation work (Section 6.3.5) but which could be incorporated earlier.

6.2.2 Studies of the monolithic final stage

Extensive characterization (strength, dimensions, mechanical loss) of fused silica fibers as suspension elements [96, 97], produced using both oxy-hydrogen and laser-based pulling techniques [98], has been done. Welding techniques and silicate bonding techniques including characterization of associated losses [99] has been done, along with extensive exploration on the ear shape and fiber shape.

Several monolithic suspensions have been installed in Advanced LIGO. Integration of the suspensions into the Advanced LIGO interferometers will allow the first measurements of the ultimate noise performance of these systems in the 10 Hz to 40 Hz range. As the interferometer noise is improved, participation of experts will be critical to understanding the interferometer performance.

The first integration of a test mass into the interferometer resulted in 2 incidents of fiber breakage, one caused by an impact by a dropped part, and one caused by large excitations from a computer control system error. Studies of possible mechanisms for the fiber break, and methods to prevent future damage are underway.

Several areas of research could yield enhancements to Advanced LIGO suspensions. Further understanding and characterizing of losses in silica fibers including investigations of non-linear thermoelastic noise and of surface losses could lead to improvements. Changes in fiber neck shape including shorter neck and thicker stock could lead to enhanced thermal noise performance.

Research is also underway to further understand the role of weld loss in addition to techniques to observe and ameliorate stress in the weld regions. Furthermore, an increase in strength of the fibers could allow reduction in cross-section and in vertical bounce frequency, enhancing isolation. Investigations of the silicate bond mechanical loss and strength as a function of time and following temperature treatments are underway to reduce further the loss contribution and optimize ear design.

6.2.3 Newtonian Gravitational Noise

Gravity fluctuations caused by density changes close to the test masses generate the so-called Newtonian noise that is predicted to contribute significantly to the strain noise of aLIGO at frequencies below 20Hz. Aiming for further sensitivity improvements at low frequencies with the next detector generation, the development of techniques to mitigate the Newtonian noise will become one of the major challenges.

Several theoretical studies [100, 101, 102] indicate that the dominant contributions to Newtonian noise are due to seismic waves and atmospheric density fluctuations. Furthermore, recent studies at the sites have shown that vibrations of objects and buildings can also contribute significantly [103, 104].

Earth's Surface The most promising approach for suppressing Newtonian noise in surface GW detectors is to design an array of seismometers, microphones, etc measuring perturbations in the ground and atmosphere to derive an estimate of the associated Newtonian noise that is subtracted coherently from the strain signal. This method has recently been tested successfully in numerical simulations [103]. Future work should focus on our understanding of the seismic field and its sources at the LIGO sites, and how certain properties of the seismic field affect the efficiency of the Newtonian noise subtraction. The following list gives an idea of what an R&D program for Newtonian-noise mitigation should include:

- Analysis of data from seismic arrays deployed at the sites to characterize seismic scattering, mode content (e.g. surface versus body waves), identify seismic sources, study variability of seismic fields over longer periods of time, measure wave dispersion.
- A similar effort should be pursued to address atmospheric fluctuations. This includes a monitoring array as well as modelling of the atmospheric density fluctuations.
- Refine Newtonian-noise models based on improved understanding of the seismic fields, and other ambient vibrations or atmospheric perturbations.
- Refine Newtonian-noise subtraction schemes based on improved understanding of the seismic fields, and other ambient vibrations or atmospheric perturbations.

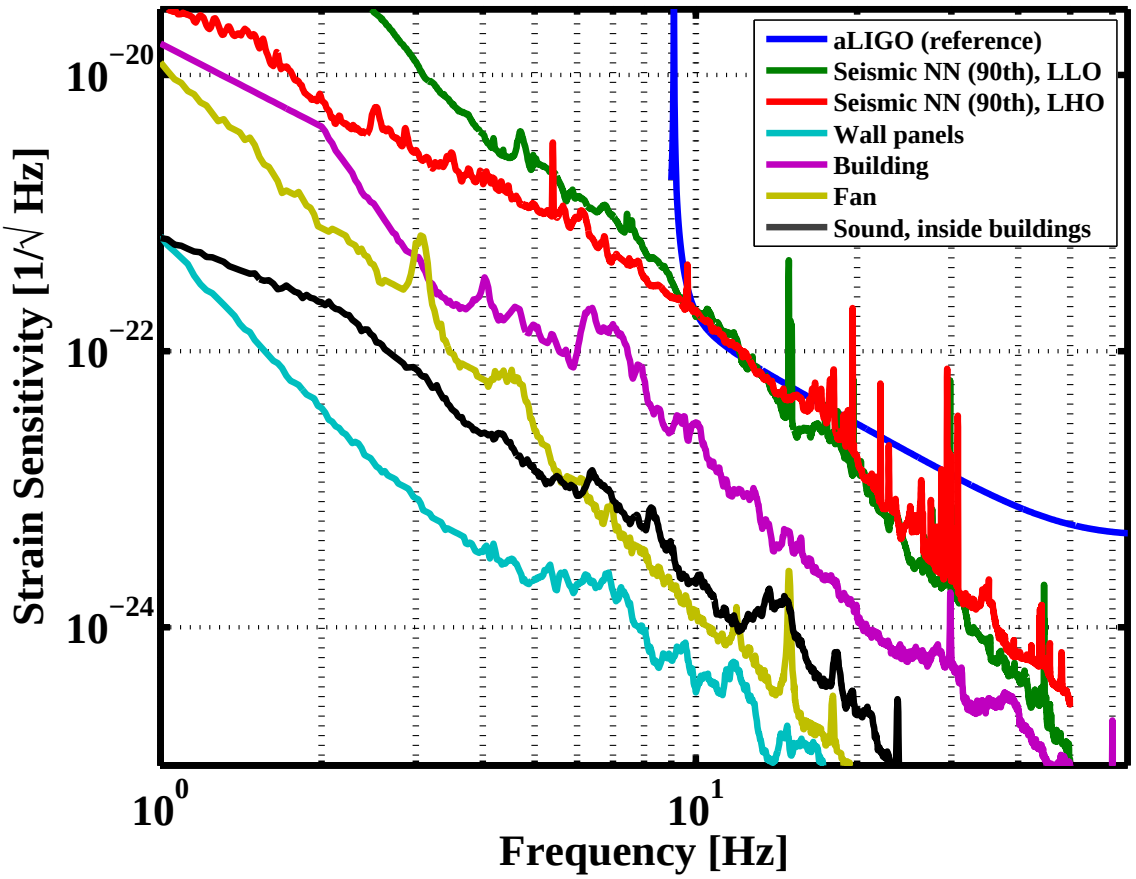

Figure 27: Newtonian noise estimates for the LIGO sites [103]

- Develop accurate models of gravity perturbations originating from vacuum chamber vibrations and rocking motion, and residual vibrations of structures very close to the test mass such as the suspension cages. These models should take into account near-field corrections from higher-order mass moments of the cylindrical test mass.

6.2.4 Violin mode damping

The silica fiber suspensions will have very high Q violin modes (of order 10^8). Such high quality factors make stable control of the interferometer with wide bandwidth more challenging and also lead to long ring-down times after any mechanical excitation. Lower Q values (of order 10^6) lead to easier operation. A prototype optical violin mode sensor has been successfully tested on a dummy suspension with silica fibers at LASTI [105, 106]. However the decision has been taken not to implement violin mode sensing in this form in Advanced LIGO. The need for violin mode damping has not been demonstrated and if it is found to be required we can use Arm Length Stabilization (ALS) system as a sensor.

6.2.5 Mechanical Upconversion: Crackling Noise

Some sources of detectable gravitational waves are expected to produce impulsive, short, rare events in an extremely large body of data, and so characterization and reduction of "background" transients of technical origin is important. Some work on looking for non-thermal noise originating in the fused silica fibers has been carried out with no non-thermal noise being seen at modest sensitivity (insufficient to exclude it as a significant noise source for aLIGO). Work has been done to study the noise associated with the violin modes of the silica suspensions in GEO 600 [107]. Further work is needed to extend these studies by modeling to put upper limits on the expected noise in Advanced LIGO. Direct experiments to characterise the level of and/or put upper limits at a meaningful sensitivity level to potential non-Gaussian transient events associated with the Advanced LIGO suspension system are challenging. However new ideas for carrying out such experiments are encouraged.

One approach which will be pursued to observe the impulsive releases of energy or acoustic emissions ("creak effect") is to strain the element statically while also driving the element through a large amplitude motion at low frequency below the measurement band, while interferometrically measuring the element at high sensitivity in band (above 10 Hz). By large amplitude motion we mean much larger (100∼1000 times) than the out of band motions estimated through modeling. We will when possible drive the large amplitude low frequency motions in a common mode fashion between two identical devices under test while measuring the noise which will be uncorrelated between the two elements.

Experiments of this type are envisaged or underway to measure or put upper limits on noise from maraging steel cantilever blades and separately from silicate bonds.

6.2.6 Control aspects and different payloads

Lock acquisition of the Advanced LIGO detectors is a challenging problem, due to the addition of the signal recycling mirror, the increased finesse of the arm cavities, and the long time needed for core optics to reach thermal equilibrium. Studies of ways to extract better information to set the detector at its operational condition would be of great value to the project. The seismic platform interferometer is an example of this type of device, because it allows some measure of the relative motion of the optics, even when the main gravitational wave interferometer is not running. Studies of additional ways to gain information about the state of the detector could also lead to shorter lock acquisition times and improved duty cycles. Future seismic isolation systems will probably have the same basic system-level function, to reduce the relative motion among payloads in vacuum tanks. However the payloads will change and may include cryogenic systems, larger suspended mirrors that could employ all reflective optics or suspensions that need to dissipate more heat.

6.2.7 Low noise sensors for the suspension system

Improved displacement sensors for the suspension system, which have the range of the existing OSEMs but with lower noise, could be used to increase the damping of pendulum modes without compromising the performance. One example of such a sensor is the 'Euclid' interferometric sensors [108] but further development would be required to integrate those

onto the existing pendulums and to make the sensors UHV compatible. Improved sensors are necessary for 3G detectors.

6.3 3rd Generation Suspensions

A range of techniques appear at first analysis to be worthwhile to pursue. In general, this starts with a program of collecting the present knowledge on the subject and making models and simulations. Small scale experiments follow to allow the utility to be evaluated and the correct path established if interesting. We list some paths currently in exploration.

6.3.1 Cryogenics: Suspension and Isolation aspects

Preliminary investigations of moving to cryogenic temperatures have shown that they can provide significant improvements in the thermal noise, even with test mass temperatures as high as 120 K to 130 K.

The 'Blue Team' design (cf. Section 3.1.3) incorporates radiative coupling of a mass at about 120 K to a cold-shield held at around 77 K.

This design requires test masses and heat links (either to the mass or to the cooling shield) with excellent thermal properties, most likely silicon or sapphire, as described in the following sections. Any cold system will require an ultimate heat sink. Current cryocoolers, even those designed for gravitational wave detectors [109] are not free from vibration, and the heat transport properties of heat links are limited. Thus, it is essential that studies of systems with suspension elements of suitable design and dimensions to provide an efficient path for required heat conduction while still maintaining good thermal noise and mechanical isolation performance be carried out, and followed with experimental demonstrations.

One of the challenges of implementing a cryogenic silicon suspension is extracting the required heat in a reasonable amount of time. A purely radiative cooled suspension with a 143 kg silicon test mass will require cool down periods to 120 K on the order of weeks at best to months at worst. Research is currently underway to investigate the benefits and feasibility of introducing a cool down period which incorporates aggressive cooling technology that would not be permitted during science runs. Current research is focussing on the methods of convectively cooling the suspension in a dry atmosphere and contacting the suspension stages with a movable cold link.

Methods of maintaining room temperature detector infrastructure near the cold suspension stages should be pursued. This issue is particularly relevant for Advanced LIGO hardware that will be reused in a future cryogenic system. Notable components that might be influenced are suspension springs, electronics, and sensors and actuators.

Investigations of materials suitable for construction of elements of the isolation and suspension systems with good properties for use at cryogenic temperatures should be studied ,e.g. silicon carbide which has excellent stiffness to weight ratio (specific stiffness) and low thermal expansion constant and silicon, which has excellent thermal conduction properties and high specific stiffness.

Passive damping of structures at low temperatures is also an area of concern. Viton is

quite lossy at room temperature, and is vacuum compatible, and so is used extensively in Advanced LIGO to help control structural vibrations above 80 Hz. Unfortunately, handbook values [110] indicate that it is not effective at cryogenic temperatures, so investigations into replacements should be undertaken.

6.3.2 Low noise cantilever blade springs and improved suspension thermal noise

There are a variety of techniques being explored which could improve the room temperature thermal noise of the suspensions [111]. It is possible to improve dissipation dilution by increasing suspension length or thickening fibre ends to enhance energy distribution (e.g. 5 mm stock rather than 3 mm stock).

Studies are also underway to understand how to lower the first 'bounce' mode of the test mass. Development of fused silica or silicon blade springs which could be incorporated in the final monolithic stage for improved vertical isolation compatible with lower thermal noise is an attractive option to explore for possible upgrades to Advanced LIGO and future interferometers. Sapphire is also a possible material choice. Experiments are already underway to investigate the breaking stress for such materials when used as blades.

6.3.3 Silicon Suspensions

Silicon has attractive thermal and thermo-mechanical properties making it a strong candidate for the suspension elements in future detectors possibly operating at cryogenic temperatures to reduce thermal noise. It is also conductive which may have advantages for controlling charging effects (discussed elsewhere). Development and measurement of suitable suspension flexure elements, including studies of the optimum material, thermal noise properties, and the geometry and assembly of elements including methods of bonding to test masses are being pursued. Analysis techniques include the use of FEA to study the various contributions to thermal noise such as surface loss and bond loss. Investigation of fabrication techniques, properties of silicon- silicon bonds such as strength and thermal conductivity and thermo-mechanical properties of silicon, for example as a function of doping, are examples of areas which can be addressed.

Attachment techniques A slightly modified version of silicate bonding for silicon-silicon attachment for, e.g., the attachment of interface pieces to silicon test masses is well underway. Strength measurements at both cryogenic and room temperatures of these bonds has shown it is a viable attachment technique and investigations are ongoing to further understand the influence of different parameters on strength like the nature and thickness of the oxide layer required. Bond loss measurements on silicon test masses have also started producing initial results.

Alternative attachment techniques to silicate bonding may be investigated, e.g., to eliminate shear stress in any contact point in the mirror suspensions.

6.3.4 Larger masses

Increasing the mass of the interferometer mirrors will linearly reduce the displacement noise due to (classical and quantum) radiation pressure noise. This research topic requires interfacing between the Optics Working group (see Section 5) and the Suspension and Isolation Working Group.

Particular challenges of a suspension system for such masses include maintaining low suspension thermal noise and high seismic isolation, incorporating actuation, and integrating such a system into a detector.

6.3.5 Gas Damping

Work by colleagues in the LISA area and subsequent follow-up by LSC groups has shown that enhanced gas damping in small gaps could lead to excess noise in aLIGO suspensions [112, 113, 114]. The original design of the aLIGO quad suspension had a 5 mm gap between the test mass and the reaction mass used to apply actuation through electrostatic drive (ESD). We are mitigating this effect in aLIGO with a combination of a thinner compensator plate which forms the reaction mass for the inner test mass, leading to a larger gap, and by aiming to decrease further the pressure in the tanks where the end test masses are situated where the original gap size is needed to allow enough drive. In order to reduce this noise for future detectors we will have to consider alternative ESD or reaction mass geometries, or a completely new kind of actuator.

6.4 R&D Towards Fourth Generation Detectors

Several noise sources all increase steeply as frequency decreases, combining in the Advanced LIGO design to form a noise "wall" at approximately 10 Hz. Thus for any future detector beyond Advanced LIGO, improved performance at frequencies below 10 Hz will require research and development targeted at three areas in particular within the scope of the SWG:

1. reductions in suspension thermal noise
2. improved seismic isolation
3. reduction of Newtonian Gravity Noise (a.k.a. Gravity Gradient Noise)

Forces due to time-varying electric charge is dealt with in the section on Optics. Strawman designs for future interferometric detectors have taken baselines of increased test mass size to reduce the effects of radiation pressure (up to several hundred kg), with suspensions fabricated of alternate materials (e.g., sapphire or silicon) possibly cooled to cryogenic temperatures to reduce thermal noise. These strawman designs, along with the need to reduce gravity gradient noise and increase seismic isolation, thus point towards a set of areas to which current lab R&D can be targeted.

6.4.1 Magnetically Assisted Suspensions

An alternative approach to achieving suppression of seismic noise at low frequencies is to develop magnetically assisted suspensions. The basic idea is to use magnetic fields to partially cancel the gravitational restoring force in a pendulum. This can be achieved, for example, by deploying magnets of opposite polarity on the suspended mass and at the suspension point. The net result is to lower the spring constant of the system, and the corresponding resonant frequency. Preliminary attempts using ∼0.5m long magnetically assisted pendula have demonstrated resonant frequencies below 0.2 Hz (corresponding to ∼6 m long pendula) [**?**]. However, more detailed studies of such systems are needed to understand their applicability to future generations of detectors: tilt, angular degrees of freedom, chainability etc. Most significantly, it is not yet clear that such a system can be made to have low displacement noise in presence of Barkhausen noise.

6.4.2 Newtonian Noise: Underground

Newtonian noise is expected to become increasingly important at frequencies below 10 Hz: at 1 Hz the theoretical expectation for the seismic gravity gradient contribution (strain equivalent) is in the vicinity of $10^{-20}/\sqrt{\text{Hz}}$. Hence, a suppression by a factor of 1000 (or larger) is required in order to reach the strain sensitivity of Advanced LIGO scale ($10^{-23}/\sqrt{\text{Hz}}$) at this frequency.

One of the priorities for the 4G detectors is to probe frequencies below 10 Hz [100]. Consequently, detailed studies of the Newtonian noise are needed. Such studies should be performed both on the surface (potentially enhancing the performance of second-generation detectors) and underground (informing the design of potential 4G detectors). We summarize below some of the directions to be explored.

There are several potential advantages for building underground GW detectors (as compared to the surface). Forces on the mirrors due to atmospheric density fluctuations are reduced; local disturbances (such as humans and their incessant activity) are much reduced and controllable; the seismic noise is expected to be reduced, with the suppression factor depending on the frequency, depth, and the rock structure. The speed of sound (and correspondingly the seismic wavelengths) underground is much larger than on the surface, implying kilometer-scale correlation lengths in the 0.1-10 Hz band. This opens the possibility of having correlated gravity gradients across the entire detector, resulting in a suppression of this noise source. It also implies that an array of seismometers needed for the active suppression of Newtonian noise could be significantly smaller.

Even though it is believed that Newtonian gravity perturbations from the atmosphere and other surface sources like moving objects can largely be avoided by going underground, this is certainly not true anymore when extending the detection band to frequencies below 1 Hz. Atmospheric Newtonian noise is in fact predicted to be the dominant form of Newtonian noise at these frequencies even underground unless the detector depth equals several sound wavelengths.

Accordingly, we propose the following research directions:

Seismic Newtonian noise

- Continue developing the array of underground seismic stations at the Homestake mine [115] (and preferably in other locations as well) to understand the dependence of the seismic noise amplitude, correlation length, and modal structure, on depth, frequency, and rock composition and structure.
- Such studies should be complemented with optical strainmeters, tilt-meters, dilatometers etc, to further understand the modal structure of the seismic noise.
- Pursue R&D to improve the sensitivity of the above instruments if needed.
- As in the surface case, develop a finite element model that would use the above measurements as input to produce an estimate of the Newtonian noise underground. Such a model would determine the size of the array necessary for the active subtraction: volume to be covered, spacing between instruments, number of instruments and their sensitivity requirements etc. The model should include effects such as surface reflection, scattering off of density fluctuations and fault lines etc.
- Study the effects of the cavity size and shape.

Atmospheric and object Newtonian noise

- Characterize atmospheric Newtonian noise with infrasound arrays and develop models of sound propagation at the low-frequency range around 0.1 Hz.
- Ideally complement this study with direct measurements of atmospheric Newtonian noise at frequencies around 0.1 Hz (direct measurements above this frequency are increasingly challenging).
- Study gravity perturbations from moving objects especially below 1 Hz (see section 6.2.3 for studies at higher frequencies).
- Study gravity perturbations from air turbulence.
- The development of alternative methods/sensors to measure air turbulence and infrasound fields over long distances could have significant impact on subtractability of atmospheric Newtonian noise.

7 Lasers and Auxiliary Systems

The Lasers and Auxiliary Systems (LAX) working group developed out of the Lasers working group. In addition to all types of *classical* lasers (squeezing is part of the Quantum Noise WG), this group now includes auxiliary systems which encompasses all technologies which are not part of any of the other working groups.

7.1 Pre-Stabilized Laser

7.1.1 Advanced LIGO Laser - Background

The development of the aLIGO prestabilized laser system (PSL) is effectively finished [116]. A four stage Nd:YVO amplifier system is used to increase the 2 W power of a Nd:YAG non-planar ring-oscillator (NPRO) to 35 W [117]. An injection locked Nd:YAG end-pumped rod system was chosen as the high power oscillator. An output power of more than 200 W was demonstrated in a linear polarized single spatial and frequency mode with such a laser system [118]. The laser has been developed and built by the GEO group in Hannover (Laser Zentrum Hannover (LZH) and Max-Planck-Insitut fr Gravitationsphysik / Albert-Einstein-Institut AEI). The first laser system has been installed at LLO and the other two systems at LHO will follow soon.

The goal of the current phase is to provide technical support to the LIGO-lab and to monitor the long term stability of the laser.

7.1.2 PSL for third generation gravitational wave detector

The road map for the third generation PSL follows the three strawman designs described in section 3.1. The designs call for lasers either at 1064 nm or 1560 nm, compatible with silicon optics. As the final sensitivity depends only on the power inside the interferometer the input power can be traded against power recycling gain without affecting the fundamental noise limits. However, the power recycling gain is limited by the optical losses inside the arm cavities as well as the contrast defect at the beam splitter and typical power levels for a third generation detector are:

- 300 to 700 W laser at 1550-1650 nm
- 1-3 kW at 1064 nm (or 1030 nm)

High power concepts - 1030-1064nm At this time the Nd doped YAG gain medium is the best choice for 100 W class gravitational wave interferometers. However, in the future if kilowatt class lasers become necessary Yb doped YAG, which operates at 1030 nm, could replace the Nd system because of its higher efficiency, lower quantum defect, better thermal management and potentially longer-lived laser diode pumps. Its main disadvantages are that it is a quasi-3-level system at room temperature and thus more sensitive to increased temperatures within the gain medium, and that it has a much lower pump absorption coefficient. However, at cryogenic temperatures, the quasi-3-level system turns into an efficient 4

level system. The Adelaide group demonstrated already 200 W at 1030 nm from a cryogenic Yb:YAG laser using a zig-zag slab [119].

There is a substantial commercial interest driving the development of both Yb lasers and their pump diodes for very high power applications.

High power concepts: 1550-1650nm Erbium doped fiber lasers and Er:YAG lasers emit between 1550 and 1600 nm where the absorption in silicon is expected to be very low. Commercially available erbium fiber systems include a master laser and a fiber amplifier and achieve output powers of 10 W in single mode, single frequency operation and higher power levels are expected in the near future.

The GEO group is currently working on the development of a 1550 nm light source with a power level of 50 W while the Adelaide group plans to transfer their cryogenic Yb:YAG technology to a resonantly pumped cryogenic Er:YAG lasers to generate several 100 W of laser power at 1617 nm.

Additional Requirements Many different applications drive the laser development worldwide and it appears that nearly every year improved laser systems become commercially available. However, there is currently no application which has similar stringent requirements on the temporal and spatial stability as gravitational wave detectors. Hence a specific laser development program for third generation detectors will be required to design and build a reliable laser with sufficiently low free-running noise, an appropriate spatial beam profile and good controllability. Such a program could include spatial mode filters and adaptive optics to improve and match the spatial eigenmode to the interferometer eigenmode.

7.1.3 PSL for fourth generation gravitational wave detectors

Most ideas regarding forth generation gravitational wave detectors target the low frequency performance where the sensitivity is limited by radiation pressure noise, thermal noise and Newtonian noise and not by shot noise or the available laser power. The laser needs for silicon test masses for these detectors can probably be met by third generation PSLs assuming that **both** types of lasers will be developed in time. To further explore the high frequency region of the GW-spectrum, potential further increases of the laser power might be required.

If new test mass materials other than silicon become available changes towards a shorter wavelength might be advantageous. Shorter wavelengths generally require thinner coating layers which could reduce coating thermal noise; however, it should be kept in mind that shorter wavelength also generate smaller beam sizes for identical cavity g-parameters. The general scaling of coating thermal noise with thickness of coating layers and beamsize is in first order independent of the wavelength (for identical cavity g-parameters). The most obvious way to reduce the wavelength is via frequency doubling a powerful 1064 or 1030nm laser but many other laser concepts are currently being explored by industry and many scientific institutions.

High power concepts - spatial mode filtering and adaptive optics To convert distorted laser beam profiles into the target eigenmode of the interferometer either static or dynamic wave front correction systems or passive filtering will be required. Advanced LIGO uses optical cavities (the mode cleaner) to filter the fundamental 00-mode and suppress all higher order modes. This technology is slowly reaching its limits as the high power build up inside these optical cavities starts to distort the filter cavities themselves. Other spatial modes such as Laguerre Gauss 33-modes or Mesa beams require modified filter cavities which are resonant only for these specific spatial modes.

For higher power levels intrinsic problems are expected with the filtering method and hence dynamic adaptive beam correction methods should be designed. These could be based on well known Shack-Hartmann detectors and adaptive optic techniques currently employed in astronomical telescopes. These techniques have also significant commercial potential for many other high power laser applications.

7.1.4 Auxiliary Lasers

Auxiliary lasers serve several functions in interferometric gravitational wave detectors.

- CO_2 lasers at 10 μm are used to write a heating pattern into the compensation plate placed next to the ITM.
- Diode lasers at various wavelengths are used together with Hartmann sensors to sense thermal deformations in the test masses and the compensation plate.
- Frequency doubled Nd:YAG lasers are injected at the end stations for lock acquisition of interferometer length degrees of freedom.

The status and planned R&D on these laser types is described as part of the subsystems they are used in: CO_2 lasers as part of the TCS actuation in Section 7.2, diode lasers for Hartmann sensors as part of TCS sensing and control in the AIC working group.

7.2 Thermal Correction System

The goal of the Thermal Correction System is to optimize the spatial mode inside the interferometer. This spatial mode can be degraded by imperfections in the mirrors caused by radii of curvature or surface figure errors as well as non-homogeneous heating of the optics by the science beam. Untreated, this will reduce the mode matching between the two arm cavities and the recycling cavities and change the beam size inside the interferometer. Advanced LIGO uses ring heaters to optimize the radii of curvatures of the ITMs and ETMs and CO_2 lasers to compensate the thermal lens in the ITM substrate by acting on the compensation plate [25].

7.2.1 Ring Heater

The ring heater has to meet several requirements. It has to generate a homogeneous heating profile with minimal heating of the suspension structure. Its location very close to the test

masses requires that it has to meet very stringent cleanliness requirements. Advanced LIGO is currently using a ringheater which uses nichrome wire wound around a bended glass rod, an alternative design developed by the UF group sandwiches the nichrome wire between two alumina coated aluminum surfaces [120]. Both heaters are embedded inside a gold coated thermal shield to maximize the heat transferred to the mirror and minimize the radiative heat transfer into the suspension.

The heat loss at the end points due to thermal conductivity generates an asymmetric heating profile which will also distort the mirror surface and the thermal lens inside the substrate. At higher heating powers, these asymmetries will start to reduce the optical build-up inside the arm cavities and increase the contrast defect at the beam splitter. The development of ring heaters which produce more symmetric heating profiles could already be crucial for high power operation in Advanced LIGO.

One way to reduce the heating by the ringheater or even eliminate it is to coat the barrel of the optic with a thin layer (a few microns) or an IR reflecting metal such as gold [25]. This would reduce the radial heat flow and homogenize the temperature distribution inside the substrate. Adding a gold barrel coating to the optics would have implication for other aspects of the design, notably thermal noise, charge mitigation, and parametric instabilities. Measurements of the mechanical loss of a thin gold coating indicate that the gold coating can be applied without adversely affecting thermal noise. Gold coating applied to the barrel for thermal compensation purposes might not reduce the optics modal Q's enough to cause significant improvement in parametric instability performance. Tests of a gold coatings interaction with possible charge mitigation schemes, including UV, should be explored. Results of these tests might require follow-ups with other materials and/or coating methods or with additional modeling. This technique may be ready for use in a third generation detector.

7.2.2 CO_2 laser

Power fluctuations of the CO_2 laser are one of the dominant noise sources associated with the TCS. Commercially available CO_2 lasers do not meet the stringent requirements on power stability for Advanced LIGO during high power operation (125 W input power in the science beam) and R&D has started to develop better CO_2 lasers for Advanced LIGO.

A scanning (or, more generally, a directed-beam) thermal compensation system that can vary the compensation profile in real time without injecting noise into the signal band would be very valuable to correct non-radial symmetric beam distortions. Such a system could already be important for high power operation in third generation detectors. This will require research on carbon dioxide or other potential heating lasers, to reduce noise and possibly boost power, and potentially on measurement and control issues. In addition, by moving to shorter wavelengths it might be possible to develop MEMS or other technology based spatial light modulators to allow a programmable heating beam profile.

7.3 Laser Stabilization

Power stabilization will probably be the most demanding laser stabilization task in future gravitational wave detectors. Technical power noise on the laser can couple via many paths

into the gravitational wave channel: asymmetric arms and radiation pressure noise, deviation from the dark fringe, radiation pressure noise. Advanced LIGO requires a relative intensity noise (RIN) of around $10^{-9}/\sqrt{\text{Hz}}$ in the interferometer input beam. The accurate sensing of the needed 500 mW laser power at that location is difficult and the signal is still contaminated by pointing, polarization, and potentially even frequency noise. Ongoing research is needed to understand these couplings and reach the required stabilities.

7.3.1 Photodiodes

Advanced LIGO is currently using four in-vacuum photodiodes in parallel to measure the required 500 mW of light [121]. This is a sub-optimal arrangements for several reasons including reliability and alignment issues. To get a quantum limited measurement of the power fluctuation of 500 mW of light, new photodetectors need to be developed with sufficient power handling capability, spatial uniformity and quantum efficiency. First experiments showed that back-illuminated InGaAs diodes show promising features. However neither the spatial uniformity nor a sufficiently high quantum efficiency has been demonstrated so far. Furthermore current power stabilization experiments seem to be limited by 1/f electronic noise in photodiodes. The origin of this noise needs to be better understood and either the noise source has to be reduced or easily applicable selection criteria need to be found to get the best devices from the available vendors.

Further R&D in close collaboration between the material and device experts, electrical engineers and groups that can test the photodiodes is needed to develop better photodiodes for maybe third but certainly for forth generation gravitational wave detectors.

7.4 Electro- and magneto-optical devices

7.4.1 Electro-Optic Modulators

Length and alignment sensing schemes rely heavily on the generation of optical sidetones which co-propagate with the carrier field into the interferometer. These sidetones are currently generated by RTP-based electro-optic modulators which withstand several 100 W of continuous laser power without degrading the beam profile. Third generation gravitational wave detectors might and forth generation detectors are likely to work at different wavelengths and/or at higher power levels for which suitable electro-optic modulators are not yet available or have not been tested. The main problems encountered in high power applications are photo refractive damage and variations in optical path length across the beam profile caused by the residual absorption of the laser beam.

Photo refractive damage has a fairly well defined threshold in specific nonlinear crystals and can be increased by doping the crystal. The most promising family of crystals in the near infrared region are crystals belonging to the $MTiOXO_4$-family such as RTP; M is an alkaline metal such as K, Rb, or Cs, and X is either P or As. These crystals have fairly large electro-optical coefficients, good thermal properties, and, in principle, very low optical absorption coefficients between 1 and 1.6 um laser wavelength. Optical absorption in the $MTiOXO_4$-family increases at lower wavelength and potentially limits the laser power to a 10's of Watts for visible lasers.

β-barium borate (BBO) and its derivatives are often used in the visible and near-UV region of the spectrum. BBO is uniaxial and has a very high damage threshold. Values larger than 3 kW/cm^2 for cw-light have been quoted by multiple vendors. It's negative thermo-optical coefficient prevents self-focusing. However, the electro-optical coefficient is low compared to other electro-optical crystals and BBO appears to be of limited value unless the laser wavelengths is reduced to well below 500 nm.

Magnesium-oxide doped lithium niobate (MgO:$LiNbO_3$) might be a potential alternative for IR lasers. The doping increases the photo refractive damage threshold significantly [122] and the crystal has a ∼10% larger modulation coefficient than RTP. However, going to laser powers beyond 1kW and laser wavelength below 1 um requires significant testing of electro-optical materials to ensure that electro-optical modulators will be available in time for third generation detectors.

7.4.2 Faraday isolators

Faraday isolators are required to separate the counter-propagating beam from the incoming beam. The aLIGO Faraday isolators use TGG as the Faraday material. The TGG rotates the polarization angle by an amount proportional to the length of the crystal, the Verdet constant, and to the applied magnetic field. The main issues with the Faraday isolator are beam distortion due to laser heating and subsequent thermal lensing, a reduction of the optical isolation due to depolarization and changes in the temperature dependent Verdet constant. This is further complicated by the fact that the FI is usually placed inside the vacuum chamber following the suspended input optic mode cleaner.

The aLIGO Faraday isolator uses two TGG crystals, a quartz rotator, and a waveplate to compensate the depolarization inside the TGG crystals. The radial symmetric thermal lensing is then compensated with a DKDP crystal which has a negative thermo-optic coefficient. Scaling this to kW-class power levels requires further reductions in the optical absorption in TGG while the large number of components already increases the number of ghost beams significantly. Other options are to increase the Verdet constant by cooling the crystal, to use stronger magnetic fields, and to use other magneto-optical materials such as GGG or YAG.

Increased absorption in TGG will likely prevent us from using it at wavelength longer than 1.3 μm. But the telecommunication sector developed ferromagnetic rare earth iron garnets (RIGs) such as yttrium iron garnet (YIG) and more recently $\{BiRE\}_3(FeGaAl)_5O_{12}$ to rotate the polarization. Unlike paramagnetic Faraday materials, these ferromagnetic materials can be magnetized such that they don't require any external magnetic field. These materials are typically grown in sub-mm thick films on lattice-matched substrates such as GGG for 45 deg rotation. However, the absorption is still in the 1-10 ppm/cm range at interesting wavelengths which prohibits high power laser operation. At shorter wavelength, optical absorption increases in all materials pronouncing thermal effects. Faraday isolators using potassium dihydrogen phosphate (KDP) and its isomorphs have been developed for the UV but the absorption is still fairly high. A targeted research program to study these materials at higher power levels at all interesting wavelength is required to develop Faraday isolators for the next generation of gravitational wave detectors.

Faraday Isolator in Squeezing Systems The power handling capabilities of the output Faraday isolator are far less critical. However, the optical losses inside the Faraday would currently limit the amount of useable squeezing. Since squeezing is one of the leading ideas to third generation detectors, any improvement in the optical losses could directly improve the range of these detectors.

Figure 28 shows how the losses in the squeezed beam path are strongly affecting the amount of squeezing detectable in the interferometer and therefore the improvement in the sensitivity. With 10 dB of squeezing injected, for instance, the losses need to be less than 20% in order to be able to detect at least 6 dB of squeezing.

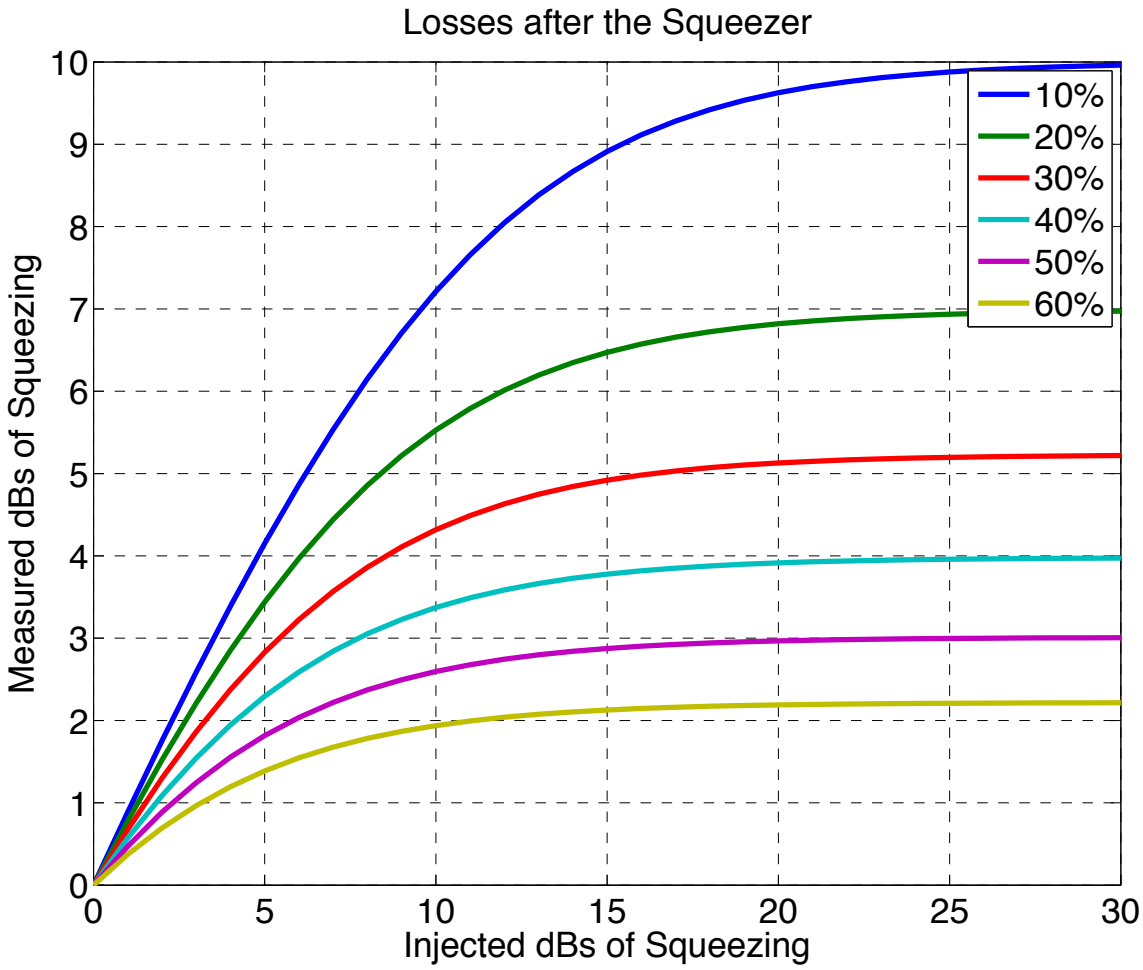

Figure 28: Measured squeezing as function of the injected squeezing for different levels of losses in the squeezed path.

In a typical layout for injecting squeezing in the interferometer the squeezed beam needs to pass through not only the main output Faraday of the IFO (twice), but also at least one additional Faraday to isolate the interferometer from the squeezer and mitigate noise from back scattered light. The losses of the new Advanced LIGO Faraday have been measured to be $\sim$ 4%. Similar measurements in initial LIGO Faradays give losses of 4 - 6%. With the current losses the Faradays themselves will account for about 15% of the losses in the squeezed path. In order to maximize the benefit from the injection of squeezed light, it is

important to reduce the losses of a single Faraday to 1 - 2%.

For the main dark port Faraday, it is also important to reduce the amount of light which leaks into the squeezed beam path, as this is a source of noise once it is back scattered back into the IFO from the squeezer source. In the new Advanced LIGO Faraday about 0.5% of the light which passes through the Faraday is reflected by the thin film polarizer. By improving the mechanical design of the Faraday one can hope to reduce this percentage down to ∼0.01%.

7.5 Cryogenics

It has long been known that cryogenically cooled test masses can have much improved material parameters which lead to significant reductions in thermal noise. However, operating at cryogenic temperatures presents multiple new challenges which need to be addressed. The most pressing is to find ways to cool the temperature, to isolate the mirrors from their hot surroundings and to constantly extract the deposited laser heat without short-circuiting the suspension and seismic isolation system. Detailed thermal models have to be developed and tested to maximize radiative and conductive cooling paths.

An additional challenge is the strong possibility of contamination through condensation on the surfaces. Methods will need to be developed to (i) mitigate the level of contamination in cryogenic mirrors, (ii) quantify the magnitude and type of contaminants, and (iii) if necessary, clean contaminated mirrors in situ. One idea which should be pursued is to use fs laser spectroscopy to identify the contaminant and potentially also to remove it.

7.5.1 Cryogenics: Radiative Cooling

Operation at cryogenic temperatures poses formidable challenges including heat extraction from the cooled test masses, required both under steady state operation and for cooling from room temperature in a reasonable time. The system needs to work without adding noise or short-circuiting the mechanical isolation. In the steady state, the circulating power may be in the range 0.5 to 1 MW, and with anticipated coating losses of 0.5 to 1 ppm, power loss in the arm coatings is of order 0.3 to 1 W per optic. For cooling a reasonable estimate is between 2 and 100 W of heat conduction from the test masses to the cold environment.

Studies are underway of a novel method of heat removal: near-field radiative coupling between two objects: one hot and one cold. The basic idea is that many thermal fluctuations in the hot object do not couple to radiation; instead, they produce evanescent fields outside the object. If a cold object with appropriate properties is introduced into this evanescent field region, energy is transferred, cooling the hot object. This approach is potentially capable of removing more than 200 W from a test mass. The heat transfer can be greatly enhanced using a small gap but this is accompanied by force coupling and this effect needs to be taken into account. Room-temperature experiments to explore this method of heat transfer have observed and are characterizing in detail the heat transfer in the near-field regime. Cryogenic experiments are planned, as are measurements to determine the effects of coatings on the heat transfer, and to attempt to optimize the coatings for maximum transfer with spacing around 0.1-1 μm.

7.6 Beam Shaping

Mirror thermal noise is one of the fundamental factors limiting the sensitivity of gravitational wave detectors. A Gaussian beam profile is not the best shape to average over thermal fluctuations and different, carefully chosen shapes allow for sensitivity improvements. Non-spherical mirrors, shaped to support flat intensity mesa profile beams, have been designed and fabricated using specialized coating techniques. These mirrors are being tested on a dedicated interferometer to assess ease of mode-matching and locking. Recent efforts have shown that the tilt sensitivity of the fundamental mesa mode agrees with expectations. It is possible to extend this study, producing useful alignment correction signals via the wavefront sensing technique. The Sidles-Sigg tilt instabilities must also be examined. In addition, continued modeling needs to examine how thermal effects alter the mode profile in a detector arm cavity and help develop thermal compensation strategies. One option involves depositing a static thermal compensation profile to mitigate these effects.

Modeling and experimental work is being carried out on Laguerre-Gauss and other optical modes that show promise for reducing thermal noise. Laguerre-Gauss modes may avoid some of the instability issues that cause concern with mesa beams. There are, however, questions about the strict requirements on the figure and polish of the optics necessary for these higher order modes. There has been modeling of the effects of different beam shapes on parametric instabilities. Further modeling and experimental testing will be necessary to truly evaluate the potential and limitations of these beam shapes.

7.7 Other auxiliiary systems

7.7.1 Photon Calibrator

The calibration of the interferometer requires to move the mirrors by a known amount and observe the changes in the gravitational wave channel. One way to apply the required forces to the test masses is photon pressure. This photon calibrator uses an amplitude modulated auxiliary laser which is reflected off the test mass. The integration, calibration, and performance of the photon calibrator is still an ongoing research subject and will already be tested in Advanced LIGO.

A Advanced LIGO Installation Status

The project started officially in April of 2008 after years of focused research and development in the LSC. aLIGO is fully funded to date, is three-quarters complete in the formal project earned-value system (as of June 2012). In a change in scope in June 2012 the Project baseline was modified to build three 4-km armlength Advanced LIGO detectors in total, and to install one in Livingston, one 4 km in Hanford, and to place the third detector in storage for ultimate installation in a new facility to be constructed in India.

All of the subsystems have completed design, most of the hardware fabrication is done, and the first components are in June 2012 being installed and readied for integrated testing (of a 4km long single cavity using a pre-lock length stabilization system, and of the suspended mode-cleaner with the pre-stabilized laser). The two US-based instruments are planned to be installed by 2013, and capable of being locked for a few hours at a time by mid-2014. It is expected that the third LIGO-India instrument will be observing in 2020.

A.1 Overview of the Sub-Systems

- **FMP** The Facilities have been changed to move the Hanford 2 km test mass chambers to 4 km (although with the advent of LIGO-India, those chambers are not planned to be used for the immediate future), and the input-output tubes were increased in diameter to accommodate wider beam paths.

- **SEI** The seismic isolation is now more active, with servo-control systems to hold isolate against vibrations in the 0.1-10 Hz band. Several units of both kinds – test mass 'BSC' chambers and multi-use HAM chambers – have been installed, tested, and accepted.

- **SUS** The suspensions for the test masses have four pendulums in series (a quadruple design based on GEO-600 triple suspensions) with the final stage made of fused silica to reduce thermal noise. Several suspensions have been installed.

- **PSL** The pre-stabilized laser supplies 200 W (as compared with 35 W in eLIGO) of frequency, amplitude, and position stabilized light. The two U.S. lasers are in place and operating, and the third LIGO-India laser is ready for shipping.

- **IOO** The input optics employ a similar configuration to initial LIGO but capable of handling the full laser power. All main optics and most smaller auxiliary optics, modulators, and isolators have been received; the components shared on the laser table are installed, and several of the in-vacuum suspended optics, in their triple suspensions, as well.

- **COC** The test masses are fused silica, 40 kg to reduce the motion from radiation pressure noise, and 32 cm diameter to reduce the thermal noise. The coating is also optimized to reduce its thermal noise. All substrates have been very successfully polished. Several input test masses with suitable HR coatings have been received. The coating vendor is making progress on meeting hte end test mass coatings.

- **AOS** The Auxiliary Optics System includes thermal compensation, a baffling design to combat scattered light, initial alignment, photon calibration, and coupling of light out of the interferometer. This is the last subsystem to complete design, and the first baffles and in-vacuum thermal-compensation components have been fabricated and installed.

- **ISC** A signal recycling cavity is added to the power-recycled Fabry-Perot interferometer to allow tuning for astrophysical sources and to manage quantum noise. There is a pre-lock arm-length stabilization system to aid and accelerate locking. This pre-lock system will be tested in the 4km-arm integrated test to start in June 2012.

- **DAQ** The data acquisition system can handle the significant increase in channels due to the active seismic isolation and multi-stage suspension, and delivers low-latency data via several means. This system has been installed.

- **DCS** The project includes a significant computing capability for the data analysis. This system will be procured close to the end of the project to allow Moore's 'law' to help get the desired computing power with the least cost.

The ever-improving understanding of what we can actually build has not led to any significant changes inour expectation for the ultimate performance (see Fig. 2). There are now well-developed plans for the incremental approach to those curves. The first activity will be a single 4 km Fabry-Perot cavity at Hanford, locked with an Arm Length Stabilization system, with integrated testing starting in June 2012. The hardware elements for that are now installed and pumpdown of the chambers is underway.

At Livingston, we are gearing up to make a power recycled Michelson interferometer with the two near mirrors of the arm cavities as the initial integration focus, with integrated testing starting in Summer 2012. All components are installed in one of the two mode-cleaner 'HAM' vacuum chambers, and the other is being populated in June 2012.

A.2 Further Reading

- M060056: Advanced LIGO Reference Design

- G1000061: aLIGO Current Installation Schedule

- P0900255: Advanced LIGO: The next generation of gravitational wave detectors

References

[1] Einstein Telescope Science Team, "Einstein gravitational wave Telescope conceptual design study," *ET Document: ET-0106C-10*, 2011. http://www.et-gw.eu/.

[2] C. D. Ott, Y. Chen, and R. X. Adhikari, "Astrophysical Motivations for the Third Generation LIGO Detectors," *LIGO Document: LIGO-P1200099*, 2012. https://dcc.ligo.org/cgi-bin/private/DocDB/ShowDocument?docid=87934.

[3] R. Adhikari, K. Arai, S. Hild, S. Ballmer, and E. Gustafson, "LIGO III Strawman Design Workshop Report," *LIGO Document: LIGO-T1200031*, 2012. https://dcc.ligo.org/cgi-bin/private/DocDB/ShowDocument?docid=85610.

[4] S. Hild, B. Barr, A. Bell, C. Bell, C. Bond, D. Brown, F. Brueckner, L. Carbone, K. Craig, A. Cumming, S. Danilishin, K. Dooley, A. Freise, T. Fricke, P. Fulda, S. Giampanis, N. Gordon, H. Grote, G. Hammond, J. Harms, J. Hough, S. Huttner, R. Kumar, H. Lück, N. Lockerbie, J. Macarthur, I. Martin, P. Murray, S. Reid, S. Rowan, D. Shoemaker, B. Sorazu, K. Strain, S. Tarabrin, K. Tokmakov, and N. Voronchev, "LIGO 3 Strawman Design, Team Red," *LIGO Document: LIGO-T1200005*, 2012. https://dcc.ligo.org/cgi-bin/private/DocDB/ShowDocument?docid=78100.

[5] Y. Aso, M. Ando, K. Kawabe, S. Otsuka, and K. Tsubono, "Stabilization of a Fabry–Perot interferometer using a suspension-point interferometer," *Phys. Lett. A*, **327**, no. 1, pp. 1–8, 2004. http://dx.doi.org/10.1016/j.physleta.2004.04.066.

[6] Y. Aso, M. Ando, S. Otsuka, and K. Tsubono, "Active vibration isolation using a Suspension Point Interferometer," *J. Phys.: Conf. Ser.*, **32**, pp. 451–456, 2006. http://dx.doi.org/10.1088/1742-6596/32/1/069.

[7] R. Abbott, R. Adhikari, S. Ballmer, L. Barsotti, M. Evans, P. Fritschel, V. Frolov, G. Mueller, B. Slagmolen, and S. Waldman, "AdvLIGO Interferometer Sensing and Control Conceptual Design," *LIGO Document: LIGO-T070247-01*, 2007. https://dcc.ligo.org/cgi-bin/DocDB/ShowDocument?docid=5306.

[8] K. Arai, M. Ando, S. Moriwaki, K. Kawabe, and K. Tsubono, "New signal extraction scheme with harmonic demodulation for power-recycled Fabry-Perot-Michelson interferometers," *Phys. Lett. A*, **273**, pp. 15–24, 2000. http://dx.doi.org/10.1016/S0375-9601(00)00467-9.

[9] J. Abadie and et al., "Squeezed light injection in a gravitational wave detector," *in preparation*, 2012.

[10] T. Fricke, N. Smith-Lefebvre, R. Abbott, R. Adhikari, K. L. Dooley, M. Evans, P. Fritschel, V. Frolov, K. Kawabe, J. S. Kissel, and S. Waldman, "DC readout experiment in Enhanced LIGO," *Class. Quantum Grav.*, 2012. http://dx.doi.org/10.1088/0264-9381/29/6/065005.

[11] The LIGO Scientific Collaboration, J. Abadie, B. P. Abbott, R. Abbott, T. D. Abbott, M. Abernathy, C. Adams, R. Adhikari, C. Affeldt, B. Allen, and et al., "A gravitational

wave observatory operating beyond the quantum shot-noise limit," *Nature Physics*, **7**, pp. 962–965, 2011. http://dx.doi.org/10.1038/nphys2083.

[12] S. Hild, H. Grote, J. Degallaix, S. Chelkowski, K. Danzmann, A. Freise, M. Hewitson, J. Hough, H. Lück, M. Prijatelj, K. A. Strain, J. R. Smith, and B. Willke, "DC-readout of a signal-recycled gravitational wave detector," *Class. Quantum Grav.*, **26**, no. 5, 055012, 2009. http://dx.doi.org/10.1088/0264-9381/26/5/055012.

[13] K. Goda, O. Miyakawa, E. E. Mikhailov, S. Saraf, R. Adhikari, K. McKenzie, R. Ward, S. Vass, A. J. Weinstein, and N. Mavalvala, "A quantum-enhanced prototype gravitational-wave detector," *Nature Physics*, **4**, pp. 472–476, 2008. http://dx.doi.org/10.1038/nphys920.

[14] O. Miyakawa, R. Ward, R. Adhikari, M. Evans, B. Abbott, R. Bork, D. Busby, J. Heefner, A. Ivanov, M. Smith, R. Taylor, S. Vass, A. Weinstein, M. Varvella, S. Kawamura, F. Kawazoe, S. Sakata, and C. Mow-Lowry, "Measurement of optical response of a detuned resonant sideband extraction gravitational wave detector," *Phys. Rev. D*, **74**, 022001, 2006. http://link.aps.org/doi/10.1103/PhysRevD.74.022001.

[15] R. L. Ward, R. Adhikari, B. Abbott, R. Abbott, D. Barron, R. Bork, T. Fricke, V. Frolov, J. Heefner, A. Ivanov, O. Miyakawa, K. McKenzie, B. Slagmolen, M. Smith, R. Taylor, S. Vass, S. Waldman, and A. Weinstein, "DC readout experiment at the Caltech 40m prototype interferometer," *Class. Quantum Grav.*, **25**, no. 11, 114030, 2008. http://dx.doi.org/10.1088/0264-9381/25/11/114030.

[16] S. Hild, H. Grote, M. Hewitson, H. Lück, J. R. Smith, K. A. Strain, B. Willke, and K. Danzmann, "Demonstration and comparison of tuned and detuned signal recycling in a large-scale gravitational wave detector," *Class. Quantum Grav.*, **24**, no. 6, 1513, 2007. http://dx.doi.org/10.1088/0264-9381/24/6/009.

[17] R. L. Ward, *Length Sensing and Control of an Advanced Prototype Interferometric Gravitational Wave Detector*. PhD thesis, California Institute of Technology, 2010. https://dcc.ligo.org/cgi-bin/private/DocDB/ShowDocument?docid=9237.

[18] M. Evans, P. Fritschel, D. McClelland, J. Miller, A. Mullavey, D. Shaddock, B. Slagmolen, S. Waldman, and et al., "Adv. LIGO Arm Length Stabilization Design," *LIGO Document: LIGO-T0900144*, 2012. https://dcc.ligo.org/cgi-bin/private/DocDB/ShowDocument?docid=1625.

[19] A. J. Mullavey, B. J. J. Slagmolen, J. Miller, M. Evans, P. Fritschel, D. Sigg, S. J. Waldman, D. A. Shaddock, and D. E. McClelland, "Arm-length stabilisation for interferometric gravitational-wave detectors using frequency-doubled auxiliary lasers," *Opt. Express*, **20**, pp. 81–89, 2012. http://dx.doi.org/10.1364/OE.20.000081.

[20] K. Izumi, K. Arai, B. Barr, J. Betzwieser, A. Brooks, K. Dahl, S. Doravari, J. C. Driggers, W. Z. Korth, H. Miao, J. G. Rollins, S. Vass, D. Yeaton-Massey, and R. Adhikari, "Multi-color Cavity Metrology," *LIGO Document: LIGO-P1200019*, 2012. https://dcc.ligo.org/cgi-bin/private/DocDB/ShowDocument?docid=87878.

[21] N. Smith-Lefebvre and N. Mavalvala, "Modematching feedback control for interferometers with an output mode cleaner," *LIGO Document: LIGO-P1200034*, 2012. https://dcc.ligo.org/cgi-bin/private/DocDB/ShowDocument?docid=89076.

[22] J. A. Sidles and D. Sigg, "Optical torques in suspended Fabry–Perot interferometers," *Phys. Lett. A*, **354**, pp. 167–172, 2006. http://dx.doi.org/10.1016/j.physleta.2006.01.051.

[23] N. Smith-Lefebvre, S. Ballmer, M. Evans, S. Waldman, K. Kawabe, V. Frolov, and N. Mavalvala, "Optimal alignment sensing of a readout mode cleaner cavity," *Opt. Lett.*, **36**, no. 22, pp. 4365–4367, 2011. http://dx.doi.org/10.1364/OL.36.004365.

[24] M. Smith, K. Mailand, A. Brooks, and P. Willems, "Advanced LIGO Thermal Compensation System Preliminary Design," *LIGO Document: LIGO-T0900304-v2*, 2009. https://dcc.ligo.org/cgi-bin/private/DocDB/ShowDocument?docid=3162.

[25] M. Evans and P. Fritschel, "TCS and the Golden Shield," *LIGO Document: LIGO-T0900359-v2*, 2009. https://dcc.ligo.org/cgi-bin/private/DocDB/ShowDocument?docid=3967.

[26] R. Lawrence, *Active Wavefront Correction in Laser Interferometric Gravitational Wave Detectors*. PhD thesis, Massachusetts Institute of Technology, 2003. http://dspace.mit.edu/handle/1721.1/29308.

[27] P. Willems, "TCS Actuator Noise Couplings," *LIGO Document, LIGO-T060224-v7*, 2006. https://dcc.ligo.org/cgi-bin/private/DocDB/ShowDocument?docid=9248.

[28] H. Yamamoto, "SIS (Stationary Interferometer Simulation) manual," *LIGO Document, LIGO-T070039-v6*, 2007. https://dcc.ligo.org/cgi-bin/DocDB/ShowDocument?docid=160.

[29] P. Willems, "Implications of ETM02 HR Coating Absorption for Thermal Compensation," *LIGO Document, LIGO-T1100250-v2*, 2011. https://dcc.ligo.org/cgi-bin/private/DocDB/ShowDocument?docid=60664.

[30] A. F. Brooks and et al., "Ultra-sensitive wavefront measurement using a Hartmann sensor," *Opt. Express*, **15**, pp. 10370–10375, 2007. http://www.opticsinfobase.org/oe/abstract.cfm?uri=oe-15-16-10370.

[31] A. F. Brooks, *Hartmann Wavefront Sensors for Advanced Gravitational Wave Interferometers*. PhD thesis, The University of Adelaide, 2007. http://digital.library.adelaide.edu.au/dspace/handle/2440/57100.

[32] J. C. Driggers, M. Evans, K. Pepper, and R. Adhikari, "Active noise cancellation in a suspended interferometer," *Rev. Sci. Instrum.*, **83**, 2012. http://dx.doi.org/10.1063/1.3675891.

[33] B. N. Shapiro, *Adaptive Modal Damping for Advance LIGO Suspensions*. PhD thesis, Massachusetts Institute of Technology, 2012. https://dcc.ligo.org/cgi-bin/private/DocDB/ShowDocument?docid=91198.

[34] K. Arai, J. Betzwieser, P. Kalmus, and R. Adhikari, "Simulated Plant Approach," *LIGO Document: LIGO-G1000546*, 2010. https://dcc.ligo.org/cgi-bin/private/DocDB/ShowDocument?docid=11804.

[35] H. Yamamoto, B. Bhawal, M. Evans, E. Maros, M. Rakhmanov, J. R. L. Savage, G. Cella, S. Klimenko, and S. Mohanty, "End to End Simulation Program for Gravitational-Wave Detectors," , in *Gravitational Wave Detection II* (S. Kawamura and N. Mio, eds.), vol. 32 of *Frontiers Science Series*, pp. 331–336, Universal Academy Press, 2000.

[36] LIGO, "GWINC: Gravitational Wave Interferometer Noise Calculator." http://ilog.ligo-wa.caltech.edu:7285/advligo/GWINC.

[37] A. Freise, "FINESSE." http://www.gwoptics.org/finesse/.

[38] T. Corbitt, Y. Chen, and N. Mavalvala, "Mathematical framework for simulation of quantum fields in complex interferometers using the two-photon formalism," *Physical Review A*, **72**, pp. 013818+, July 2005. http://dx.doi.org/10.1103/physreva.72.013818.

[39] T. Corbitt and N. Mavalvala, "Review: Quantum noise in gravitational-wave interferometers," *Journal of Optics B: Quantum and Semiclassical Optics*, **6**, no. 8, S675, 2004. http://dx.doi.org/10.1088/1464-4266/6/8/008.

[40] Y. Chen, "Macroscopic quantum mechanics: theory and experimental concepts of optomechanics," *Journal of Physics B Atomic Molecular Physics*, **46**, 104001, May 2013.

[41] H. J. Kimble, Y. Levin, A. B. Matsko, K. S. Thorne, and S. P. Vyatchanin, "Conversion of conventional gravitational-wave interferometers into quantum nondemolition interferometers by modifying their input and/or output optics," *Phys. Rev. D*, **65**, 022002, 2001. http://link.aps.org/doi/10.1103/PhysRevD.65.022002.

[42] S. P. Vyatchanin and E. A. Zubova, "Quantum variation measurement of a force," *Phys. Lett. A*, **201**, pp. 269–274, 1995. http://dx.doi.org/10.1016/0375-9601(95)00280-G.

[43] F. Y. Khalili and Y. Levin, "Speed meter as a quantum nondemolition measuring device for force," *Phys. Rev. D*, **54**, pp. 4735–4737, 1996. http://link.aps.org/doi/10.1103/PhysRevD.54.4735.

[44] P. Purdue, "Analysis of a quantum nondemolition speed-meter interferometer," *Phys. Rev. D*, **66**, 022001, 2002. http://link.aps.org/doi/10.1103/PhysRevD.66.022001.

[45] P. Purdue and Y. Chen, "Practical speed meter designs for quantum nondemolition gravitational-wave interferometers," *Phys. Rev. D*, **66**, 122004, 2002. http://link.aps.org/doi/10.1103/PhysRevD.66.122004.

[46] Y. Chen, "Sagnac interferometer as a speed-meter-type, quantum-nondemolition gravitational-wave detector," *Phys. Rev. D*, **67**, 122004, 2003. http://link.aps.org/doi/10.1103/PhysRevD.67.122004.

[47] H. Rehbein, H. Müller-Ebhardt, K. Somiya, S. L. Danilishin, R. Schnabel, K. Danzmann, and Y. Chen, "Double optical spring enhancement for gravitational-wave detectors," *Phys. Rev. D*, **78**, 062003, 2008. http://link.aps.org/doi/10.1103/PhysRevD.78.062003.

[48] H. Rehbein, H. Müller-Ebhardt, K. Somiya, C. Li, R. Schnabel, K. Danzmann, and Y. Chen, "Local readout enhancement for detuned signal-recycling interferometers," *Phys. Rev. D*, **76**, 062002, 2007. http://link.aps.org/doi/10.1103/PhysRevD.76.062002.

[49] A. Buonanno and Y. Chen, "Scaling law in signal recycled laser-interferometer gravitational-wave detectors," *Phys. Rev. D*, **67**, 062002, 2003. http://link.aps.org/doi/10.1103/PhysRevD.67.062002.

[50] V. B. Braginsky and F. Y. Khalili, *Quantum Measurement*. ed. K. S. Thorne, Cambridge University Press, 1992. http://www.amazon.com/Quantum-Measurement-Vladimir-B-Braginsky/dp/052141928X.

[51] A. Wade, K. Mckenzie, Y. Chen, D. Shaddock, J. Chow, and D. McClelland, "A Polarization Speed Meter for Gravitational-Wave Detection," *LIGO Document: P1100205*, 2011. https://dcc.ligo.org/cgi-bin/private/DocDB/ShowDocument?docid=77471.

[52] H. Miao, H. Yang, R. Adhikari, and Y. Chen, "Comparison of Quantum Noise in 3G Interferometer Configurations," *LIGO Document: LIGO-T1200008-v3*, 2012. https://dcc.ligo.org/cgi-bin/private/DocDB/ShowDocument?docid=78229.

[53] N. A. Robertson, G. Cagnoli, D. R. M. Crooks, E. Elliffe, J. E. Faller, P. Fritschel, S. Goßler, A. Grant, A. Heptonstall, J. Hough, H. Lück, R. Mittleman, M. Perreur-Lloyd, M. V. Plissi, S. Rowan, D. H. Shoemaker, P. H. Sneddon, K. A. Strain, C. I. Torrie, H. Ward, and P. Willems, "Quadruple suspension design for Advanced LIGO," *Class. Quantum Grav.*, **19**, pp. 4043–4058, 2002.

[54] A. V. Cumming, A. S. Bell, L. Barsotti, M. A. Barton, G. Cagnoli, D. Cook, L. Cunningham, M. Evans, G. D. Hammond, G. M. Harry, A. Heptonstall, J. Hough, R. Jones, R. Kumar, R. Mittleman, N. A. Robertson, S. Rowan, B. Shapiro, K. A. Strain, K. Tokmakov, C. Torrie, and A. A. van Veggel, "Design and development of the advanced LIGO monolithic fused silica suspension," *Class. Quantum Grav.*, **29**, no. 3, 035003, 2012. http://stacks.iop.org/0264-9381/29/i=3/a=035003.

[55] N. A. Robertson for the LSC, "Seismic isolation and suspension systems for Advanced LIGO," *Proceedings of SPIE*, **5500**, 81, 2004.

[56] P. R. Saulson, "Terrestrial gravitational noise on a gravitational wave antenna," *Phys. Rev. D*, **30**, pp. 732–736, 1984.

[57] J. C. Driggers, J. Harms, and R. Adhikari, "Newtonian noise subtraction." in prep., 2012.

[58] G. M. Harry, M. R. Abernathy, A. E. Becerra-Toledo, H. Armandula, E. Black, K. Dooley, M. Eichenfield, C. Nwabugwu, A. Villar, D. R. M. Crooks, G. Cagnoli, J. Hough, C. R. How, I. MacLaren, P. Murray, S. Reid, S. Rowan, P. H. Sneddon, M. M. Fejer, R. Route, S. D. Penn, P. Ganau, J.-M. Mackowski, C. Michel, L. Pinard, and A. Remillieux, "Titania-doped tantala/silica coatings for gravitational-wave detection," *Class. Quantum Grav.*, **24**, no. 2, 405, 2007.

[59] T. Hong, H. Yang, E. K. Gustafson, R. Adhikari, and Y. Chen, "Brownian Thermal Noise in Multlayer Coated Mirrors," *in prep.*, 2012. in prep.

[60] G. de Vine, D. A. Shaddock, and D. E. McClelland, "Variable reflectivity signal mirrors and signal response measurements," *Class. Quantum Grav.*, **19**, 1561, 2002. http://dx.doi.org/10.1088/0264-9381/19/7/345.

[61] S. L. Danilishin and F. Y. Khalili, "Practical design of the optical lever intracavity topology of gravitational-wave detectors," *Phys. Rev. D*, **73**, 022002, 2006. http://link.aps.org/doi/10.1103/PhysRevD.73.022002.

[62] T. Corbitt, Y. Chen, F. Khalili, D. Ottaway, S. Vyatchanin, S. Whitcomb, and N. Mavalvala, "Squeezed-state source using radiation-pressure-induced rigidity," *Phys. Rev. A*, **73**, 023801, 2006. http://link.aps.org/doi/10.1103/PhysRevA.73.023801.

[63] S. Wise, V. Quetschke, A. J. Deshpande, G. Mueller, D. H. Reitze, D. B. Tanner, B. F. Whiting, Y. Chen, A. Tünnermann, E. Kley, and T. Clausnitzer, "Phase Effects in the Diffraction of Light: Beyond the Grating Equation," *Phys. Rev. Lett.*, **95**, 013901, 2005. http://link.aps.org/doi/10.1103/PhysRevLett.95.013901.

[64] G. S. Pati, M. Salit, K. Salit, and M. S. Shahriar, "Demonstration of a Tunable-Bandwidth White-Light Interferometer Using Anomalous Dispersion in Atomic Vapor," *Phys. Rev. Lett.*, **99**, 133601, 2007. http://link.aps.org/doi/10.1103/PhysRevLett.99.133601.

[65] H. N. Yum, M. Salit, G. S. Pati, S. Tseng, P. R. Hemmer, and M. S. Shahriar, "Fast-light in a photorefractive crystal forgravitational wave detection," *Opt. Express*, **16**, no. 25, pp. 20448–20456, 2008. http://www.opticsexpress.org/abstract.cfm?URI=oe-16-25-20448.

[66] E. E. Mikhailov, K. Goda, T. Corbitt, and N. Mavalvala, "Frequency-dependent squeeze-amplitude attenuation and squeeze-angle rotation by electromagnetically induced transparency for gravitational-wave interferometers," *Phys. Rev. A*, **73**, 053810, 2006. http://link.aps.org/doi/10.1103/PhysRevA.73.053810.

[67] S. Kawamura and Y. Chen, "Displacement-Noise-Free Gravitational-Wave Detection," *Phys. Rev. Lett.*, **93**, 211103, 2004. http://link.aps.org/doi/10.1103/PhysRevLett.93.211103.

[68] V. B. Braginsky, M. L. Gorodetsky, F. Y. Khalili, and K. S. Thorne, "Energetic Quantum Limit in Large-Scale Interferometers," *AIP Conf. Proc.*, **523**, pp. 180–190, 2000. http://link.aip.org/link/doi/10.1063/1.1291855.

[69] R. Adhikari, "Upgrades to the Advanced LIGO Interferometer," *LIGO Document: LIGO-G1000524*, 2010. https://dcc.ligo.org/cgi-bin/private/DocDB/ShowDocument?docid=11613.

[70] G. Rempe, R. J. Thompson, H. J. Kimble, and R. Lalezari, "Measurement of Ultralow Losses in an Optical Interferometer," *Opt. Lett.*, **17**, pp. 363–365, 1992. http://www.opticsinfobase.org/abstract.cfm?id=11045.

[71] N. Uehara, A. Ueda, K. Ueda, H. Sekiguchi, T. Mitake, and et al., "Ultralow-loss mirror of the parts-in 10^{-6} level at 1064 nm," *Opt. Lett.*, **20**, pp. 530–532, 1995. http://www.opticsinfobase.org/abstract.cfm?uri=ol-20-6-530.

[72] S. Dwyer. personal communication, 2012.

[73] C. F. McCormick, A. M. Marino, V. Boyer, and P. D. Lett, "Strong low-frequency quantum correlations from a four-wave-mixing amplifier," *Physical Review A*, **78**, 043816, Oct. 2008.

[74] N. V. Corzo, Q. Glorieux, A. M. Marino, J. B. Clark, and P. D. Lett, "Rotation of the noise ellipse for squeezed vacuum light generated via four-wave-mixing," *ArXiv e-prints*, May 2013.

[75] Y. Levin, "Internal thermal noise in the LIGO test masses: A direct approach," *Phys. Rev. D*, **57**, pp. 659–663, 1998. http://link.aps.org/doi/10.1103/PhysRevD.57.659.

[76] W. A. Phillips, "Two-level states in glasses," *Reports on Progress in Physics*, **50**, 1657, 1987. http://dx.doi.org/10.1088/0034-4885/50/12/003.

[77] S. D. Penn, P. H. Sneddon, H. Armandula, J. C. Betzwieser, G. Cagnoli, J. Camp, D. R. M. Crooks, M. M. Fejer, A. M. Gretarsson, G. M. Harry, J. Hough, S. E. Kittelberger, M. J. Mortonson, R. Route, S. Rowan, and C. C. Vassiliou, "Mechanical loss in tantala/silica dielectric mirror coatings," *Class. Quantum Grav.*, **20**, no. 13, 2917, 2003. http://dx.doi.org/10.1088/0264-9381/20/13/334.

[78] G. D. Cole, W. Zhang, M. J. Martin, J. Ye, and M. Aspelmeyer, "Tenfold reduction of Brownian noise in optical interferometry," *ArXiv e-prints*, Feb. 2013.

[79] A. C. Lin, J. S. Harris, and M. M. Fejer, "Two-dimensional III-V nucleation on Si for nonlinear optics," *Journal of Vacuum Science Technology B: Microelectronics and Nanometer Structures*, **29**, no. 3, 030000, 2011.

[80] M. Evans, L. Barsotti, and P. Fritschel, "A general approach to optomechanical parametric instabilities," *Phys. Lett. A*, **374**, no. 4, pp. 665–671, 2010. http://dx.doi.org/10.1016/j.physleta.2009.11.023.

[81] R. X. Adhikari, "Gravitational Radiation Detection with Laser Interferometry," *Reviews of Modern Physics*, 2013.

[82] J. Driggers, V. Frolov, D. Atkinson, H. Miao, M. Landry, R. Adhikari, and R. DeRosa, "Global feed-forward vibration isolation in a km scale interferometer," *LIGO-Document: LIGO-P1000088*, 2010. https://dcc.ligo.org/cgi-bin/private/DocDB/ShowDocument?docid=14511.

[83] R. Kurdyumov, C. Kucharczyk, and B. Lantz, "Blend Switching User Guide," *LIGO-Document: LIGO-T1200126*, 2012. https://dcc.ligo.org/cgi-bin/private/DocDB/ShowDocument?docid=88466.

[84] K.-F. J. Tseng, "System Failure Diagnosis for the Advanced LIGO HAM Chamber Seismic Isolation System," *LIGO Document: LIGO-P1000086*, 2010. https://dcc.ligo.org/cgi-bin/private/DocDB/ShowDocument?docid=14285.

[85] B. Lantz, R. Schofield, B. O'Reilly, D. E. Clark, and D. DeBra, "Review: Requirements for a Ground Rotation Sensor to Improve Advanced LIGO," *Bulletin of the Seismological Society of America*, **99**, pp. 980–989, 2009. http://bssa.geoscienceworld.org/cgi/content/abstract/99/2B/980.

[86] V. Dergachev and R. DeSalvo, "A high precision mechanical ground rotation sensor ," *LIGO Document: LIGO-G1200187*, 2012. https://dcc.ligo.org/cgi-bin/private/DocDB/ShowDocument?docid=88971.

[87] K. Venkateswara, "TiltWash: Update on tiltmeter work at UW," *LIGO Document: LIGO-G1200225*, 2012. https://dcc.ligo.org/cgi-bin/private/DocDB/ShowDocument?docid=89051.

[88] W. Korth, A. Heptonstall, R. Adhikari, E. Gustafson, and B. Lantz, "Status of the Caltech Laser Gyro," *LIGO Document: LIGO-G1200261*, 2012. https://dcc.ligo.org/cgi-bin/private/DocDB/ShowDocument?docid=89111.

[89] M. Evans and F. Matichard, "Tilt Free Inertial Sensing," *LIGO Document: LIGO-T0900628*, 2009. https://dcc.ligo.org/cgi-bin/private/DocDB/ShowDocument?docid=7974.

[90] D. Clark, B. Lantz, and D. DeBra, "Seismic Platform Interferometer - Progress at Stanford," *LIGO Document: LIGO-G1200178*, 2012. https://dcc.ligo.org/cgi-bin/private/DocDB/ShowDocument?docid=88918.

[91] D. Clark, "Control of Differential Motion Between Adjacent Advanced LIGO Seismic Isolation Platforms," Tech. Rep. P1300043, LIGO Laboratory, Mar 2013. https://dcc.ligo.org/LIGO-P1300043.

[92] K. Dahl, A. Bertolini, M. Born, Y. Chen, D. Gering, S. Goßler, C. Gräf, G. Heinzel, S. Hild, F. Kawazoe, O. Kranz, G. Kühn, H. Lück, K. Mossavi, R. Schnabel, K. Somiya, K. A. Strain, J. R. Taylor, A. Wanner, T. Westphal, B. Willke, and K. Danzmann, "Towards a Suspension Platform Interferometer for the AEI 10 m Prototype Interferometer," *J. Phys.: Conf. Ser.*, **228**, 012027, 2010. http://dx.doi.org/10.1088/1742-6596/228/1/012027.

[93] N. Robertson and et al., "Quadruple suspension design for Advanced LIGO," *Class. Quantum Grav.*, **19**, pp. 4043–58, 2002. http://dx.doi.org/10.1088/0264-9381/19/15/311.

[94] N. Robertson, K. Strain, J. Greenhalgh, and G. Hammond, "Update on Quadruple Suspension Design for Advanced LIGO," *LIGO Document: LIGO-P1200056*, 2012. https://dcc.ligo.org/cgi-bin/private/DocDB/ShowDocument?docid=91155.

[95] P. Fritschel, "Potential Advanced LIGO post-Project upgrades," Tech. Rep. T1300176, LIGO Laboratory, Mar 2013. https://dcc.ligo.org/LIGO-T1300176.

[96] A. Cumming, R. Jones, M. Barton, G. Cagnoli, C. A. Cantley, D. R. M. Crooks, G. D. Hammond, A. Heptonstall, J. Hough, S. Rowan, and K. A. Strain, "Apparatus for dimensional characterization of fused silica fibers for the suspensions of advanced gravitational wave detectors," *Rev. Sci. Instrum.*, **82**, 044502, 2011. http://link.aip.org/link/doi/10.1063/1.3581228.

[97] A. Heptonstall, M. Barton, C. Cantley, A. Cumming, G. Cagnoli, J. Hough, R. Jones, R. Kumar, I. Martin, S. Rowan, C. Torrie, and S. Zech, "Investigation of mechanical dissipation in CO2 laser-drawn fused silica fibres and welds," *Class. Quantum Grav.*, **27**, 035013, 2010. http://dx.doi.org/10.1088/0264-9381/27/3/035013.

[98] A. Heptonstall, M. A. Barton, A. Bell, G. Cagnoli, C. A. Cantley, and et al., "Invited Article: CO2 laser production of fused silica fibers for use in interferometric gravitational wave detector mirror suspensions," *Rev. Sci. Insrum.*, **82**, 011301, 2011. http://link.aip.org/link/doi/10.1063/1.3532770.

[99] L. Cunningham, P. Murray, A. Cumming, E. Elliffe, G. Hammond, K. Haughian, J. Hough, M. Hendry, R. Jones, I. Martin, S. Reid, S. Rowan, J. Scott, K. Strain, K. Tokmakov, C. Torrie, and A. van Veggel, "Re-evaluation of the mechanical loss factor of hydroxide-catalysis bonds and its significance for the next generation of gravitational wave detectors," *Phys. Lett. A*, **374**, no. 39, pp. 3993 – 3998, 2010. http://dx.doi.org/10.1016/j.physleta.2010.07.049.

[100] M. Beker, G. Cella, R. DeSalvo, M. Doets, H. Grote, J. Harms, E. Hennes, V. Mandic, D. Rabeling, J. van den Brand, and C. van Leeuwen, "Improving the sensitivity of future GW observatories in the 1–10 Hz band: Newtonian and seismic noise," *General Relativity and Gravitation*, **43**, pp. 623–656, 2010. http://dx.doi.org/10.1007/s10714-010-1011-7.

[101] M. Beccaria, M. Bernardini, S. Braccini, C. Bradaschia, A. Bozzi, C. Casciano, G. Cella, A. Ciampa, E. Cuoco, G. Curci, E. D'Ambrosio, V. Dattilo, G. D. Carolis, R. D. Salvo, A. D. Virgilio, A. Delapierre, D. Enard, A. Errico, G. Feng, I. Ferrante, F. Fidecaro, F. Frasconi, A. Gaddi, A. Gennai, G. Gennaro, A. Giazotto, P. L. Penna, G. Losurdo, M. Maggiore, S. Mancini, F. Palla, H. B. Pan, F. Paoletti, A. Pasqualetti, R. Passaquieti, D. Passuello, R. Poggiani, P. Popolizio, F. Raffaelli, S. Rapisarda, A. Viceré, and Z. Zhang, "Relevance of Newtonian seismic noise for the VIRGO interferometer sensitivity," *Class. Quantum Grav.*, **15**, 3339, 1998. http://dx.doi.org/10.1088/0264-9381/15/11/004.

[102] S. A. Hughes and K. S. Thorne, "Seismic gravity-gradient noise in interferometric gravitational-wave detectors," *Phys. Rev. D*, **58**, 122002, 1998. http://prd.aps.org/abstract/PRD/v58/i12/e122002.

[103] J. C. Driggers, J. Harms, and R. Adhikari, "Subtraction of Newtonian Noise Using Optimized Sensor Arrays," *LIGO Document: P1200017*, 2012. https://dcc.ligo.org/cgi-bin/private/DocDB/ShowDocument?docid=87606.

[104] J. Driggers and J. Harms, "Results of Phase 1 Newtonian Noise Measurements at the LIGO Sites," *LIGO Document: LIGO-T1100237*, 2011. https://dcc.ligo.org/cgi-bin/DocDB/ShowDocument?docid=60064.

[105] N. A. Lockerbie and K. V. Tokmakov, "A 'Violin-Mode' shadow sensor for interferometric gravitational wave detectors," *LIGO Document: LIGO-P1100046*, 2011. https://dcc.ligo.org/cgi-bin/private/DocDB/ShowDocument?docid=58851.

[106] N. A. Lockerbie, L. Carbone, B. Shapiro, K. V. Tokmakov, A. Bell, and K. A. Strain, "First results from the 'Violin-Mode' tests on an advanced LIGO suspension at MIT," *Class. Quantum Grav.*, **28**, no. 24, 245001, 2011. http://dx.doi.org/10.1088/0264-9381/28/24/245001.

[107] B. Sorazu, K. A. Strain, I. S. Heng, , and R. Kumar, "Violin mode amplitude glitch monitor for the presence of excess noise on the monolithic silica suspensions of GEO 600," *Class. Quantum Grav.*, **27**, 155017, 2010. http://dx.doi.org/10.1088/0264-9381/27/15/155017.

[108] C. C. Speake and S. M. Aston, "An interferometric sensor for satellite drag-free control," *Class. Quantum Grav.*, **22**, S269, 2005. http://dx.doi.org/10.1088/0264-9381/22/10/019.

[109] Y. Ikushima, R. Li, T. Tomaru, N. Sato, T. Suzuki, T. Haruyama, T. Shintomi, and A. Yamamoto, "Ultra-low-vibration pulse-tube cryocooler system - cooling capacity and vibration," *Cryogenics*, **48**, no. 9-10, pp. 406 – 412, 2008. http://www.sciencedirect.com/science/article/pii/S0011227508000490.

[110] D. I. G. Jones, *Handbook of Viscoelastic Vibration Damping*. Chichester: J. Wiley, 2001. pp. 171-174.

[111] G. Hammond, "suspension thermal noise," *LIGO Document: LIGO-G1200579*, 2012. https://dcc.ligo.org/cgi-bin/DocDB/ShowDocument?docid=91524.

[112] N. A. Robertson and J. Hough, "Gas Damping in Advanced LIGO Suspensions," *LIGO Document: LIGO-T0900416-v2*, 2009. https://dcc.ligo.org/cgi-bin/DocDB/ShowDocument?docid=5085.

[113] A. Cavalleri, G. Ciani, R. Dolesi, A. Heptonstall, M. Hueller, D. Nicolodi, S. Rowan, D. Tombolato, S. Vitale, P. J. Wass, and W. J. Weber, "Increased Brownian Force Noise from Molecular Impacts in a Constrained Volume," *Phys. Rev. Lett.*, **103**, 140601, 2009. http://link.aps.org/doi/10.1103/PhysRevLett.103.140601.

[114] R. Dolesi, M. Hueller, D. Nicolodi, D. Tombolato, S. Vitale, P. J. Wass, W. J. Weber, M. Evans, P. Fritschel, R. Weiss, J. H. Gundlach, C. A. Hagedorn, S. Schlamminger, G. Ciani, and A. Cavalleri, "Brownian force noise from molecular collisions and the sensitivity of advanced gravitational wave observatories," *Phys. Rev. D*, **84**, 063007, 2011. http://link.aps.org/doi/10.1103/PhysRevD.84.063007.

[115] J. Harms, F. Acernese, F. Barone, I. Bartos, M. Beker, J. F. J. van den Brand, N. Christensen, M. Coughlin, R. DeSalvo, S. Dorsher, J. Heise, S. Kandhasamy, V. Mandic, S. Márka, G. Mueller, L. Naticchioni, T. O'Keefe, D. S. Rabeling, A. Sajeva, T. Trancynger, and V. Wand, "Characterization of the seismic environment at the Sanford Underground Laboratory, South Dakota," *Class. Quantum Grav.*, **27**, 225011, 2010. http://dx.doi.org/10.1088/0264-9381/27/22/225011.

[116] L. Winkelmann, O. Puncken, R. Kluzik, C. Veltkamp, P. Kwee, J. Poeld, C. Bogan, B. Willke, M. Frede, J. Neumann, P. Wessels, and D. Kracht, "Injection-locked single-frequency laser with an output power of 220 W," *Applied Physics B: Lasers and Optics*, **102**, pp. 529–538, 2011. http://www.springerlink.com/content/t2r71860p9631681/.

[117] M. Frede, B. Schulz, R. Wilhelm, P. Kwee, F. Seifert, B. Willke, and D. Kracht, "Fundamental mode, single-frequency laser amplifier for gravitational wave detectors," *Opt. Express*, **15**, pp. 459–465, 2007. http://www.opticsinfobase.org/oe/abstract.cfm?URI=oe-15-2-459.

[118] M. Frede, R. Wilhelm, D. Kracht, and C. Fallnich, "Nd:YAG ring laser with 213 W linearly polarized fundamental mode output power," *Opt. Express*, **13**, pp. 7516–7519, 2005. http://www.opticsinfobase.org/oe/abstract.cfm?URI=oe-13-19-7516.

[119] M. Ganija, D. Ottaway, P. Veitch, and J. Munch, "Cryogenic, high power, near diffraction limited, Yb:YAG slab laser," *Opt. Express*, **21**, pp. 6973–6978, Mar 2013. http://www.opticsexpress.org/abstract.cfm?URI=oe-21-6-6973.

[120] G. Mueller, M. Arain, P. Sainathan, and G. Ciani, "aLIGO TCS Ring Heater development at UF - Krakow 2010 talk," *LIGO Document: LIGO-G1000945-v1*, 2010. https://dcc.ligo.org/cgi-bin/private/DocDB/ShowDocument?docid=21294.

[121] P. Kwee, B. Willke, and K. Danzmann, "Shot-noise-limited laser power stabilization with a high-power photodiode array," *Opt. Lett.*, **34**, pp. 2912–2914, 2009. http://www.opticsinfobase.org/abstract.cfm?URI=ol-34-19-2912.

[122] D. A. Bryan, R. Gerson, and H. E. Tomaschke, "Increase optical damage resistance in lithium niobate," *Appl. Phys. Lett.*, **44**, 847, 1984. http://dx.doi.org/10.1063/1.94946.